1994

In situ determination of hydraulic conductivity and hydraulic head in shallow coastal sediments

Michael D. Wetzel
Lehigh University

AUTHOR:

Wetzel, Michael David

TITLE:

In Situ Determination of Hydraulic Conductivity and Hydraulic Head in Shallow Coastal Sediments

DATE: January 15, 1995

In Situ Determination of Hydraulic Conductivity and Hydraulic Head in Shallow Coastal Sediments

by

MICHAEL D. WETZEL

A Thesis

Presented to the Graduate and Research Committee

of Lehigh University

in Candidacy for the Degree of

Master of Science

in

Civil Engineering

Lehigh University

December 1994

This thesis is accepted and approved in partial fulfillment for the degree of Master of Science.

12/8/94
Date

Dr. Gerard P. Lennon
Thesis Advisor

Dr. Le-Wu Lu
Chairman of Department

Acknowledgements

The author wishes to thank the New Jersey Sea Grant College Program, National Oceanographic and Atmospheric Administration for funding this study under the project number R/S-17 entitled "Field Test and Calibration of an In Situ Instrument to Determine Groundwater/Surface Water Exchange in the Salt Marsh Complex at Stone Harbor, New Jersey".

The author would like to express his great appreciation to Dr. Gerard P. Lennon, Associate Professor, Department of Civil and Environmental Engineering, Lehigh University, for his continuous insight, guidance, and especially patience.

Thanks to Elias Dittbrenner, Dr. Bobb Carson, George Yasko, and Scott Mastronianni for their provided expertise with the instrumentation and for assistance during field experiments. Andrew Bennett's previous work was essential in this study, and for that the author is grateful. Assistance with grain size analysis and field experiments by Deanne Sabarese and Christina Stauffer and document preparation by Catherine Miller was also appreciated.

Finally, the author wishes to thank his fiancee Rachel for her continuous inspiration and support.

Table of Contents

List of Tables vi

List of Figures vii

Abstract 1

1. Introduction 2
    1.1 Premise and Background 2
    1.2 Project Goal/Overview 4
    1.3 Literature Review 5

2. Water Extraction Device 7
    2.1 Introduction 7
    2.2 Early Design/Testing 8
        2.2.1 Previous Study 8
        2.2.2 Preliminary Instrument Design 8
        2.2.3 Laboratory Testing 9
        2.2.4 Analysis of Observed Laboratory Response 10
        2.2.5 Computer Simulations of Observed Laboratory Data 11
        2.2.6 Analysis of Laboratory Computer Simulations 11
        2.2.7 Preliminary Field Tests 12
    2.3 Current Design/Testing 13
        2.3.1 Instrumentation 13
        2.3.2 Field Deployments 13
        2.3.3 Analysis of Observed Field Response 15
        2.3.4 Computer Simulation of Observed Field Data 16
        2.3.5 Analysis of Field Computer Simulations 16
        2.3.6 Estimate of Hydraulic Conductivity Using Type Curves 17
    2.4 Effects of Heterogeneous and Anisotropic Conditions on Field Tests 18
    2.5 Conclusions 19

3. Insertion Device (PISPPI-2) 21
    3.1 Introduction 21
    3.2 Early Testing 22
        3.2.1 Previous Study 22
        3.2.2 Preliminary PISPPI-2 Design 23
    3.3 Current Design/Testing 23
        3.3.1 Instrumentation 23
        3.3.2 Field Deployments 24
        3.3.3 Typical PISPPI-2 Probe Insertion Sequence 25

3.3.4 PISPPI-2 Field Insertion Data 27
3.3.5 PISPPI-2 Field Insertion Data Analysis 27
3.4 Conclusions 30

4. Estimate of Groundwater/ Surface Water Exchange 31
4.1 Estimate of Residual Pore Pressures 31
4.2 Groundwater and Surface Water Exchange 31

5. Summary and Recommendations 33
5.1 Summary 33
5.2 Recommendations 34

Tables 36

Figures 39

Bibliography 104

Vita 108

List of Tables

Table 2.1	Water Extraction Device Summary.	37
Table 3.1	PISPPI-2 Summary and Estimate of Groundwater Flux.	38

List of Figures

Figure 2.1	Normalized Observed Laboratory Water Extraction Device Data (Semi-logarithmic Scale).	40
Figure 2.2	MODFLOW Laboratory Simulated Water Extraction (Semi-logarithmic Scale).	41
Figure 2.3	MODFLOW Simulated - Observed Laboratory Water Extraction Comparison (Semi-logarithmic Scale).	42
Figure 2.4	Configuration of PISPPI-2 (Water Extraction Device): (1) the electronics package (programmable data logger, signal conditioner, and battery pack) contained in a water-tight pressure case; (2) a differential pressure transducer in compensated manifold; (3) 9.5 mm diameter probe (well) with No. 200 stainless steel mesh screen for water extraction; (4) PVC reservoir (r_c = 1.03 cm) with flotation attachment for rising water levels.	43
Figure 2.5	Site 1, Test Mode 1, Raw Observed Field Water Extraction Data.	44
Figure 2.6	Site 2, Test Mode 1, Raw Observed Field Water Extraction Data.	45
Figure 2.7	Site 3, Test Mode 2, Raw Observed Field Water Extraction Data.	46
Figure 2.8	Site 4, Test Mode 2, Raw Observed Field Water Extraction Data.	47
Figure 2.9	Site 5, Test Mode 4, Raw Observed Field Water Extraction Data.	48
Figure 2.10	Site 6, Test Mode 4, Raw Observed Field Water Extraction Data.	49
Figure 2.11	Site 7, Test Mode 3, Raw Observed Field Water Extraction Data.	50

Figure 2.12	Site 8, Test Mode 1, Raw Observed Field Water Extraction Data.	51
Figure 2.13	Site 10, Test Mode 1, Raw Observed Field Water Extraction Data.	52
Figure 2.14	Site 1, Normalized Observed Field Water Extraction Data (Semi-logarithmic Scale).	53
Figure 2.15	Site 2, Normalized Observed Field Water Extraction Data (Semi-logarithmic Scale).	54
Figure 2.16	Site 3, Normalized Observed Field Water Extraction Data (Semi-logarithmic Scale).	55
Figure 2.17	Site 4, Normalized Observed Field Water Extraction Data (Semi-logarithmic Scale).	56
Figure 2.18	Site 5, Normalized Observed Field Water Extraction Data (Semi-logarithmic Scale).	57
Figure 2.19	Site 6, Normalized Observed Field Water Extraction Data (Semi-logarithmic Scale).	58
Figure 2.20	Site 7, Normalized Observed Field Water Extraction Data (Semi-logarithmic Scale).	59
Figure 2.21	Site 8, Normalized Observed Field Water Extraction Data (Semi-logarithmic Scale).	60
Figure 2.22	Site 10, Normalized Observed Field Water Extraction Data (Semi-logarithmic Scale).	61
Figure 2.23	Normalized MODFLOW Field Simulated Water Extraction Type Curves (Semi-logarithmic Scale).	62
Figure 2.24	Match of the Silty-Sand Observed Field Extraction (slug) Test Response Curve (solid line) with the $S = 1 \cdot 10^{-5}$ Type Curve from Figure 2.23 (dotted line).	63
Figure 2.25	MODFLOW Simulated - Observed Field Water Extraction of Beltzville Layered Sediment.	64

Figure 3.1	Configuration of the PISPPI-2 (Pressure Pulse Technique): (1) the electronics package (programmable data logger, signal conditioner, and battery pack) contained in a water-tight pressure case; (2) a differential pressure transducer in compensated manifold; (3) the 9.5 mm diameter probe on the end of flexible hydraulic tubing.	65
Figure 3.2	Location of 1993 and 1994 sampling locations in Great Sound, New Jersey.	66
Figure 3.3	Normalized Observed Field Pressure Decay Curve, Station 1.	67
Figure 3.4	Normalized Observed Field Pressure Decay Curve, Station 2.	68
Figure 3.5	Normalized Observed Field Pressure Decay Curve, Station 4.	69
Figure 3.6	Normalized Observed Field Pressure Decay Curve, Station 5.	70
Figure 3.7	Normalized Observed Field Pressure Decay Curve, Station 6.	71
Figure 3.8	Normalized Observed Field Pressure Decay Curve, Station 7.	72
Figure 3.9	Normalized Observed Field Pressure Decay Curve, Station 8.	73
Figure 3.10	Normalized Observed Field Pressure Decay Curve, Station 9.	74
Figure 3.11	Normalized Observed Field Pressure Decay Curve, Station 10.	75
Figure 3.12	Normalized Observed Field Pressure Decay Curve, Station 11.	76
Figure 3.13	Normalized Observed Field Pressure Decay Curve, Station 12.	77

Figure 3.14	Normalized Observed Field Pressure Decay Curve, Station 13.	78
Figure 3.15	Normalized Observed Field Pressure Decay Curve, Station 14.	79
Figure 3.16	Normalized Observed Field Pressure Decay Curve, Station 15.	80
Figure 3.17	Normalized Observed Field Pressure Decay Curve, Station 16.	81
Figure 3.18	Normalized Observed Field Pressure Decay Curve, Station 17.	82
Figure 3.19	Normalized Observed Field Pressure Decay Curve, Station 18.	83
Figure 3.20	Normalized Observed Field Pressure Decay Curve, Station 19.	84
Figure 3.21	Normalized Observed Field Pressure Decay Curve, Station 20.	85
Figure 3.22	Normalized Observed Field Pressure Decay Curve, Station 21.	86
Figure 3.23	Normalized Observed Field Pressure Decay Curve, Station 22.	87
Figure 3.24	Normalized Observed Field Pressure Decay Curve, Station 23.	88
Figure 3.25	Normalized Observed Field Pressure Decay Curve, Station 24.	89
Figure 3.26	Normalized Observed Field Pressure Decay Curve, Station 25.	90
Figure 3.27	Normalized Observed Field Pressure Decay Curve, Station 26.	91
Figure 3.28	Normalized Observed Field Pressure Decay Curve,	92

Station 30.

Figure 3.29 Normalized Observed Field Pressure Decay Curve, Station 31. 93

Figure 3.30 Normalized Observed Field Pressure Decay Curve, Station 32. 94

Figure 3.31 Normalized Observed Field Pressure Decay Curve, Station A. 95

Figure 3.32 Normalized Observed Field Pressure Decay Curve, Station B1. 96

Figure 3.33 Normalized Observed Field Pressure Decay Curve, Station B2. 97

Figure 3.34 Grain Size Distribution and PISPPI-2 Normalized Observed Field Pressure Decay Curves for Selected Stations in Great Sound Proceeding from (a) Coarser (low ϕ units) to (c) Finer (high ϕ units) Sediment. 98

Figure 3.35 T_{50} (Time to 50% Pressure Decay) vs. Laboratory Permeameter Hydraulic Conductivity. 99

Figure 3.36 Equivalent Casing Radius Squared (r_c^2) vs. Laboratory Permeameter Hydraulic Conductivity (K). 100

Figure 3.37 Ratio of K to Equivalent Casing Radius Squared (r_c^2) vs. Laboratory Permeameter Hydraulic Conductivity. 101

Figure 3.38 Estimate of Hydraulic Conductivity from PISPPI-2 Normalized Observed Field Pressure Decay Using the Equivalent Casing Radius Matching Technique. 102

Figure 4.1 Observed Raw Field Pressure Decay Curve with Apparent Residual Pressure. 103

Abstract

Accurately quantifying groundwater/surface water exchange rates in coastal lagoons is extremely difficult. Hydraulic conductivity and hydraulic gradient of the sediment must first be estimated in order to obtain the flux rate. Determining hydraulic conductivity alone is typically very cumbersome due to the need for permanent structures, test expense, time constraints, and the accuracy of the test method.

Two field techniques were developed and tested to estimate hydraulic conductivity and hydraulic gradient to obtain flux rates. The methods used a water extraction device and an insertion instrument (PISSPI-2).

The water extraction device is comparable to a miniature slug test. Hydraulic conductivity is estimated by matching observed field data to simulated field type curves created by MODFLOW (a 3-Dimensional Finite Difference Groundwater Flow Model), resulting in curves similar to Cooper et al. (1967). Hydraulic conductivity (K) varied by a factor of approximately 2.2 when comparing the laboratory permeameter determined K and the water extraction K.

The PISPPI-2 is similar to tests using a piezocone, where monitored pressure decay due to device insertion is analyzed using an empirical approach. Bredehoeft et al.'s (1980) theory of an equivalent casing radius (r_c) for pressurized slug tests is used in conjunction with laboratory determined hydraulic conductivities to develop an empirical matching process that identifies r_c^2 and subsequently K.

1. Introduction

1.1 Premise and Background

Hydraulic conductivity of a soil depends on a variety of physical factors including porosity, particle size and distribution, shape of particles, arrangement of particles, and other factors (Todd, 1980). Hydraulic conductivity is a function of both soil and pore fluid, compared to permeability which is only a function of the soil medium. Hydraulic Conductivity is defined as the D'Arcy velocity divided by the hydraulic gradient, and is a measure of the ease with which water/fluid moves through the ground. The D'Arcy velocity multiplied by the cross-sectional area at a location yields the volumetric groundwater flux at that location. Hydraulic conductivity has dimensions of velocity [L/T].

Hydraulic conductivity of a geologic formation can be a difficult parameter to quantify. Numerous methods are used to calculate hydraulic conductivity for a formation, but each has disadvantages or inaccuracies related to the particular test method. Examples are laboratory permeameter tests, slug tests, pump tests, and piezocone tests (Todd, 1980).

Permeameter testing is traditionally conducted in a laboratory using a sample from a sediment core taken in the field. Using D'Arcy's Law, hydraulic conductivity is determined using a constant or unsteady flow rate through the sample. Disturbance of the material occurs during coring and during transfer of the sediment from the core to the permeameter device. This disturbance of the sediment can lead to permeameter results with little relation to actual field hydraulic conductivities

(Todd, 1980). In addition, cores are only representative of the point locations and depths sampled. Variations of several orders of magnitude frequently occur for depths and locations even a short distance away (Todd, 1980). Slug testing, also known as single-well permeability testing, permits measurements of hydraulic conductivity of a formation with a single permanent well or piezometer. The method consists of quickly lowering or raising the water level in the well and monitoring its subsequent response until returning to static (equilibrium) conditions. Bouwer and Rice (1989), Cooper et al. (1967), and Hvorslev (1951), each present a method of interpreting slug test data to determine values of hydraulic conductivity and storativity using different assumptions. However, hydraulic conductivities based on slug tests are only indicative of the medium in the immediate vicinity of the well. Therefore, characterizing a large area is expensive, as single wells are needed throughout a study area.

Pump (aquifer) tests traditionally use one pumping well with one or more observation wells or piezometers. The time-drawdown response in observation wells is used in conjunction with pumping rate and other well dimensions to estimate aquifer parameters, including hydraulic conductivity. Two methods in common use for calculating aquifer characteristics from time-drawdown data are the Theis and Jacob methods (Freeze and Cherry, 1979). Each use a combination of analytical and graphical solutions. A definite advantage of pump tests over other tests is the value of hydraulic conductivity determined is usually representative of the aquifer between the wells. However, disadvantages include high costs of well installation, and

problems with disposal of discharge water. Pump tests also require extensive testing time, typically 24 hours or more, as compared to a slug test which requires times as short as a few minutes.

Piezocones are used to determine hydraulic conductivity of a saturated soil by monitoring decay of pressure in the formation caused by the instruments insertion. The pressure response is related to the soil's parameters and therefore can be used to calculate hydraulic conductivity. Bennett et al. (1987) empirically related time of pressure decay to consolidation coefficient and coefficient of volume change to estimate hydraulic conductivity. Piezocones do not require a permanent structure, which reduces testing costs, compared to a permanently installed well or piezometer.

In summary, most current tests are expensive, time consuming, and require permanent structures. Many tests are intended for pristine field conditions, and are often difficult to conduct in terrains such as marine environments.

1.2 Project Goal/Overview

The goal of this project was to develop methods for the in situ determination of hydraulic conductivity of surficial saturated sediments. Following Bennett (1993), the purpose of this study was to develop a non-permanent, non-time consuming, less expensive, portable instrument.

Similar to Bennett, two methods were studied and developed for field testing. They include a water extraction device and an insertion instrument (PISPPI-2). The water extraction device is comparable to a miniature slug test, while the insertion

device is similar to an analysis of pressure decay from a piezocone insertion and analyzed similar to a pressurized slug test (Bredehoeft et al., 1980) using an empirical approach.

It should be noted that the test methods developed are supplemental to existing methods which are more appropriate for greater depths. Hydraulic conductivity values are only indicative of the shallow sediment formation near the test apparatus. These tests in no way indicate values of hydraulic conductivity at greater depths nor the direction of groundwater flow at greater depths. Care must be taken to properly infer flux rates from the data, because the technique assumes the flux is vertically upward.

1.3 Literature Review

The water extraction device uses a similar technique to Cooper et al.'s (1967) slug test theory to estimate the value of hydraulic conductivity of saturated surficial sediments. They derived normalized type curves using the equation for unsteady radial flow to a well assuming a fully penetrating and developed well in a confined aquifer. Transmissivity and storage coefficient are identified using a graphical method, matching observed slug test data with the type curves. Hvorslev (1951) used a simpler approach that neglects aquifer and water compressibility.

The PISPPI-2 device is analyzed by studying the decay of the pressure head transient created by instrument probe insertion. Combining theories from Bredehoeft et al. (1980), Cooper et al. (1967) and Hvorslev (1951), a technique for estimating

hydraulic conductivity for a saturated surficial sediment is derived.

Bredehoeft et al. (1980) realized conventional slug tests (water extraction/injection) in a low hydraulic conductive material would require an extensive amount of time. They derived a method for estimating aquifer parameters (hydraulic conductivity and storage coefficient) in which the well is pressurized causing a slight compression in the water and subsequently shut-in to maintain the pressure. The pressure response was then monitored until returning to equilibrium conditions. Bredehoeft et al.'s theory uses the same equation as Cooper et al., but uses the pressurized head in the well instead of the water level in the well. The volume of water that flows into the formation is much smaller than for filling a resrvoir, resulting in a much shorter test.

In addition, according to Hvorslev (1951), test data should plot as a straight line when the logarithm of the water level differential is plotted versus time. Hydraulic conductivity values were not calculated using Hvorslev's method because the theory is not as appropriate as Cooper et al. (1967), since it neglects water and soil compressibilities. However, Hvorslev's technique is very useful in judging the consistency of the data (logarithm of differential head versus time falls on a straight line) and can be used to backcalculate an "effective" initial water level deflection.

2. Water Extraction Device

2.1 Introduction

The water extraction device developed in this study was essentially a miniature slug test modified from Bennett's (1993) design. An instantaneous change in water level in a reservoir is generated by removal of a steel slug of known volume. Water flows from the aqueous sediment via flexible tubing, and into the reservoir. The subsequent head (water level) differential was monitored over time until returning to equilibrium. The test data result in an 'S' shape curve characterized by slug test data when normalized head was plotted versus the logarithm of time.

The Three-Dimensional Finite-Difference Groundwater Flow Model (MODFLOW) was used to generate type curves simulating the transient water extraction (Bennett, 1993). Assuming a homogeneous, isotropic sediment, the boundary conditions included a zero head (recharge boundary) on the sediment surface, no flow boundaries sufficiently far from the test site to not influence the head recovery, and impermeable cells representing the extraction probe.

Configuration of the model grid lead to a domain with 4500 cells, 15 rows, 15 columns, and 20 horizontal layers. Cells were designed to get progressively larger as distance from the well screen increased. This arrangement produces better resolution closer to the well screen where larger head changes are expected.

Assuming symmetric radial flow, one-fourth of the sediment domain was modelled to reduce computational effort. Since one-fourth of the sediment domain is modelled, only one-fourth of the total flow is simulated.

A curve matching process, similar to Cooper et al. (1967), using the normalized simulated type curves was adopted. Hydraulic conductivity was interpreted by comparing observed field tests of the water extraction device with the type curves.

2.2 Early Design/Testing

2.2.1 Previous Study

Bennett (1993) studied three different size reservoir casings resulting in a slow, medium, and fast response in conjunction with the water extraction device. The fast extraction reservoir with an effective area of 3.33 cm^2 provided an adequate extraction time of approximately 6.7 minutes for the laboratory sand with hydraulic conductivity of 0.007 cm/s. Following project goals of a non-time consuming instrument, the fast reservoir was selected for further development.

2.2.2 Preliminary Instrument Design

Bennett's (1993) prototype water extraction device was modified to adapt for field use. To make handling easier, the reservoir and probe (well) were connected to form one instrument.

Bennett's (1993) apparatus was designed for laboratory testing only, because the self-jetting insertion method disturbed the sediment and required recompacting. To adapt to field situations, the well's outside diameter (equivalent to the PISPPI-2 probe diameter), and the well screen radius and length were reduced to allow the

probe to be inserted similar to the PISPPI-2, causing less disturbance of the sediment matrix, and avoided the need for recompaction. The screen length was chosen to be interchangeable with the PISPPI-2 porous stone.

Both well and screen were tested to check hydraulic conductance. One criteria is that the hydraulic conductivity of the stone be two orders of magnitude higher than the sediment. Results indicated the reduction in screen size and well diameter had no effect on flow into the reservoir.

An inverted manometer connected to the reservoir was used to read water levels inside the reservoir during initial testing. The water levels were recorded at selected time intervals using a stop watch.

Bennett's valve system (utilized to cause an instantaneous water level change) was replaced by a stainless steel slug which was removed from the reservoir to initiate the test. This test method mimics a traditional slug test in a well.

2.2.3 Laboratory Testing

Laboratory testing of the water extraction device was completed in the fluidization tank of the Herbert R. Imbt Hydraulics Laboratory at Lehigh University (Bennett, 1993). The fine sand with mean diameter of d_{50} = 0.148 mm and hydraulic conductivity of 0.007 cm/sec used in Bennett's experiments was used in these tests.

The water extraction device was tested in the configuration described in the previous section. The device was inserted into the sediment by hand or by hammering with a rubber mallet, with the slug situated inside the reservoir. Water

was allowed to flow into the reservoir so the pretest reservoir water level corresponded to the equilibrium level. A test was initiated when the slug was pulled from the reservoir, causing a deviation from equilibrium head and subsequently an inflow rate due to the driving head difference.

Following slug test procedures, the head (water level) readings were recorded manually using the inverted manometer. Water level versus time were recorded until water levels inside the reservoir returned to equilibrium.

2.2.4 Analysis of Observed Laboratory Response

The reservoir head response was normalized with respect to the initial maximum reservoir head difference caused by slug withdrawal. Normalizing eliminates any variation in the initial induced head difference. This enabled comparison of tests independent of initial head difference. The data for two laboratory water extractions using the revised laboratory prototype instrument are shown in Figure 2.1.

The 'S' shaped normalized head recovery curve is similar to Bennett's (1993) slug curves when normalized water level is plotted against the logarithm of time. During the early stages of testing, although the hydraulic gradient is large and the head recovery is fast, the expanded time scale results in a relatively flat curve. At intermediate times, the head gradient in the sediment is fully developed causing near linear head recovery with respect to the logarithm of time. In the late stages of testing, head changes slowly as water levels approach equilibrium, resulting in a

flattening of the observed response.

2.2.5 Computer Simulations of Observed Laboratory Data

Computer simulations similar to Bennett's (1993) were conducted for observed laboratory results to verify the device's applicability. Simulations consisted of a finite difference tank model with 2907 cells using the MODFLOW model (McDonald and Harbaugh, 1988). In this study, cells representing the well/probe radius and screen were reduced from Bennett's instrument size to correspond to the new instrument configuration. Reconfiguring the cells led to a domain with 17 columns, 24 rows, and 9 vertical layers for a total of 3672 cells.

Following Bennett, only half of the tank domain was modelled since flow will be symmetric on either side of the probe. Reducing the total number of nodes by 50% results in significantly less computational effort. All of the modelled flow was assigned to one cell representing the new well screen. Bennett's model consisted of two cells representing the screen, each containing half the modelled flow.

Tank boundary conditions remained the same as Bennett's. The independently determined values of hydraulic conductivity and storage coefficient, 0.007 cm/sec and 10^{-5} respectively, were used as input parameters in the model (Bennett, 1993).

2.2.6 Analysis of Laboratory Computer Simulations

A MODFLOW simulation of the observed laboratory response is presented

in Figure 2.2, with the simulated head data normalized by the peak differential head response plotted versus the logarithm of time.

Figure 2.3 is a plot of the simulated water extraction (using the expected hydraulic conductivity of 0.007 cm/sec) plotted overlain on the observed water extraction. For this simulation, there was no need to select a matchpoint since the simulated data fits the observed data without translating the time axis horizontally. Results indicated that the miniature slug test developed should be applicable for field testing.

2.2.7 Preliminary Field Tests

Preliminary field tests in Great Sound led to further revisions of the water extraction device. Initial field testing from a boat was difficult and unsuccessful. At the first test location the sediment had a lower hydraulic conductivity than expected and the extraction rate was so slow that the reservoir filling rate was exceeded by the rising tide level; thus equilibrium was never reached.

Although transient water levels due to tides can be factored out, the reliability of slug tests drops significantly when the equilibrium level is not known. Lab conditions always allowed for a constant head in the tank and this problem was not encountered. During future laboratory testing, a fluctuating tank water level will be used to represent tidal variations.

2.3 Current Design/ Testing

2.3.1 Instrumentation

As a result of preliminary field tests, a revised instrument setup and method for data collection were developed. The well and reservoir were separated and connected by 4 mm hard flexible plastic tubing. The reservoir was then tested in two modes: (1) When water level change was constant or minimal over short time periods, the reservoir was attached to a steel weight and kept at a constant elevation. (2) When water levels change over short periods of time, the reservoir was affixed to a float to factor out rising tide effects, e.g. the bottom of the reservoir was always the same distance below the water surface.

Also, the reservoir water level recovery was monitored electronically using the PISPPI-2's differential pressure transducer and recorded on the PISPPI-2 data logger. A 'T' fitting at the top of the well enabled connection of the PISPPI and reservoir tubing to the well (see Figure 2.4).

2.3.2 Field Deployments

In shallow water deployments, waves migrating on the surface will cause short-period pressure fluctuations on the order of a few seconds. To combat this effect, a clamped 6" semirigid tube with 4, 1/16" holes was placed over the negative port of the PISPPI-2. Since waves pass quickly over the PISPPI-2 negative port, the small openings in the tubing filter some of the short-period pressure signal from the waves. The pressure pulse takes longer to travel through the small openings, thus the wave

passes before the entire pressure signal affects the pressure port/transducer.

The new configuration was tested in 4 modes:

1) Reservoir positioned on bottom without wave filter.

2) Reservoir positioned on bottom with wave filter.

3) Floating reservoir without wave filter.

4) Floating reservoir with wave filter.

The first test mode proved adequate for constant water levels with little or no wave climate. As wave climate increased, the noise in the output signal from the PISPPI-2 increased. Figures 2.5 and 2.6 show raw observed data for test mode 1.

The second test was used for a constant water level with a wave climate. The clamped tubing over the negative port on the PISPPI-2 provided beneficial results. Because the lag time in the sediment is expected to be small, the filter eliminated much of the noise caused by larger waves, thus resulting in smoother data. Figures 2.7, 2.8, 2.12 and 2.13 show raw observed data for test mode 2.

The third test revealed some improvement from the first. The floating reservoir not only maintained a more reliable differential pressure, but also filtered some of the wave noise, provided the reservoir was tethered directly over the negative port. Figure 2.11 shows raw observed data for test mode 3.

The fourth test mode proved the clamp was so efficient at filtering background pressure noise that coupling with the floating reservoir added more noise to the system. This is attributed to the float fluctuating with the water surface as waves pass, while the clamp is filtering out the same waves. Although the floating reservoir

does not perform well in large wave climates, it is essential for fluctuating water levels. Figures 2.9 and 2.10 show raw observed data for test mode 4.

The tubing connecting the probe, PISPPI-2, and reservoir also added noise if allowed to swing freely and contact the sediment during testing. Precautions were taken to eliminate this noise.

Although some signals are clearer than others for certain tests, an apparent decay curve is still definable in the data. It should be noted that a signal will never be free from all noise due to the transducer sensitivity.

2.3.3 Analysis of Observed Field Response

Analysis of the observed test data was completed by performing an exponential fit (straight line fit on semi-log paper) of the first twenty data points of each test (head=logarithmic, time=arithmetic). Plotting the data on semi-logarithmic paper and projecting the best fit line to intersect the head axis at t=0 gives a graphical interpretation of H_{max}, the effective maximum water level change in the reservoir upon slug removal (Hvorslev, 1951). A moving average of every five data points filters some of the remaining noise caused by the smaller waves. The head data was normalized by H_{max}, and plotted versus the logarithm of time divided by the reservoir radius squared. The normalized plots are seen in Figures 2.14 to 2.22 which will later be compared to computer simulations. Although the plots are not entirely smooth, a definable decay curve can be interpreted from the graphs. Normalizing the graphs eliminates dependence of an individual test on H_{max} and reservoir radius.

2.3.4 Computer Simulation of Observed Field Data

The goal of modelling the field case was to generate simulated extraction curves based on known sediment parameters. Simulation data would then be normalized and used similar to Cooper et al. (1967) eliminating the dependence of test specifics. As stated earlier, the type curves would then be used to determine in situ soil parameters.

The MODFLOW model was used to generate type curves as explained in Section 2.1. The only boundary conditions affecting the flow were the impermeable well probe and constant water level at the sediment surface; the domain was terminated at a distance far enough from the probe to not affect results. Because the volume of the extracted water is small, the region of influence is small. Thus, consistent with other slug tests, using a large domain relative to the well acts as an infinite aquifer. Therefore, the side boundary conditions imposed on the flow are far enough away and have minimal negligible influence on head recovery.

2.3.5 Analysis of Field Computer Simulations

Simulations were completed for $K = 7x10^{-3}$ cm/sec and $S = 10^{-2}$ to 10^{-6}. The well water level output was normalized by the maximum water level differential. Since the well in this study was not fully-penetrating the time was normalized by the simulated hydraulic conductivity, rather than the transmissivity as in Cooper et al., divided by the reservoir radius squared. This resulted in a normalized time parameter with the dimensions of 1/cm. Cooper et al.'s (1967) normalized time

parameter results in a truly non-dimensionalized parameter. Normalizing by r_c^2 and hydraulic conductivity cancels the dependence of a particular test on these two parameters. Normalized head is plotted versus normalized time to generate the field type curves, similar to Cooper et al. (1967). The type curves indicate the test is not highly sensitive to storage coefficient (S) as shown by the similar (overlapping) type curves for a range of storage coefficient values (see Figure 2.23).

Normalized simulations of field extractions should correspond to any field test for isotropic, homogeneous aquifers of a specified depth despite reservoir radius and maximum head change.

2.3.6 Estimate of Hydraulic Conductivity Using Type Curves

Using a similar method to Cooper et al. (1967), the normalized observed water level versus time plot is overlain on the computer-simulated type curves. With time axis coincident, the type curves are translated horizontally until the observed field data fit one of the type curves. Although any point will produce consistent results, traditionally the match point is chosen as $Kt/r_c^2 = 1$ on the normalized time axis of the type curves. Therefore, reading the match point value from both type (Kt/r_c^2) and observed (t/r_c^2) data from the normalized time axis, and knowing the well casing radius from field tests, a value of hydraulic conductivity is calculated for the sediment tested. The storage coefficient is estimated using the best curve fit of observed data to the type curves of different slope corresponding to different storage coefficients (see Figure 2.23). For coarser material (e.g., sand), the storage coefficient

approaches very small values and is difficult to estimate with this approach since several type curves (one for each storage coefficient) have a similar shape (slope).

One example of the matching process is seen in Figure 2.24. An average value for hydraulic conductivity of the Beltzville Lake sediment is determined using the homogeneous, isotropic type curves. The value of hydraulic conductivity determined using a type curve match is $7.7 \cdot 10^{-3}$ cm/sec. This value corresponds well to the independently determined laboratory permeameter hydraulic conductivity of $3.5 \cdot 10^{-3}$ cm/sec for the middle sediment layer. The values only deviate a factor of (2.2), which is considered excellent. Matchpoints, calculated hydraulic conductivity, and laboratory permeameter hydraulic conductivity of individual field deployments are summarized in Table 2.1.

2.4 Effects of Heterogeneous and Anisotropic Conditions on Field Tests

Several computer simulations were conducted to determine the proximity at which impermeable sediment has an effect on the determination of the hydraulic conductivity when using the type curves. An estimate of hydraulic conductivity using the type curves where impermeable sediment affects the flow into the well may result in an underestimated hydraulic conductivity for the permeable sediment.

Computer modelling of varying thicknesses of permeable sediment confined vertically by two impermeable layers was conducted. The minimum thickness of a sediment layer to fit the type curves in Figure 2.23 was 12.5 cm. Shallow depths of permeable sediment underlain by an impermeable confining unit was also modelled.

To use the type curves, a sediment should be at least 12.5 cm in depth. Screen position was varied vertically to see if any effects were noticeable. It was found that the screen needed to be further than 5.0 cm from an impermeable layer to match the type curves presented in Figure 2.23. Modelling of permeable sediment confined radially by an impermeable unit was also tested. Type curves are applicable for impermeable layers at a radial distance of 27.0 cm from the probe.

The final computer simulation was conducted based on the layering found in the core taken from Beltzville Lake State Park, PA. The hydraulic conductivity of each layer was tested using a falling head permeameter. Permeameter hydraulic conductivity and thickness of each layer were used as input parameters in MODFLOW. Simulation resulted in a near identical match of the normalized observed field data without using the matchpoint process (see Figure 2.25).

2.5 Conclusions

The water extraction device is intended to supplement existing test methods for determining in situ hydraulic conductivity. It is intended for areas with coarse sediment where hydraulic conductivity is $\geq 5.0 \cdot 10^{-4}$ cm/sec. Sediment with hydraulic conductivities $< 5.0 \cdot 10^{-4}$ require extensive amounts of time (> 30 minutes) to complete a test. The insertion device is a better choice for determining hydraulic conductivities for sediment with values $< 5.0 \cdot 10^{-4}$ which require significantly less time to complete a test. Alternatively, a prematurely terminated slug test can be conducted, where the match is performed using only a portion of the observed curve

up to the point of termination of the test.

It is recommended to avoid data collection during large wave climates when using the water extraction device. In areas where there is minimal tidal fluctuation or where tidal change is minimal over short periods of time (approximately 10 minutes) it is suggested to use a reservoir positioned on the bottom with the filter attached to the negative port of the PISPPI to dampen wave effects. Where tidal change is noticeable over a 10 minute period, it is suggested that the floating reservoir be used. It will give a consistent driving head throughout the test, factoring out the rising tide water level which affects both water column and sediment pore pressure heads. It is important to keep the floating reservoir tethered directly above the negative port so both ports sense the wave crest or trough simultaneously as it passes. Tidal effects are also dampened in deeper water.

The type curves generated for field use thus far are for homogeneous, isotropic sediment with thicknesses >12.5 cm, and radial distances of >27.0 cm. Based on independently determined values of hydraulic conductivity, the type curves give a reasonable estimate of hydraulic conductivity for the above constraints. It should be noted that the value of hydraulic conductivity computed is representative of only a small area around the probe. However, ease, efficiency, time and accuracy of the tests allow multiple tests in an area to define hydraulic conductivity in a broader region. The existing type curves can be easily modified for other sediment geometries.

3. Insertion Device (PISPPI-2)

3.1 Introduction

The PISPPI-2 (Portable In Situ Pressure and Permeability Instrument) is inserted into a saturated sediment inducing a pressure in the surrounding sediment and subsequently a pressure differential between soil and hydrostatic pressure. Decay of the pressure transient is monitored over time until returning to background pore pressure. Pressure responses generated by driving piezocones are analyzed theoretically by investigators such as Rad and Tumay (1985).

The time for the pressure decay to return to equilibrium is affected by several factors, including the permeability and compressibility. Correlation of time to return to equilibrium versus laboratory hydraulic conductivity shows a lack of one-to-one correlation, indicating compressibility (or storage) effects need to be taken into account.

Due to the very thin probe diameter, the disruption is limited to a small region. An empirical approach was used here to attempt to include compressibility effects. The monitored pressure response yields results analogous to conventional slug test analysis by Cooper et al. (1967) and pressurized slug test analysis by Bredehoeft et al. (1980) when normalized head (pressure differential) is plotted versus the logarithm of time. Analysis of transient insertion pressure data used Bredehoeft's et al. (1980) pressurized slug test theory. The insertion probe was assumed to pressurize the sediment similar to Bredehoeft's et al. shut-in well. Therefore, Bredehoeft's et al. curve matching technique was adopted for

determination of hydraulic conductivity divided by an effective well casing radius squared. The effective well casing radius is defined as the equivalent theoretical well casing radius required to conduct a traditional (extraction/injection) slug test requiring the same amount of time as the pressurized test.

This empirical approach was used to determine the value of hydraulic conductivity for a test site. Although not as theoretically sound as techniques such as Rad and Tumay (1985), it is simplicity is attractive if reliable hydraulic conductivity estimates are obtained. Hydraulic conductivity values determined from flexible wall permeameter tests on cores from specific sites were used to formulate a log-log plot of K/r_c^2 versus permeameter hydraulic conductivity. A best fit line connects the data and is used to estimate hydraulic conductivity values for stations with no permeameter tests.

3.2 Early Testing

3.2.1 Previous Study

Bennett's (1993) preliminary laboratory tests concluded that hydraulic conductivity determination is influenced by insertion rate, especially if inserted over a long period (over 1 sec). However, the variation in hydraulic conductivity estimates from repeated insertions was deemed minor for fast insertions if the response is normalized by the maximum pressure. He found that the region of influence was much smaller for the PISPPI-1 device than the water extraction device. Bennett also determined that the observed pressure transient response, due to device insertion, yields 'S' shape curves similar to conventional slug test data and pressurized slug test

data when normalized head data is plotted versus the logarithm of time.

3.2.2 Preliminary PISPPI-1 Design

A detailed description of the preliminary PISPPI-1 design is found in Bennett (1993). The preliminary laboratory insertion technique utilized the weight of the instrument to insert the probe. Difficulties with field insertions experienced by others resulted in a modification of insertion technique. The probe was separated from the main housing unit to ease the insertion method. Instead, the probe was connected to the pressure transducer via hard flexible plastic tubing. This modification also avoided pressure pulses generated by the housing unit due to contact with the sediment surface.

3.3 Current Design/Testing

3.3.1 Instrumentation

The PISPPI-2 instrument consists of three main components: (1) an electronics package contained in a water-tight pressure case, (2) a solid state differential pressure transducer, and (3) a 9.5 mm diameter stainless steel probe (Carson et al., 1994).

The differential pressure transducer system consists of a positive and negative port. Although classified as a *pressure* transducer, as configured the transducer actually measures *head* differences between the hydrostatic water column pressure (negative port) and the induced pressure due to probe insertion (positive port). A tattletale 4A computer, capable of variable sampling intervals (0.1 sec to >1 hr) and

storage of 1-2 Mb of data, monitors the transducer output.

The probe is inserted with a 0.625" ID galvanized extension pipe. The pipe is placed over the probe guide rod and the probe is inserted manually (see Figure 3.1).

3.3.2 Field Deployments

The PISPPI-2 device was tested in Great Sound, New Jersey, a coastal lagoon surrounded by marshlands, and located between the barrier islands and the mainland. It was chosen because previous data existed on grain size distributions (Carson et al., 1988). The expected sediment was 75% or more with median diameters less than 4ϕ (0.0625 mm) existing in a belt around the margin of the sound adjacent to the shore. A smaller band of sediment, bisecting the sound from north to south, with median diameters less than 3ϕ (0.125 mm) is found in the areas of the Intracoastal Waterway (ICWW). The remainder of the sound is comprised of mixtures of fine and coarse sediment patches. Bottom sediment textures are given in Figure 7 of Carson et al. (1988).

PISPPI-2 insertions were conducted at approximately 30 locations in Great Sound (see Figure 3.2). Stations were chosen along a transect through the center of the sound from the western shore to the eastern barrier islands and to the north along a transect of one of the feeder channels of the sound.

Cores or grab samples at each site were taken to complement PISPPI-2 insertion data. Grain size analyses and permeameter testing were conducted on

useable samples. Complete details of the testing are provided in Wetzel et al. (1994). Table 3.1 lists a summary of the test results.

3.3.3 Typical PISPPI-2 Probe Insertion Sequence

1.) The PISPPI-2 is initially calibrated in the laboratory before deployment, by setting the water level in the tube connected to the positive port equal to and then 70 cm above the water level in the negative port tube. The zero and span controls are adjusted accordingly until zero and then 70 cm register on the data logger for the two locations of positive-port water level.

2.) The PISPPI-2's tattletale computer was programmed in the field before deployment. Input parameters included time, date, sampling time delay, sampling interval, and sampling duration.

3.) At the first insertion site of the day the flexible rigid tubing is attached to the transducer positive port. The positive port, negative port, and tubing are subsequently filled with distilled water.

4.) The PISPPI-2 and attachments are lowered into the water and placed on the sediment surface (resting horizontally).

5.) The PISPPI-2 probe is filled with salt water from the sound and the sintered metal porous stone and tip is attached. Removing all air from the system is essential for accurate data collection, since air bubbles may cause zero shifts in pressure readings. This also assures that the density difference between the distilled and salt water is negligible over a small vertical distance. In turn, the probe is attached to the

flexible tubing.

6.) The probe is laid horizontally on the sediment surface adjacent to the PISPPI-2 for approximately five minutes. This enables the ports to sense the same pressure (head) to verify that the calibrated differential pressure is still zero. Adjustments to data can later be made if a zero shift is detected during this phase of testing.

7.) The galvanized 'T' insertion handle is placed over the probe's guide rod and used to insert the PISPPI-2 probe.

8.) The pressure response is monitored using a wire remote attached to the PISPPI-2 which displays the approximate pressure differential via an LCD display panel. Testing is complete when the pressure decays to an equilibrium value. Each test is given adequate time to obtain a true residual background pore pressure.

9.) Upon test completion, the probe is pulled from the sediment and laid horizontally on the sediment surface for approximately 5 minutes to check for zero drift and/or blockage of the screen with fine sediment; e.g. the differential pressure reading should be zero.

10.) The PISPPI-2 and probe were pulled from the water and transferred to the next test site where steps 5 through 9 were repeated. Care was taken to avoid drainage of the probe during transport.

11.) When testing was completed for the day, data was downloaded from the PISPPI-2 data logger computer to a PC. The data for each site included time from initiation of test and pressure response in the form of voltage signals. Voltage is converted to a pressure (head) value knowing the capacity of the transducer

diaphragm.

3.3.4 PISPPI-2 Field Insertion Data

Normalized pressure decay curves (Figures 3.3 to 3.33) correlated well with grain size analyses (Wetzel et al., 1994), typically decaying to equilibrium within 1 or 2 minutes in sands, and 30 minutes in silty or clayey sediments. Figure 3.34 shows three stations in a transect from coarser to finer sediments in Great Sound; the time to recover half of the maximum pressure (T_{50}) for the three stations was 15, 100, and 400 seconds. The corresponding range of hydraulic conductivity from laboratory permeameter tests (Wetzel et al., 1994) on core samples was $4 \cdot 10^{-4}$ to $2 \cdot 10^{-6}$ cm/sec. Figure 3.35 is a plot of T_{50} versus laboratory hydraulic conductivity for stations with core samples. Although a clear straight line fit cannot be depicted from the plot, an expected inverse relationship of T_{50} and hydraulic conductivity is evident.

3.3.5 PISPPI-2 Field Insertion Data Analysis

An empirical relationship was developed using laboratory hydraulic conductivity data from selected cores to provide an approach that does not require cores to be taken at each site.

Bredehoeft et al. (1980) present an analytical solution for the decay of pressure head caused by pressurizing the volume of water stored in a shut-in well. They use the concept of an equivalent casing radius, r_c, which is defined as the casing radius used for a traditional slug test (withdrawal/injection) that would result in the

same rate of decay as a pressurized test. The volume of water stored per vertical foot of casing in the conventional test is $\pi \cdot r_c^2$ whereas for the pressurized test it is $V_w C_w \rho_w g$ where V_w is the volume of water within the pressurized section of the system, C_w is the compressibility of water, ρ_w is the density of water and g is the gravitational acceleration. Setting the two volumes equal,

$$r_c^2 = V_w C_w \rho_w g / \pi \, . \qquad \textbf{Equation 3.1}$$

In other words, the compressed volume of water in the actual casing is equivalent to a radius of a thinner (fictitious) casing that would have the same decay rate using a traditional slug test.

The insertion of the PISPPI-2 probe causes a compressed volume of water and deformed soil outside the probe but limited to a narrow adjacent region. The sediment type and shear strength will affect the decay rate, and a theoretical analysis involving soil deformation and compressibility is required (Bennett et al., 1987). Also, finer cohesive sediments will act much differently than coarser non-cohesive sediments. Currently, the data taken as part of this investigation is being analyzed by others using a more theoretical approach.

The goal of this study was to determine if an empirical approach can be used to determine hydraulic conductivity. The Bredehoeft et al. (1980) approach is used to determine the value of r_c^2 (equivalent casing radius squared) that would be required to dissipate the head in the same time. If a reasonable correlation between r_c^2 and hydraulic conductivity is found, this approach can be used to determine hydraulic conductivity.

A semi-logarithmic plot of differential pressure head (logarithmic) versus time (arithmetic) was used to estimate the maximum initial pressure head differential between the positive and negative port; Hvorslev (1951) presents this type of plot as part of his simplistic analysis where he ignores compressibility of water and soil. The pressure head data is divided by the maximum initial pressure head to normalize the data, eliminating dependence of individual tests on peak pressures. A conventional curve matching procedure described by Bredehoeft et al. (1980) yields matchpoint values of t_m from the PISPPI-2 data and $(Tt/r_c^2)_m$ from Cooper et al.'s (1967) type curves for individual tests. For sites where laboratory permeameter hydraulic conductivity is known and using the inserted probe length (L=60 cm) as the pressurized interval, r_c^2 is obtained from the relation:

$$r_c^2 = t_m \cdot (L \cdot K_{lab})/(Tt/r_c^2)_m. \qquad \textbf{Equation 3.2}$$

A plot of r_c^2 versus hydraulic conductivity for sites with laboratory determined hydraulic conductivity is seen in Figure 3.36. An additional plot of K/r_c^2 versus hydraulic conductivity with a best fit line to the data is included in Figure 3.37.

For stations with a PISPPI-2 insertion test but no laboratory-determined hydraulic conductivity, Bredehoeft's et al. matching process is again followed. Values for $(Tt/r_c^2)_m$ and t_m are estimated from the type curves in Figure 3 of Cooper et al., (1967) and normalized observed data (Figures 3.3 to 3.33) respectively. Using the probe length as the pressurized interval, a value of K/r_c^2 is obtained from the relation:

$$K/r_c^2 = (Tt/r_c^2)_m/(t_m \cdot L). \qquad \textbf{Equation 3.3}$$

A value of hydraulic conductivity for the station sediment is obtained from the K/r_c^2 versus hydraulic conductivity best fit plot, Figure 3.37. An example of the matching process which essentially uses a best fit line to estimate r_c^2, is seen in Figure 3.38.

3.4 Conclusions

The empirical approach developed in this study yields estimated hydraulic conductivities expected to be as reliable as Bennett et at. (1987) more detailed theory, but without requiring a consolidation test at each site. Using the best fit plot of Figure 3.37 results in approximately a factor of 5.5 deviation for stations with laboratory determined hydraulic conductivities deemed to be well within the order of magnitude of accuracy typically cited for slug tests. The deviation occurs due to assumptions such as the storage properties for a given hydraulic conductivity value are consistent from site to site.

Future testing will verify the best fit line of Figure 3.37 by providing data for hydraulic conductivities in the range of $1 \cdot 10^{-4}$ to $3 \cdot 10^{-6}$ cm/s.

4. Estimate of Groundwater/ Surface Water Exchange

4.1 Estimate of Residual Pore Pressures

Residual pore pressures are estimated using data from PISPPI insertion tests. Observed data from Section 3.3.3, Step 6, is compared to the background pore pressure obtained in Step 8. The residual pore pressure is evaluated as the difference of the means of the two readings. An example of apparent residual head in PISPPI-2 raw observed pressure dissipation curves is seen in Figure 4.1.

Note that six of the test sites showed significant excess pressure heads (over 5 cm) in Great Sound, mostly near the shore where excess groundwater levels are expected and where the lower hydraulic conductivity inhibits the flow and can cause higher heads. Estimated flux based on hydraulic conductivity and hydraulic gradient are also provided in Table 3.1. Other raw observed pressure decay curves are included in Wetzel et al. (1994).

4.2 Groundwater and Surface Water Exchange

The water exchange is estimated using D'Arcy's law:

$$v = - K \cdot (dh/dl) \qquad \text{Equation 4.1}$$

where v is the D'Arcy velocity (flow per unit surface area) in the vertical direction, K is the hydraulic conductivity, and dh/dl is the vertical hydraulic gradient with v and K expressed in consistent units (Todd, 1980). Many assumptions are inherent in this procedure, including that the discharge is assumed to be vertical under the sound, that lower permeability layers are not present to inhibit flow, and that the hydraulic conductivity determined is accurately determined from the empirical technique and

is representative of the horizontal value. Each of these assumptions should be examined in more detail and verified independently if possible. In summary, using the hydraulic conductivity value determined from either the water extraction device or the PISPPI device with the residual pore pressure will yield an estimate for groundwater flux. A negative residual pressure results in flow from the surface into the sediment, and vice-versa.

5. Summary and Recommendations

5.1 Summary

The goal of this project was to develop methods for the in situ determination of hydraulic conductivity of surficial sediments. The procedures or instruments were required to be non-permanent, non-time consuming, inexpensive, and portable. The two methods tested were a water extraction instrument and an insertion instrument (PISPPI-2).

The methods developed in this study are supplemental to existing methods which are more appropriate for greater depths. The techniques do not estimate hydraulic conductivities and hydraulic gradients at greater depths, but rather only in the shallow surficial sediment near the test apparatus. Hydraulic gradients are assumed to be vertical, therefore care must be taken to properly infer groundwater flux from the test results.

The water extraction instrument was used as a miniature slug test. The type curves of Figure 2.23 indicate that the water extraction device is not highly dependent on the storage coefficient so its value is difficult to determine. Fortunately, it is not an important parameter for calculating flux rates. Sediment with hydraulic conductivities $< 5 \cdot 10^{-4}$ require extensive testing times for water extractions. For that reason, the water extraction device is recommended for sediment with hydraulic conductivities $\geq 5 \cdot 10^{-4}$ cm/sec. Estimated values of hydraulic conductivity varied by a factor of only 2.2 when compared to laboratory permeameter determined hydraulic conductivity values used in this study.

The PISPPI-2 analysis uses an empirical approach to estimate the hydraulic conductivity by including the compressibility effects of water and soil. Originally, additional probes inserted previously into the sediment (analogous to observation wells) were to be used to help identify hydraulic conductivity. The alternate technique developed here is not as theoretically sound as other pressure decay analyses, but its simplicity and reliability are attractive. Future tests which improve the best fit plot in Figure 3.37 will determine its usefulness. Estimated hydraulic conductivities from this analysis method vary by a factor of only 5.5 compared to laboratory permeameter determined hydraulic conductivities.

Results from this study demonstrate the usefulness and need for further investigation of both techniques.

5.2 Recommendations

Although the water extraction device is recommended for use with coarser sediment, it can be used to estimate hydraulic conductivities in finer sediment. A prematurely-terminated slug test resulting in a partial head recovery curve can provide adequate estimates of hydraulic conductivity

A longer PISPPI-2 insertion probe is recommended for determining residual heads in coarser sediments so that a higher excess head can be measured. The coarse sediment cannot maintain a large head gradient over the length of the probe due to its high permeability, unlike finer sediments that were shown to maintain heads of up to 10 cm. Although head gradients are large in fine sediments, the

groundwater flux may be negligible due to the low hydraulic conductivity. Identifying hydraulic gradients in coarse sediment would result in a measurable groundwater flux.

Future testing should be conducted to verify the best fit line of Figure 3.37. Verifying the line will indicate the test method's usefulness in future studies.

The empirical technique used in this study was the first method developed to analyze PISPPI-2 pressure decay responses. Future testing should require a more theoretical approach of analysis. Development of type curves similar to the water extraction device using MODFLOW is recommended for future investigations.

Tables

SITE	SETUP	SCREEN INSERTION DEPTH [cm]	MATCHPOINT		PERMEAMETER HYDRAULIC CONDUCTIVITY [cm/sec]	TYPE CURVE HYDRAULIC CONDUCTIVITY [cm/sec]
			TYPE CURVE Kt/r [1/cm]	OBSERVED DATA Time, [sec]		
1	FnRb	13.5	1.00	155.0	(3.5-7.7)E-3	6.84E-3
2	FnRb	13.5	1.00	160.0	(3.5-7.7)E-3	6.63E-3
3	FRb	13.5	0.47	63.0	(3.5-7.7)E-3	7.91E-3
4	FRb	13.5	1.00	138.0	(3.5-7.7)E-3	7.69E-3
5	FRf	13.5	1.00	134.0	(3.5-7.7)E-3	7.92E-3
6	FRf	13.5	1.00	130.0	(3.5-7.7)E-3	8.16E-3
7	FnRf	13.5	1.00	116.0	(3.5-7.7)E-3	9.15E-3
8	FRb	15.5	0.47	103.0	(2.7-3.5)E-3	4.84E-3
9	FRb	17.5	-	-	-	-
10	FRb	15.5	0.40	520.0	(2.7-3.5)E-3	8.16E-3

Table 2.1 Water Extraction Device Summary.

STATION	T 50 (sec.)	GRAIN ANALYSIS	LABORATORY HYDRAULIC CONDUCTIVITY (cm/sec.)	INTERPRETABLE RAW RESPONSE	RESIDUAL HEAD (cm)	INTERPRETED HYDRAULI CONDUCTIVITY FROM CURVE MATCH (cm/sec.)	GOUNDWATER FLUX INTO GREAT SOUND (cm/sec.)
10-23-93							
1	9.0	x	(2.3-13.0)E-4	x		8.0E-5	
2	2.1	x	(5.3-20.0)E-4			-	
3	-	x				-	
4	35.0			x		2.0E-05	
5	44.0			x		2.0E-7	
6	33.0			x		4.0E-7	
7	64.0			x	-3.9	2.0E-7	-7.8E-7
8	59.0	x				2.0E-5	
9	81.0	x		x		2.0E-7	
10	96.0	x		x		3.0E-7	
11	54.0				+5.1	7.0E-8	+3.6E-7
12	52.0	x		x	+6.5	3.0E-7	+2.0E-6
13	119.0	x				7.0E-8	
14	4.0	x		x	+6.2	1.0E-4	+6.2E-4
15	7.5	x		x	+6.2	2.0E-3	+1.2E-2
16	54.5	x		x	+24.4	5.0E-7	+1.2E-5
17	20.3	x		x	+5.1	2.0E-4	+1.0E-3
18	14.0			x	+5.2	5.0E-5	+2.6E-4
19	85.0			x	+24.3	9.0E-6	+2.2E-4
20	75.0	x			+10.3	2.0E-7	+2.1E-6
21	39.0	x		x	+6.2	1.0E-7	+6.2E-7
6-1-94							
22	128.0	x	(14.0-9.0)E-5	x		2.0E-6	
23a	2.0	x	(1.7-4.3)E-4			7.0E-5	
23b	4.9	x		x			
23c	6.3	x		x			
23d	6.3	x		x			
23e	11.6	x		x			
24	101.0	x	2.4E-7	x		6.0E-6	
25	396.0	x	1.6E-6	x		2.0E-7	
26	133.0	x	2.1E-7	x	+6.7	5.0E-6	+3.4E-7
30	14.6	x	(3.6-1.6)E-4	x		6.0E-4	
31	31.6	x	5.6E-4	x		7.0E-5	
32	34.0	x	(5.1-3.6)E-4	x		2.0E-6	
33	36.0	x		x		-	
				x			

Table 3.1 PISPPI-2 Summary and Estimate of Groundwater Flux.

Figures

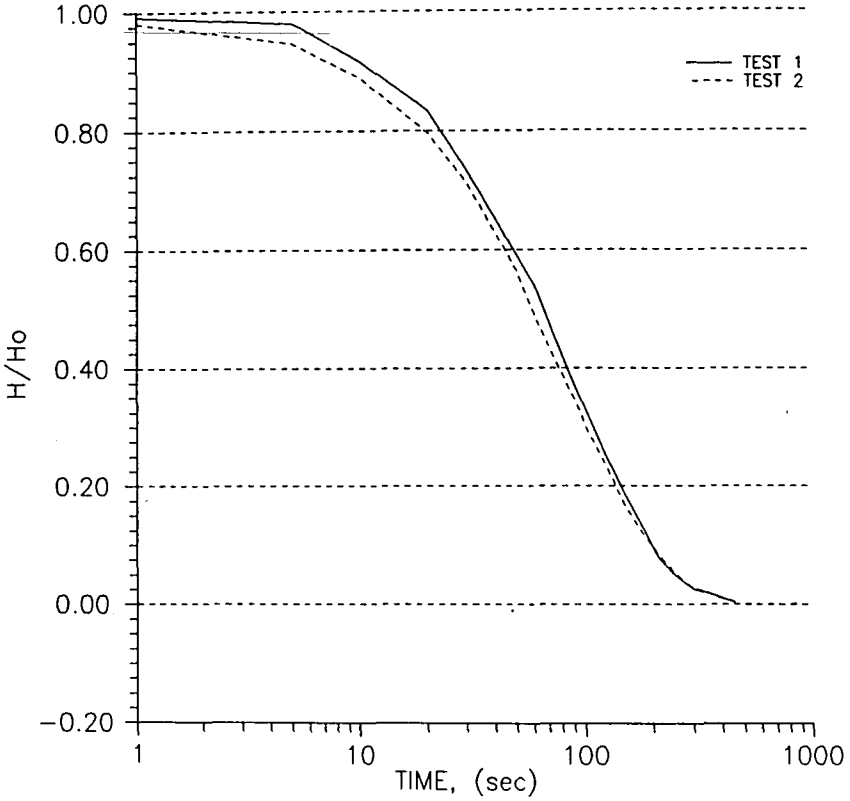

Figure 2.1 Normalized Observed Laboratory Water Extraction Device Data (Semi-logarithmic Scale).

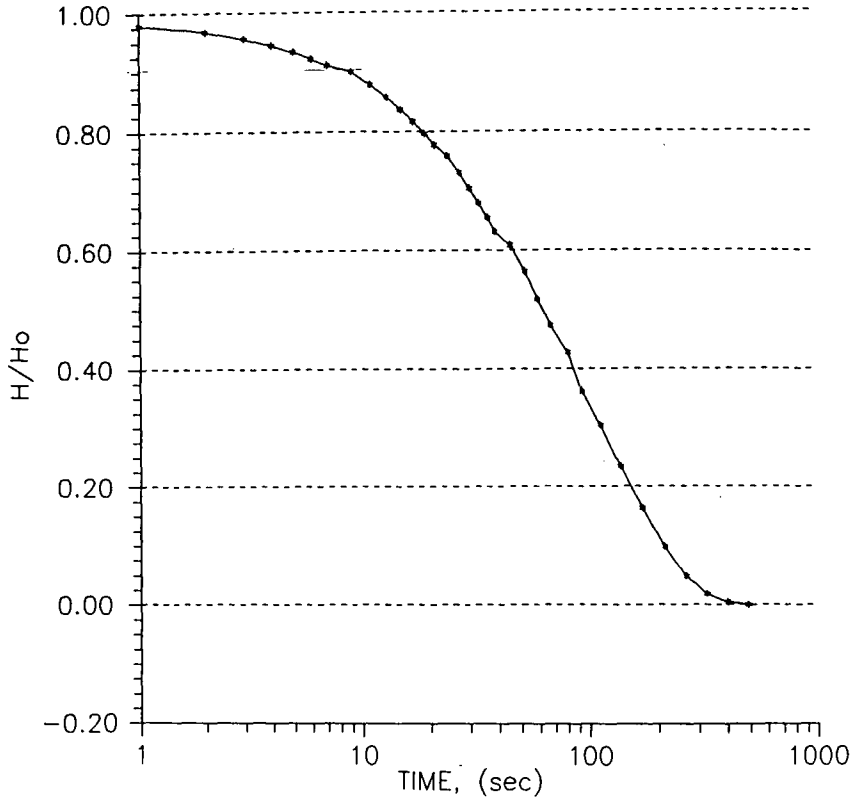

Figure 2.2 MODFLOW Laboratory Simulated Water Extraction (Semi-logarithmic Scale).

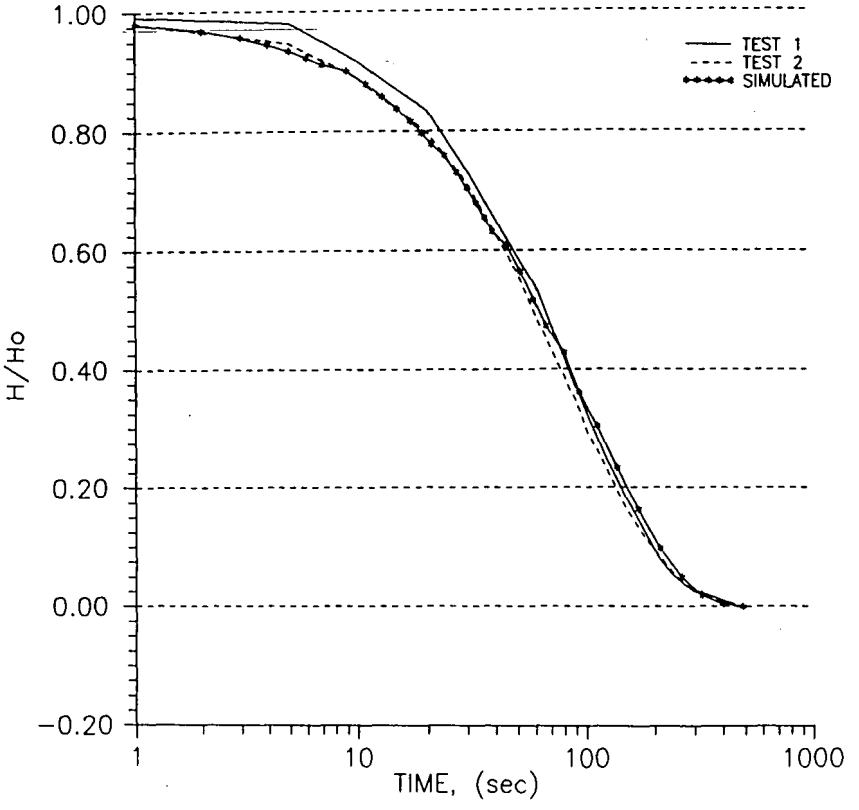

Figure 2.3 MODFLOW Simulated - Observed Laboratory Water Extraction Comparison (Semi-logarithmic Scale).

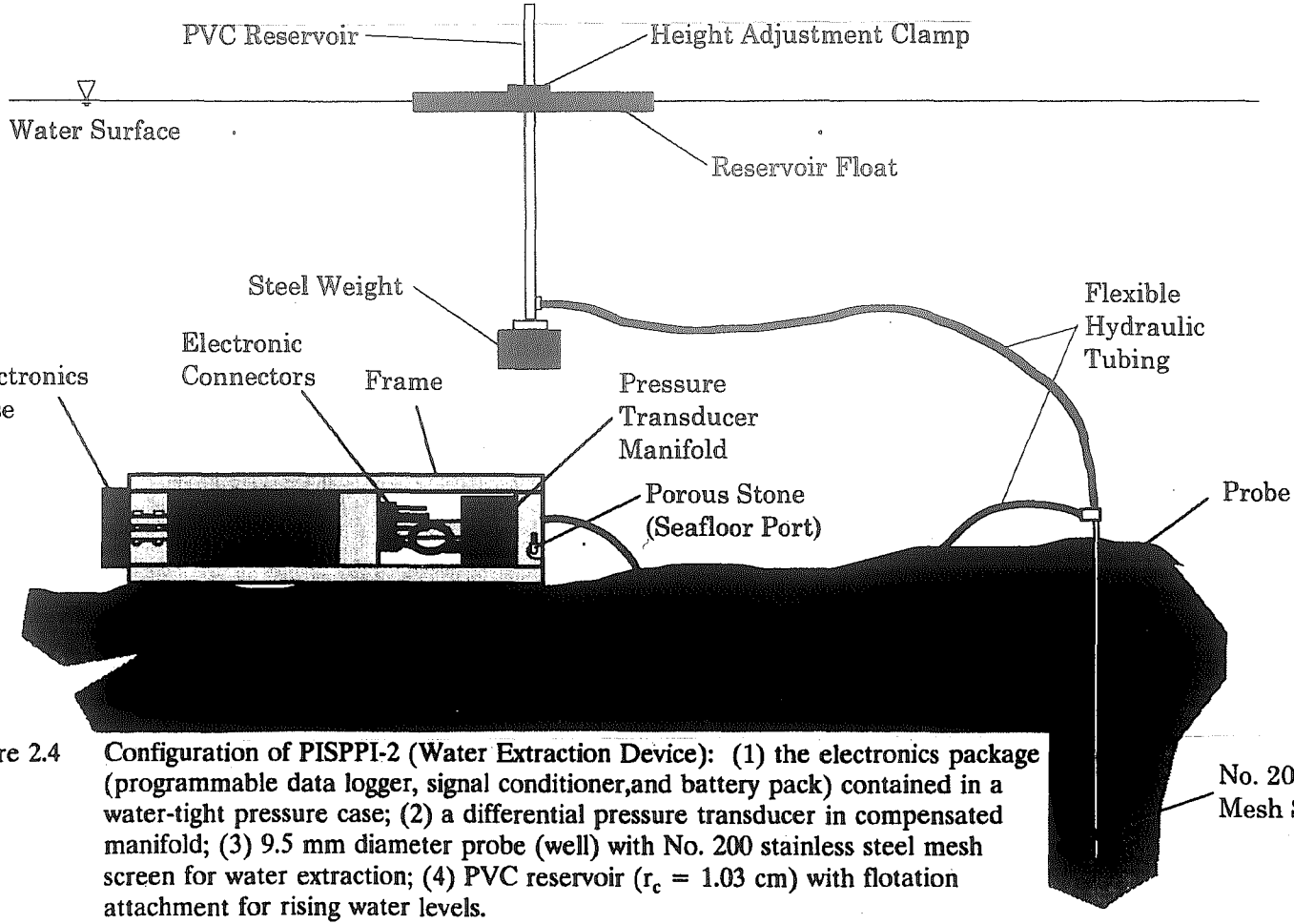

Figure 2.4 **Configuration of PISPPI-2 (Water Extraction Device): (1) the electronics package (programmable data logger, signal conditioner,and battery pack) contained in a water-tight pressure case; (2) a differential pressure transducer in compensated manifold; (3) 9.5 mm diameter probe (well) with No. 200 stainless steel mesh screen for water extraction; (4) PVC reservoir (r_c = 1.03 cm) with flotation attachment for rising water levels.**

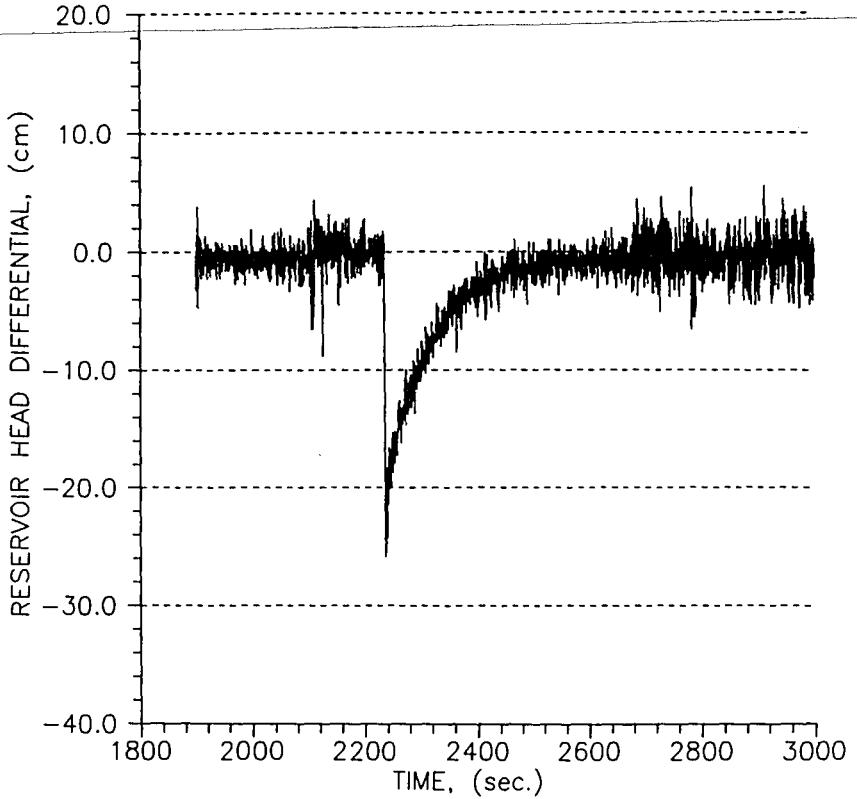

Figure 2.5 Site 1, Test Mode 1, Raw Observed Field Water Extraction Data.

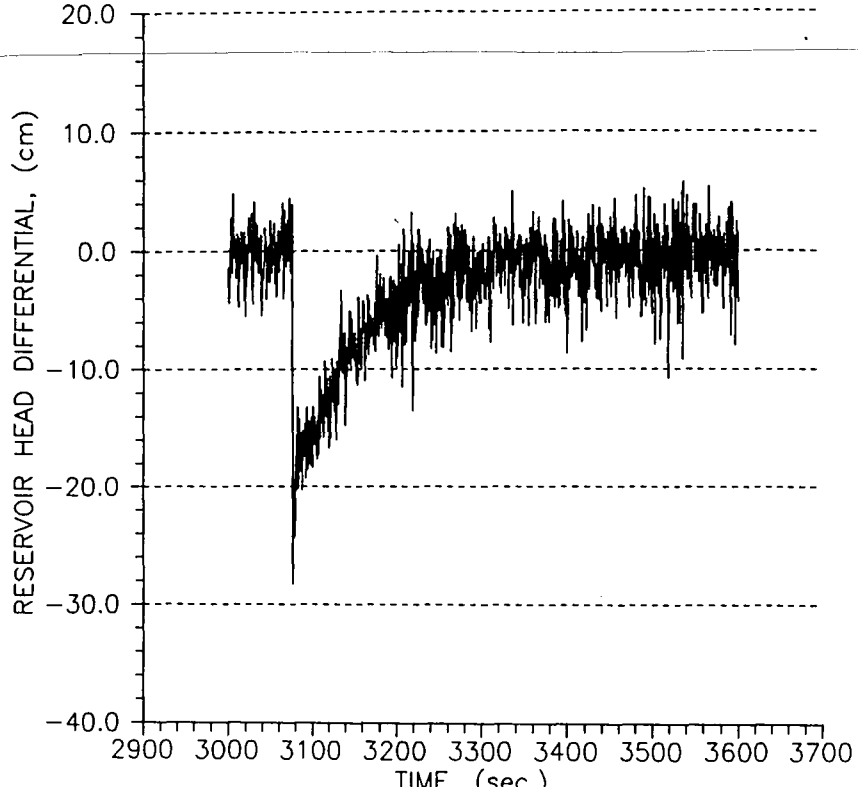

Figure 2.6 Site 2, Test Mode 1, Raw Observed Field Water Extraction Data.

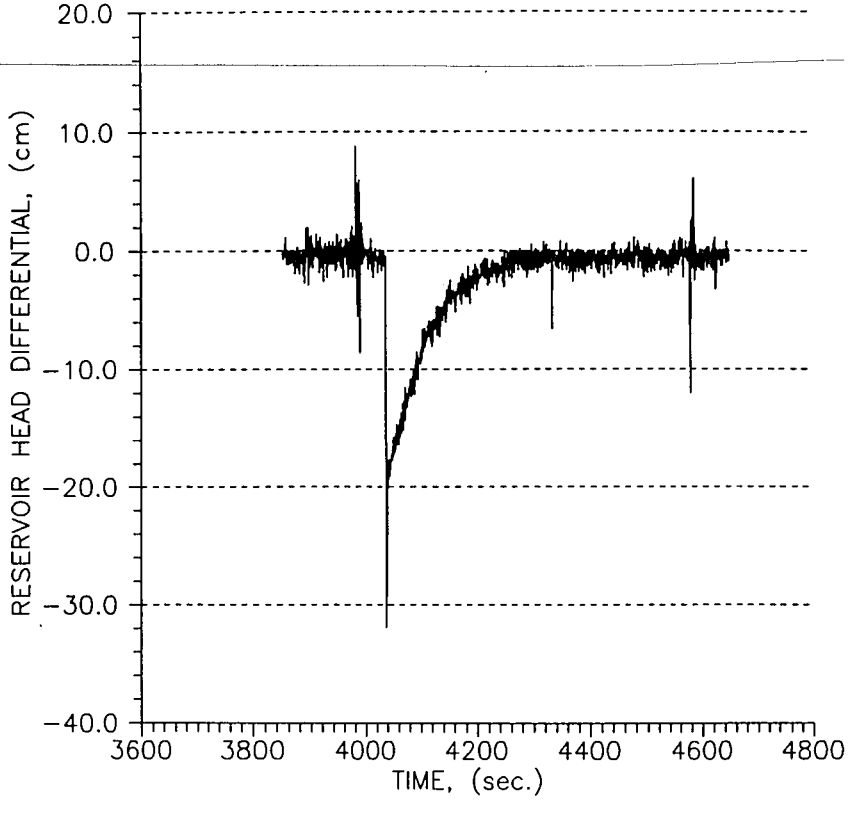

Figure 2.7 Site 3, Test Mode 2, Raw Observed Field Water Extraction Data.

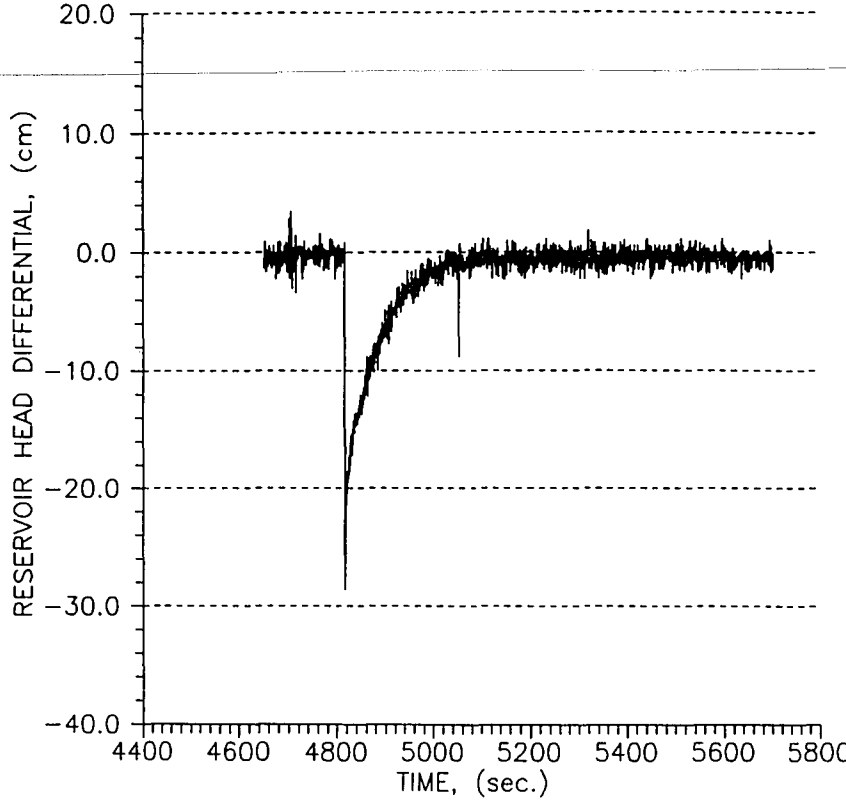

Figure 2.8 Site 4, Test Mode 2, Raw Observed Field Water Extraction Data.

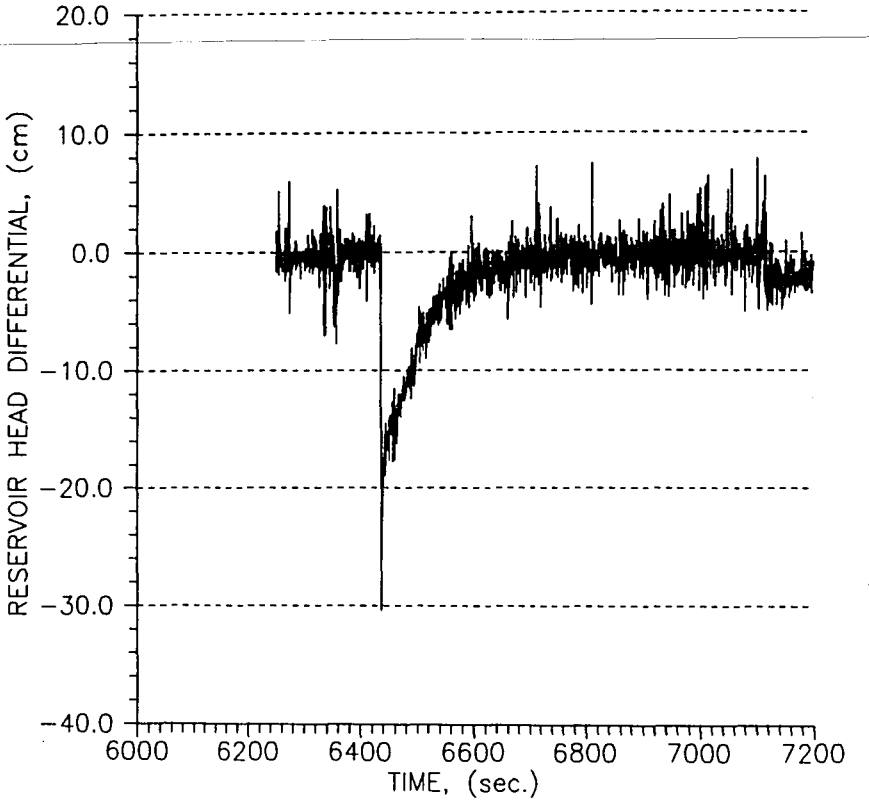

Figure 2.9 Site 5, Test Mode 4, Raw Observed Field Water Extraction Data.

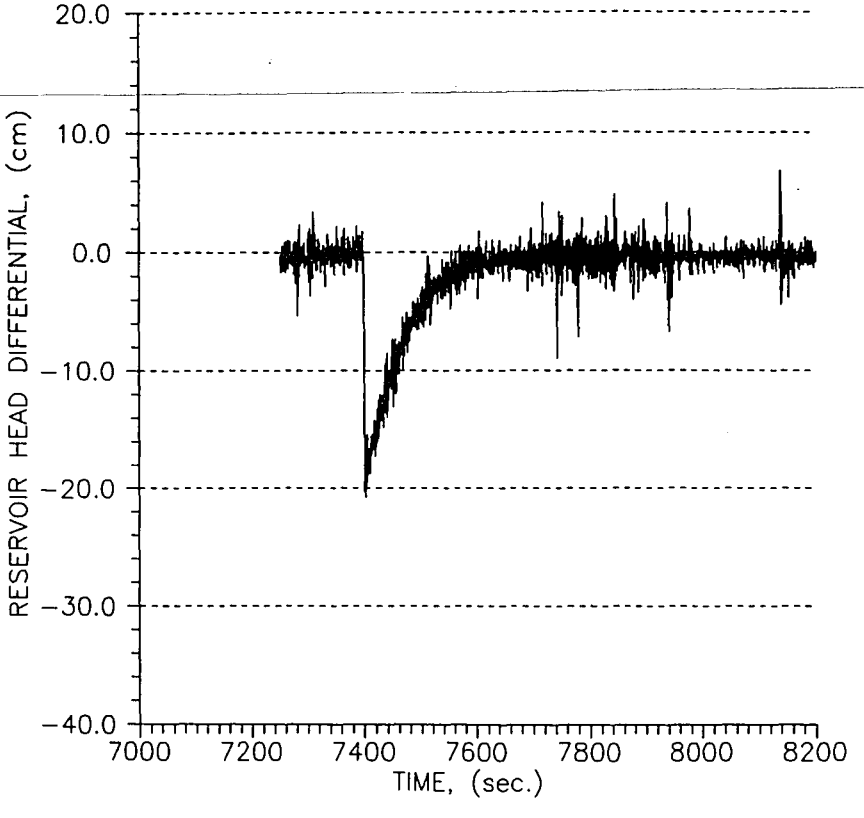

Figure 2.10 Site 6, Test Mode 4, Raw Observed Field Water Extraction Data.

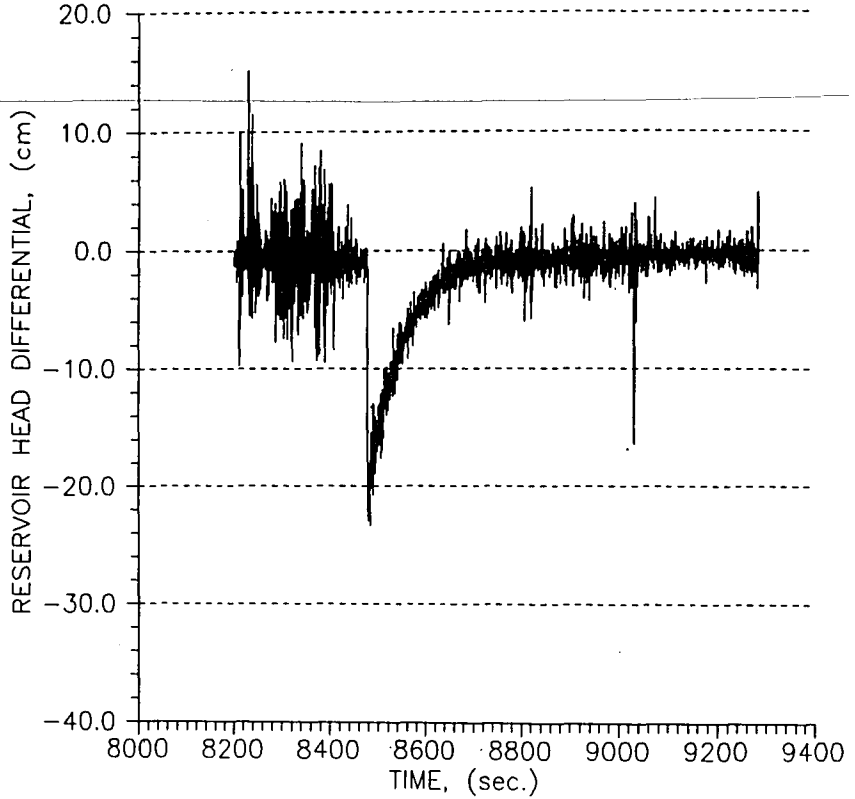

Figure 2.11 Site 7, Test Mode 3, Raw Observed Field Water Extraction Data.

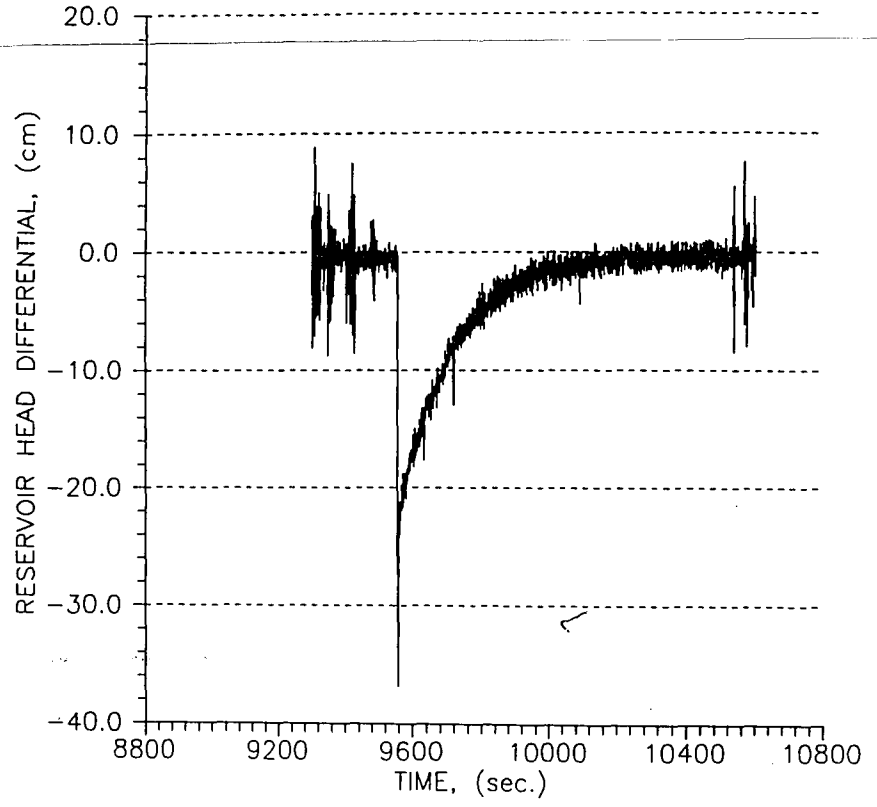

Figure 2.12 Site 8, Test Mode 1, Raw Observed Field Water Extraction Data.

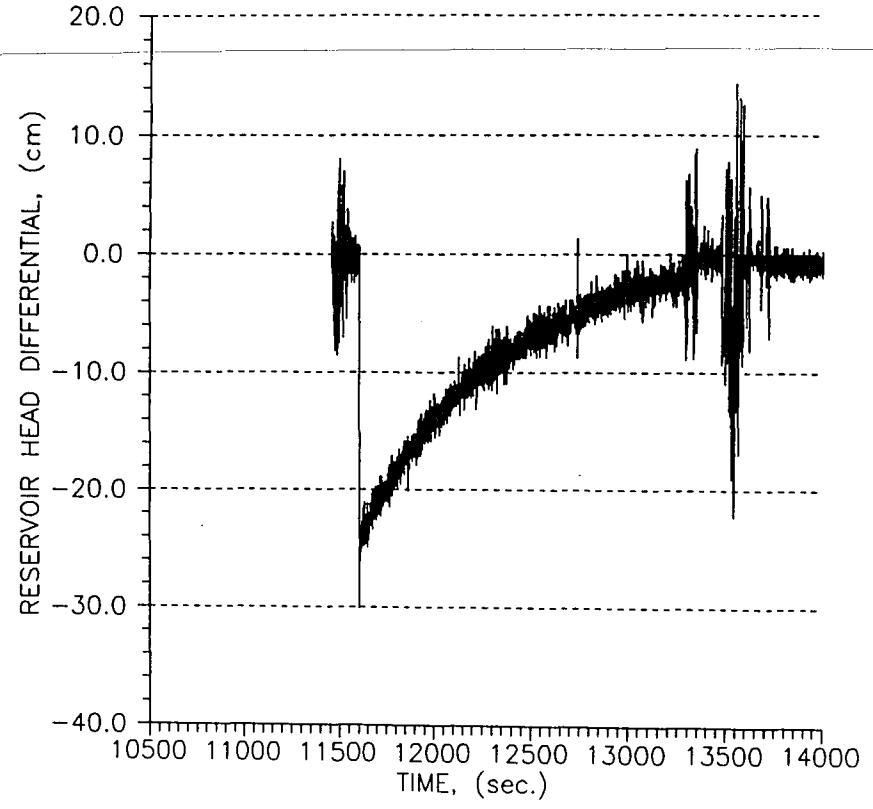

Figure 2.13 Site 10, Test Mode 1, Raw Observed Field Water Extraction Data.

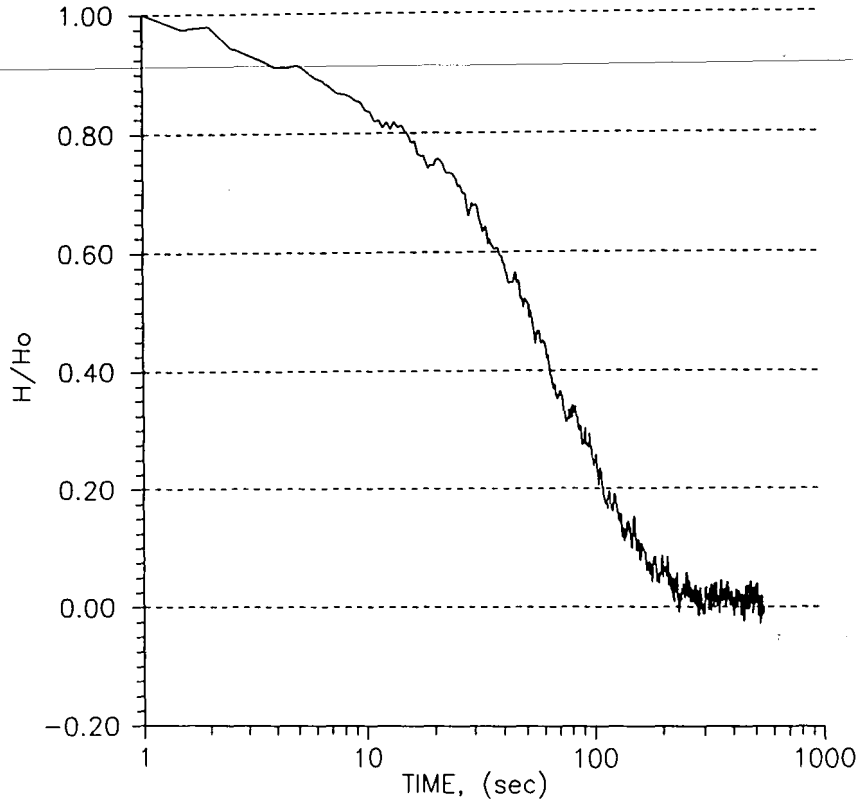

Figure 2.14 Site 1, Normalized Observed Field Water Extraction Data (Semi-logarithmic Scale).

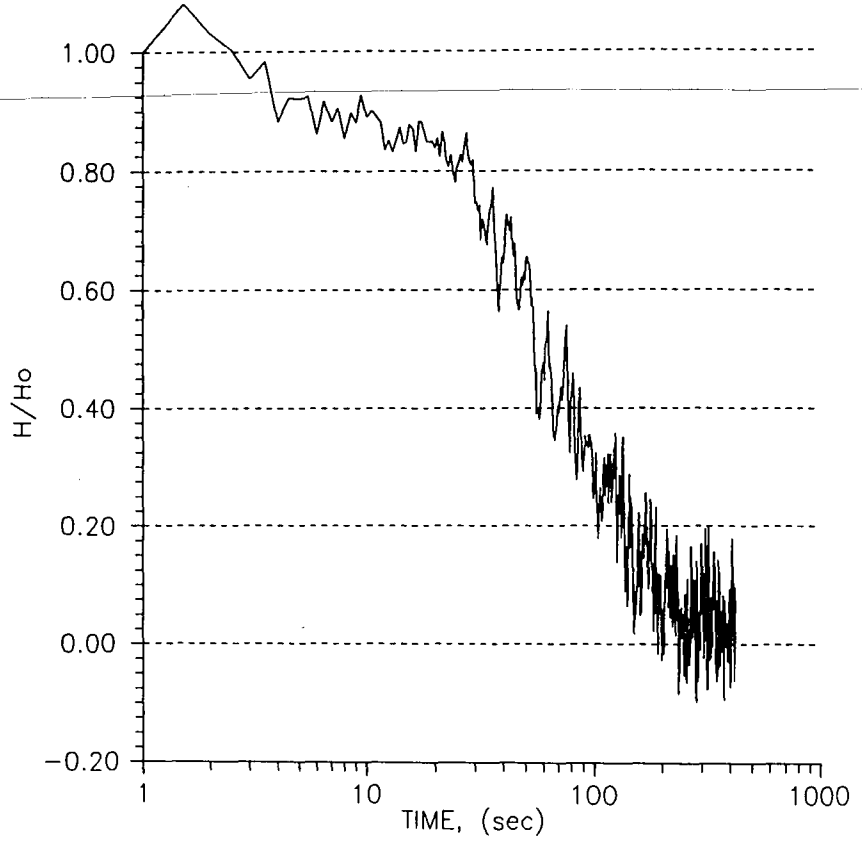

Figure 2.15 Site 2, Normalized Observed Field Water Extraction Data (Semi-logarithmic Scale).

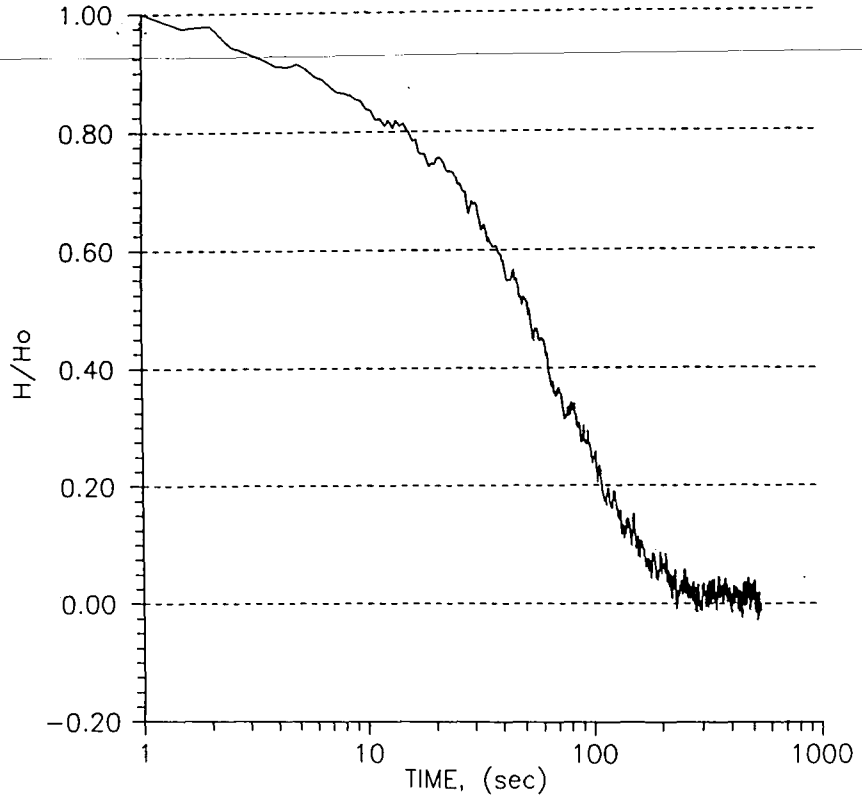

Figure 2.16 Site 3, Normalized Observed Field Water Extraction Data (Semi-logarithmic Scale).

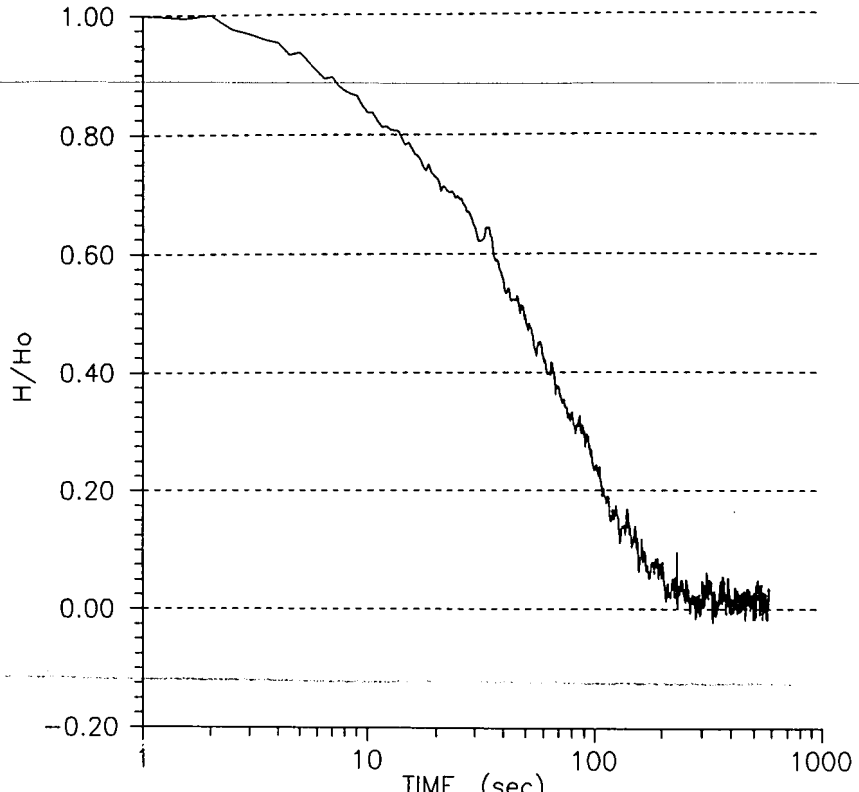

Figure 2.17 Site 4, Normalized Observed Field Water Extraction Data (Semi-logarithmic Scale).

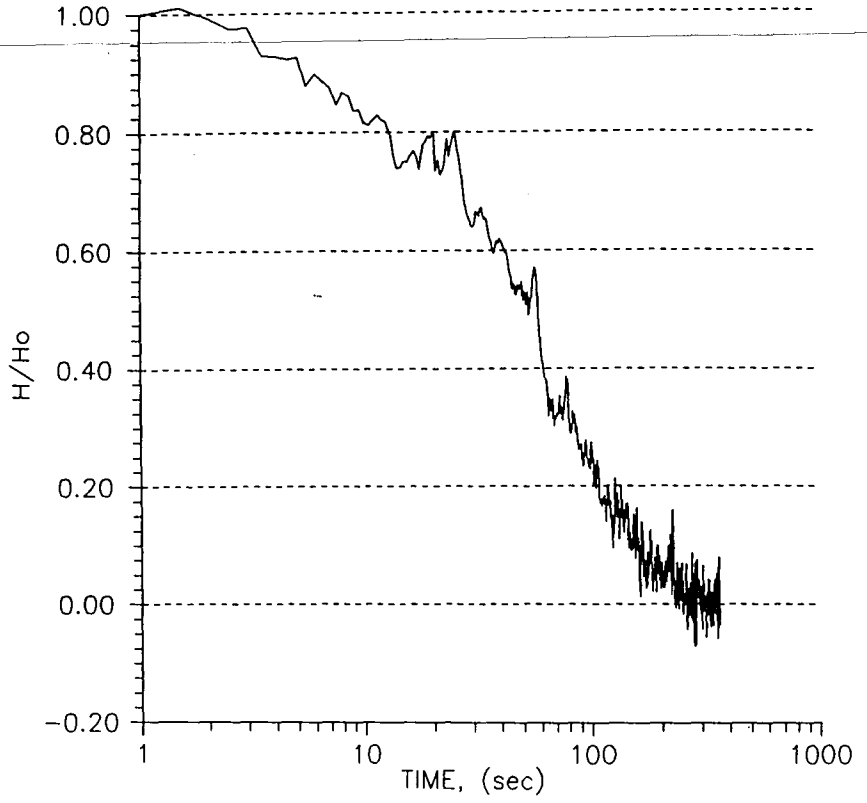

Figure 2.18 Site 5, Normalized Observed Field Water Extraction Data (Semi-logarithmic Scale).

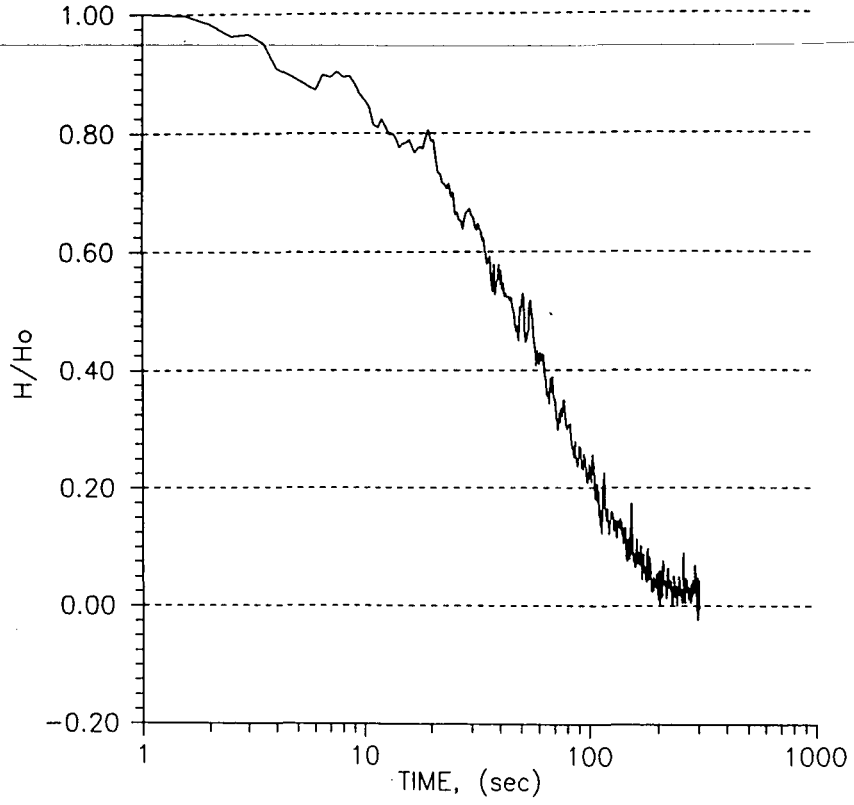

Figure 2.19 Site 6, Normalized Observed Field Water Extraction Data (Semi-logarithmic Scale).

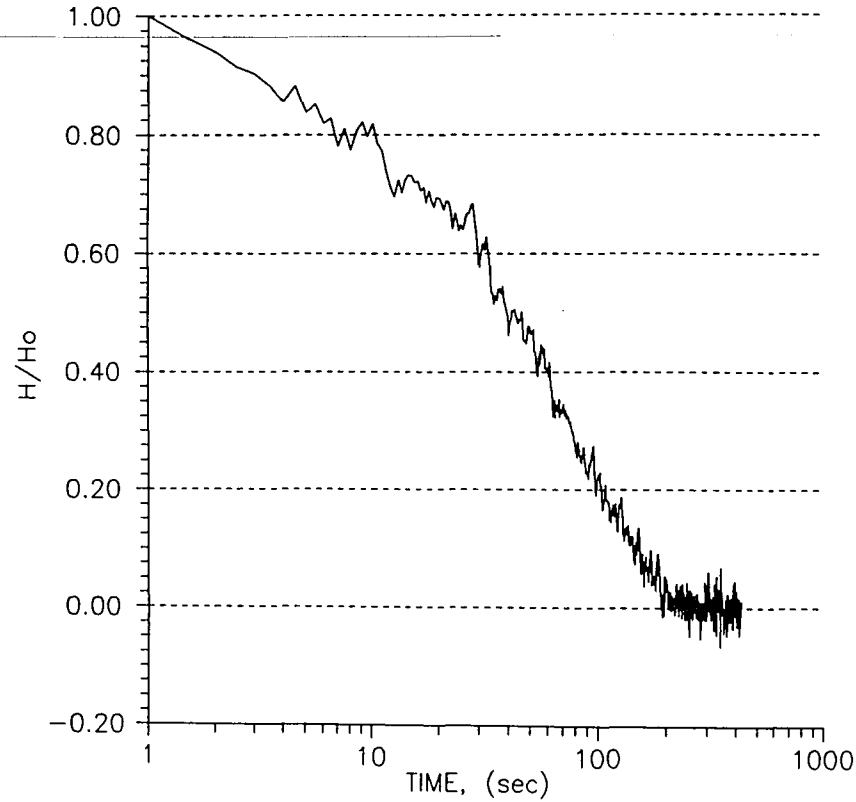

Figure 2.20 Site 7, Normalized Observed Field Water Extraction Data (Semi-logarithmic Scale).

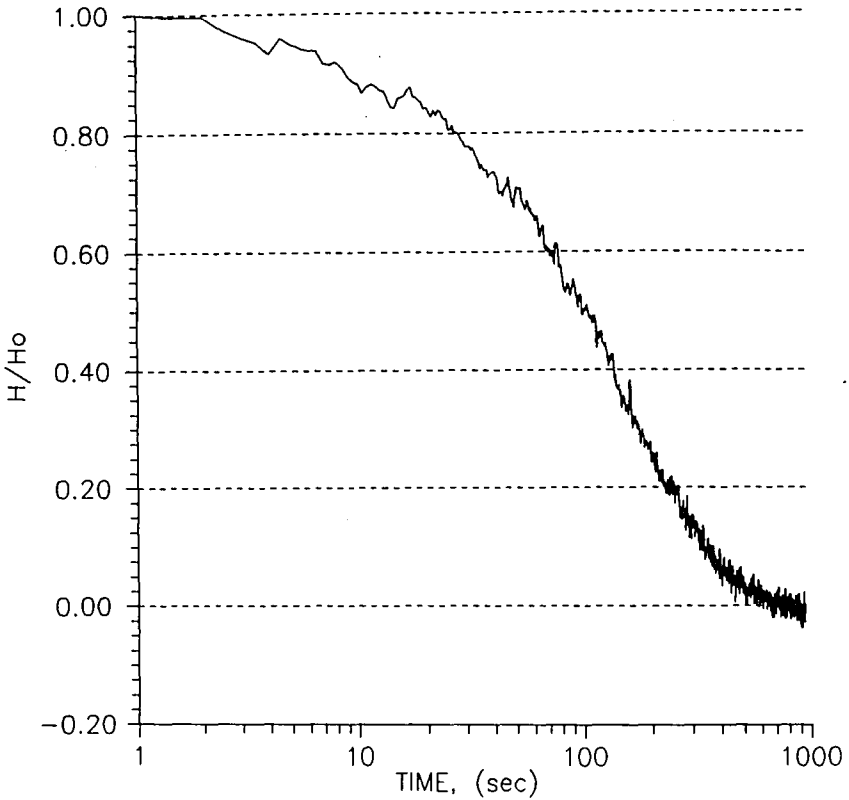

Figure 2.21 Site 8, Normalized Observed Field Water Extraction Data (Semi-logarithmic Scale).

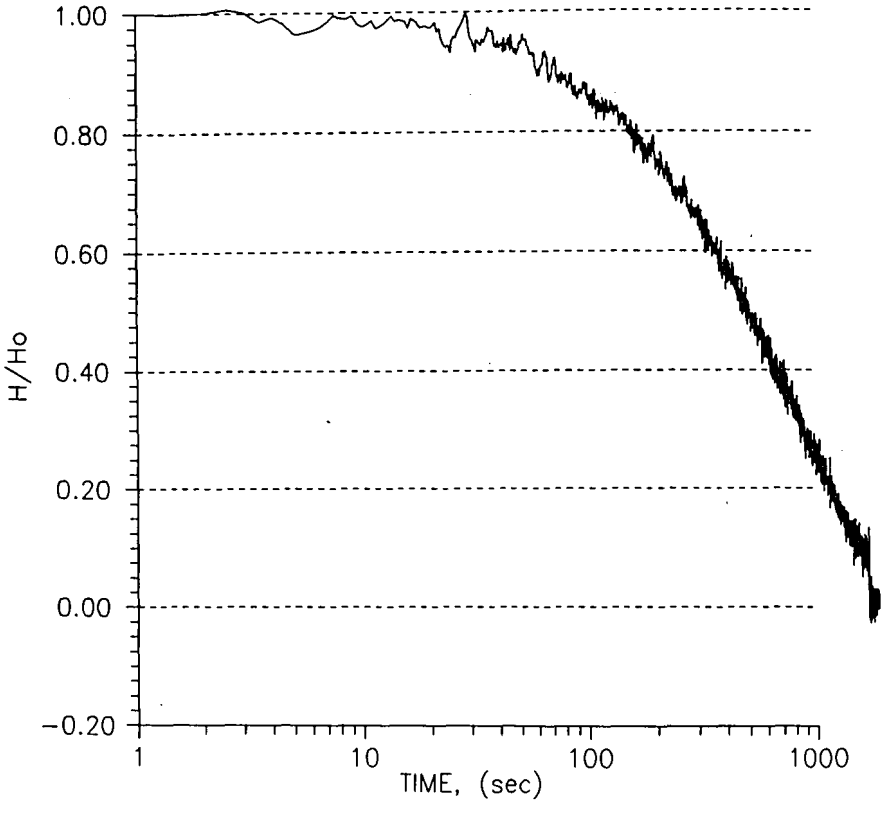

Figure 2.22 Site 10, Normalized Observed Field Water Extraction Data (Semi-logarithmic Scale).

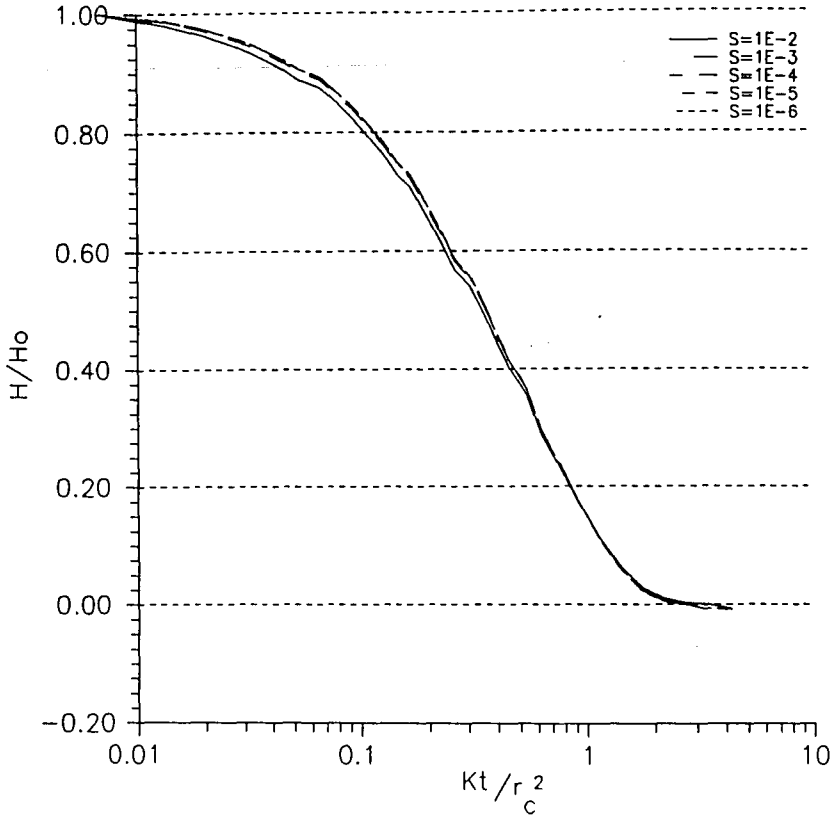

Figure 2.23 Normalized MODFLOW Field Simulated Water Extraction Type Curves (Semi-logarithmic Scale).

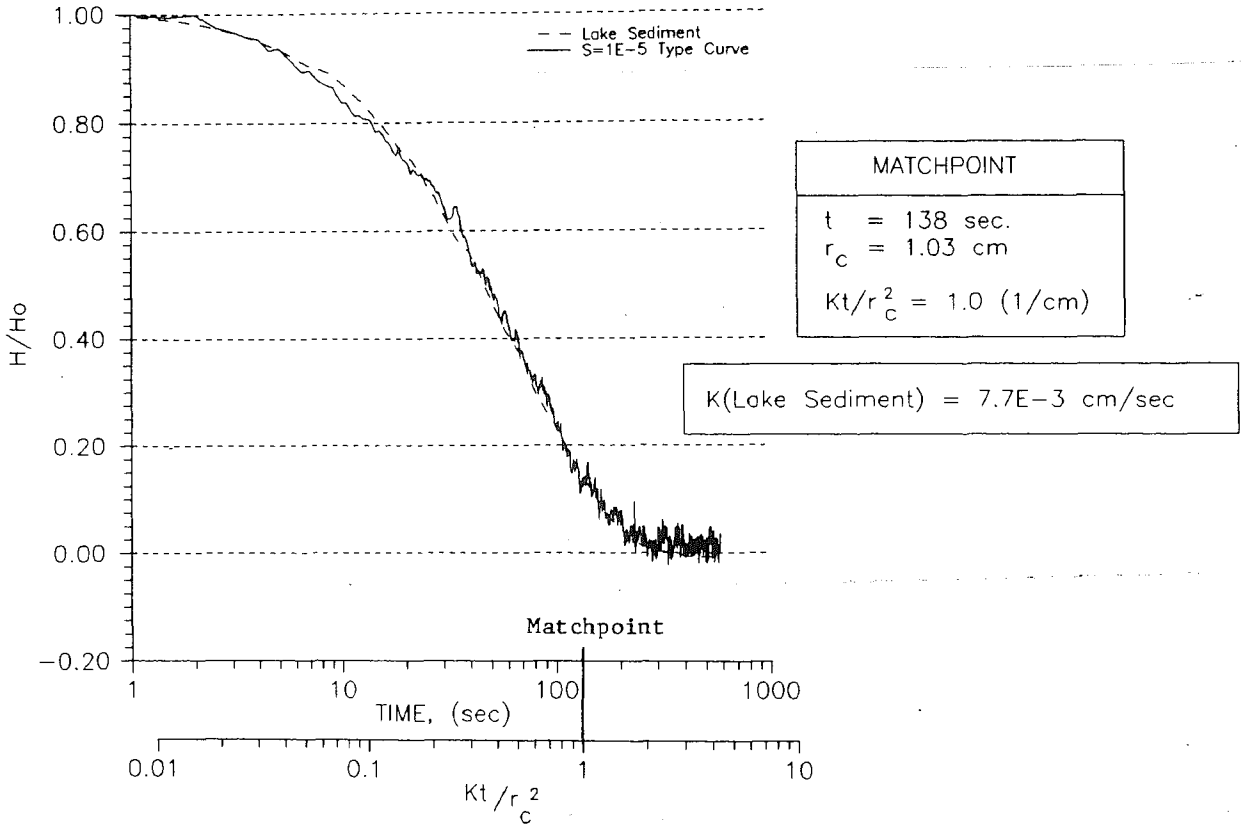

Figure 2.24 Match of the Silty-Sand Observed Field Extraction (slug) Test Response Curve (solid line) with the $S = 1 \cdot 10^{-5}$ Type Curve from Figure 2.23 (dotted line).

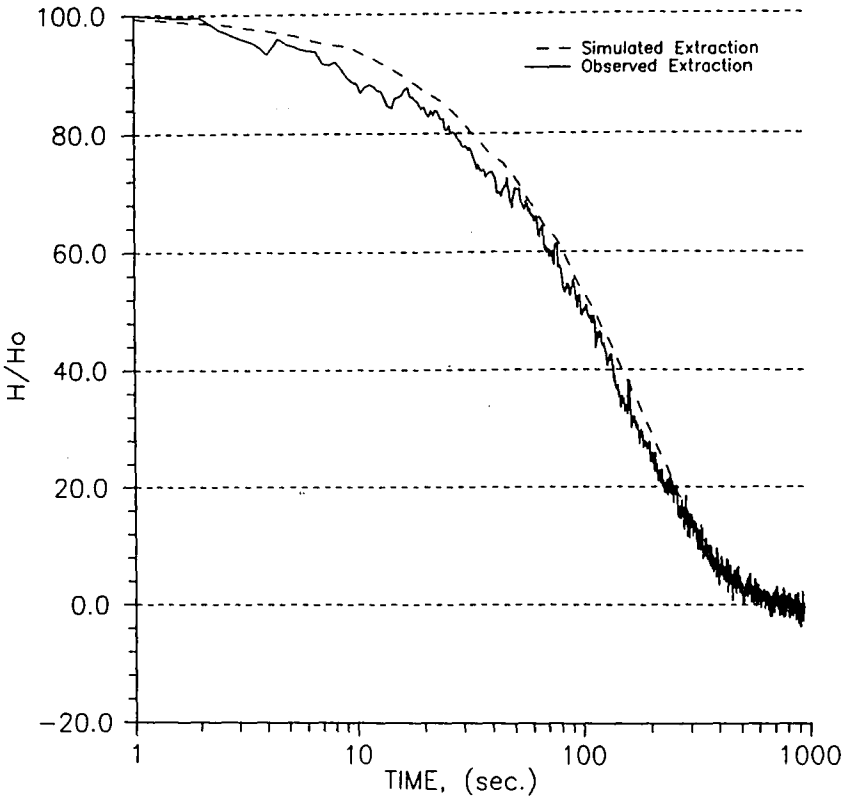

Figure 2.25 MODFLOW Simulated - Observed Field Water Extraction of Beltzville Layered Sediment.

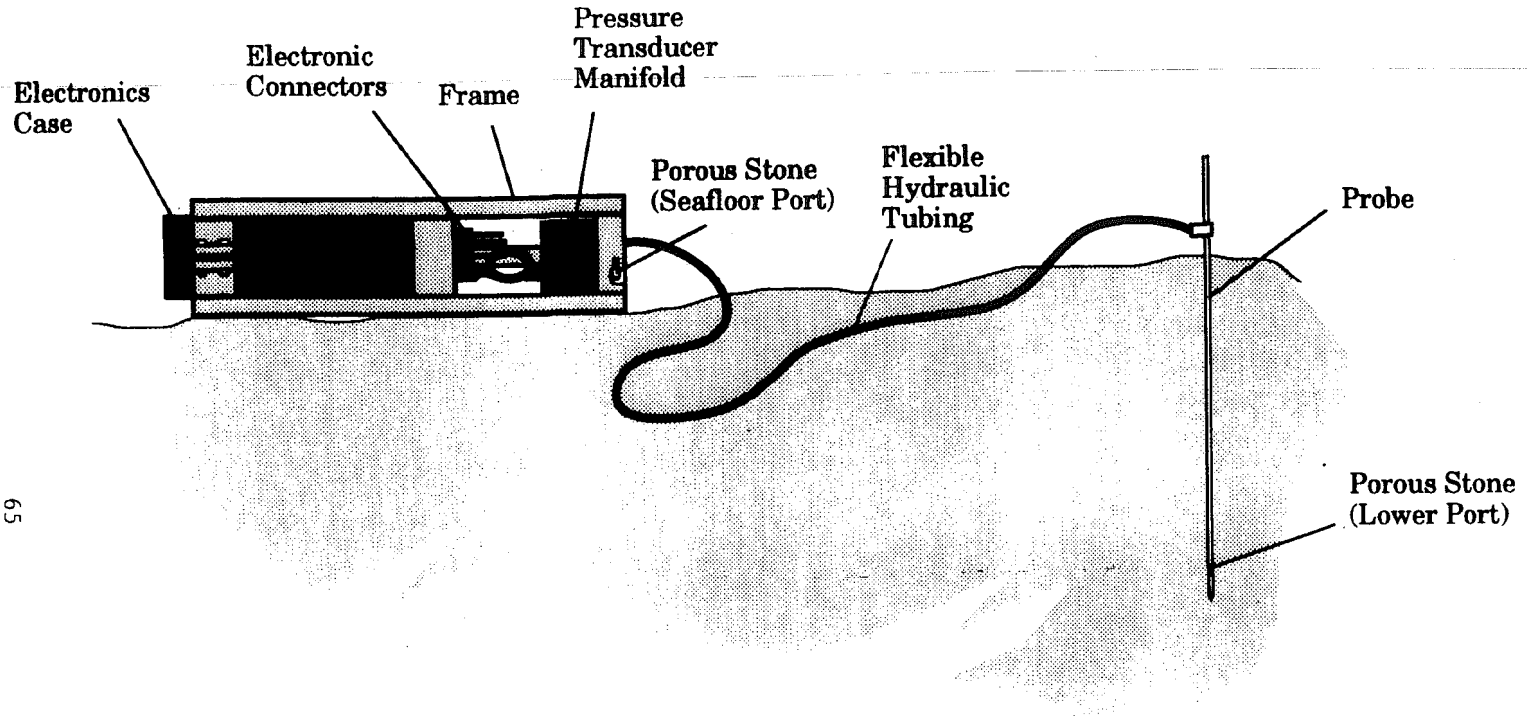

Figure 3.1 Configuration of the PISPPI-2 (Pressure Pulse Technique): (1) the electronics package (programmable data logger, signal conditioner, and battery pack) contained in a water-tight pressure case; (2) a differential pressure transducer in compensated manifold; (3) the 9.5 mm diameter probe on the end of flexible hydraulic tubing.

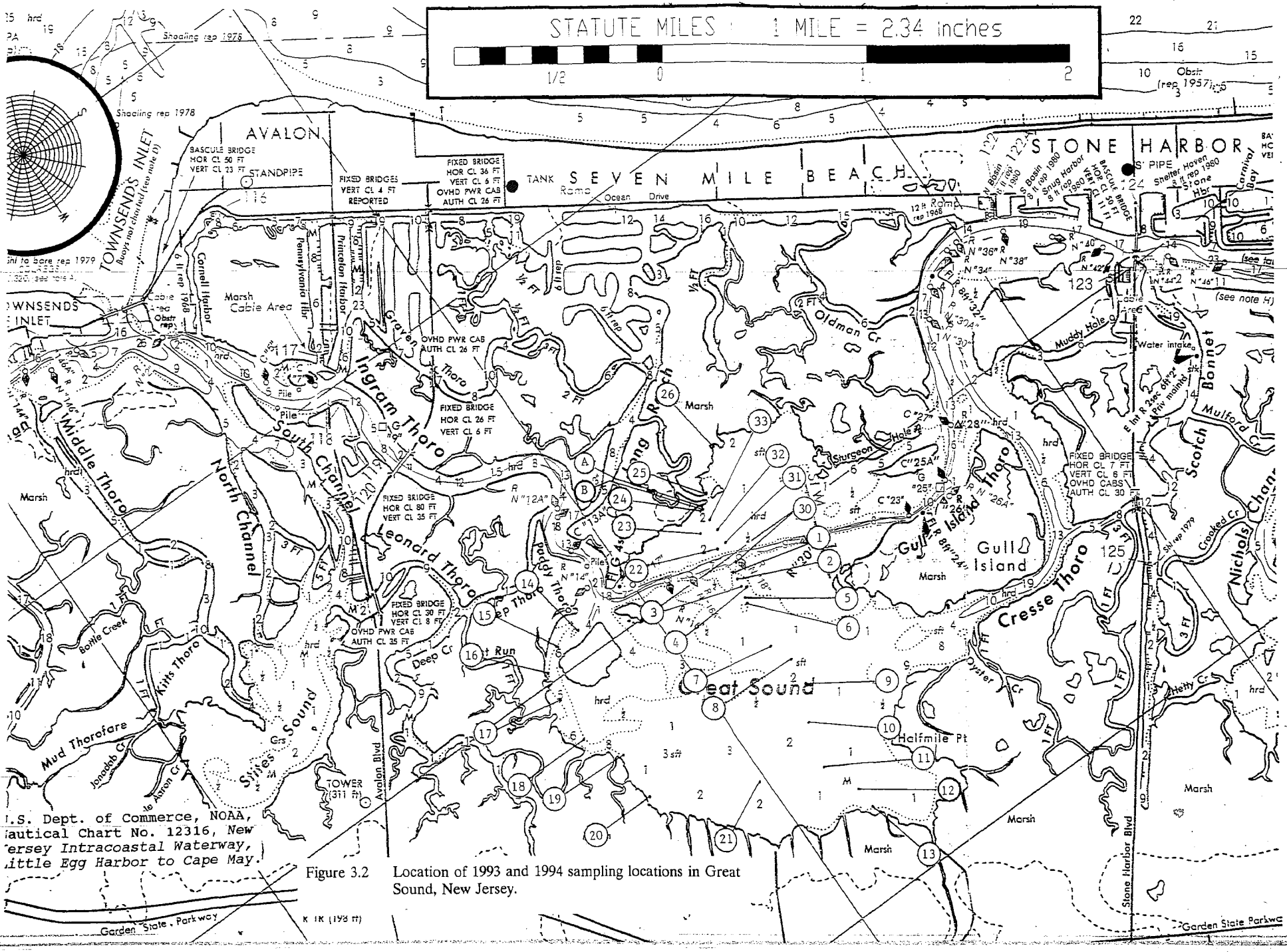

U.S. Dept. of Commerce, NOAA, Nautical Chart No. 12316, *New Jersey Intracoastal Waterway, Little Egg Harbor to Cape May.*

Figure 3.2 Location of 1993 and 1994 sampling locations in Great Sound, New Jersey.

STATION 1

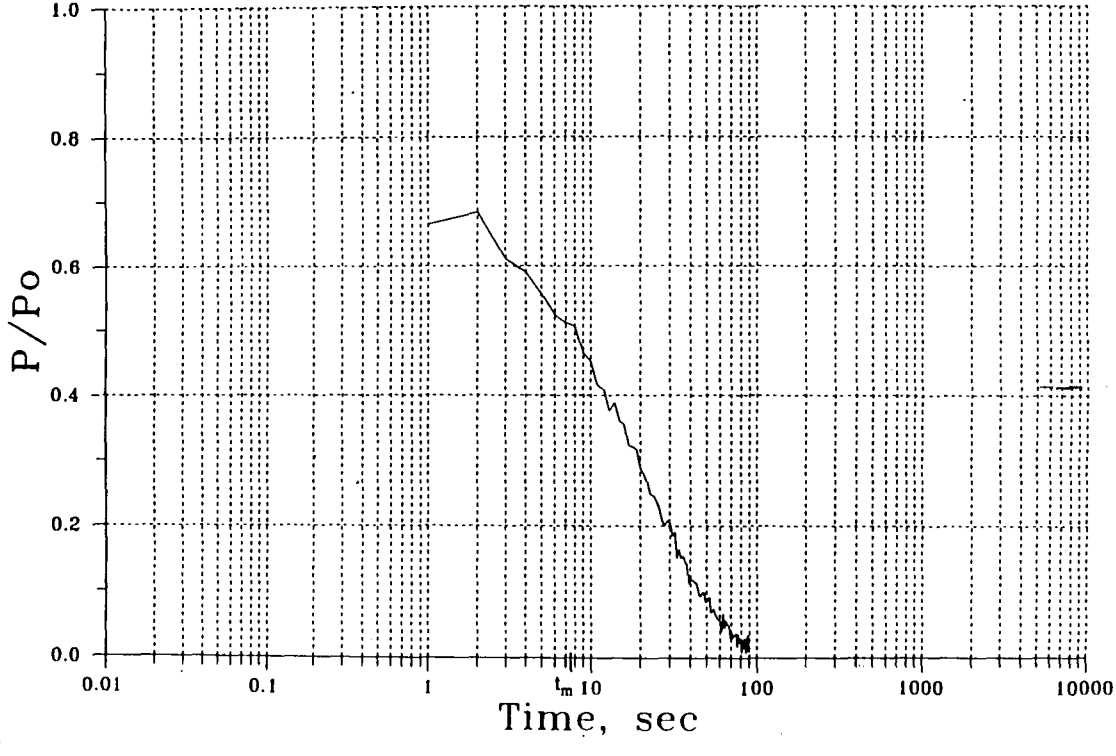

Figure 3.3 Normalized Observed Field Pressure Decay Curve, Station 1.

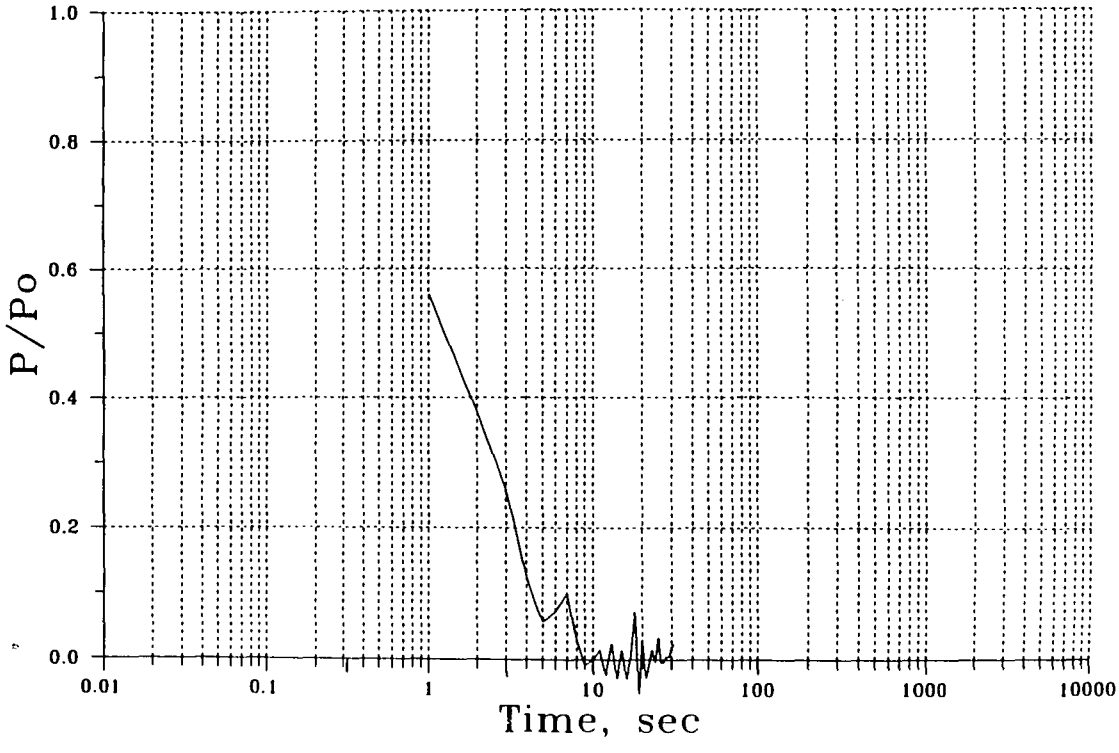

Figure 3.4 Normalized Observed Field Pressure Decay Curve, Station 2.

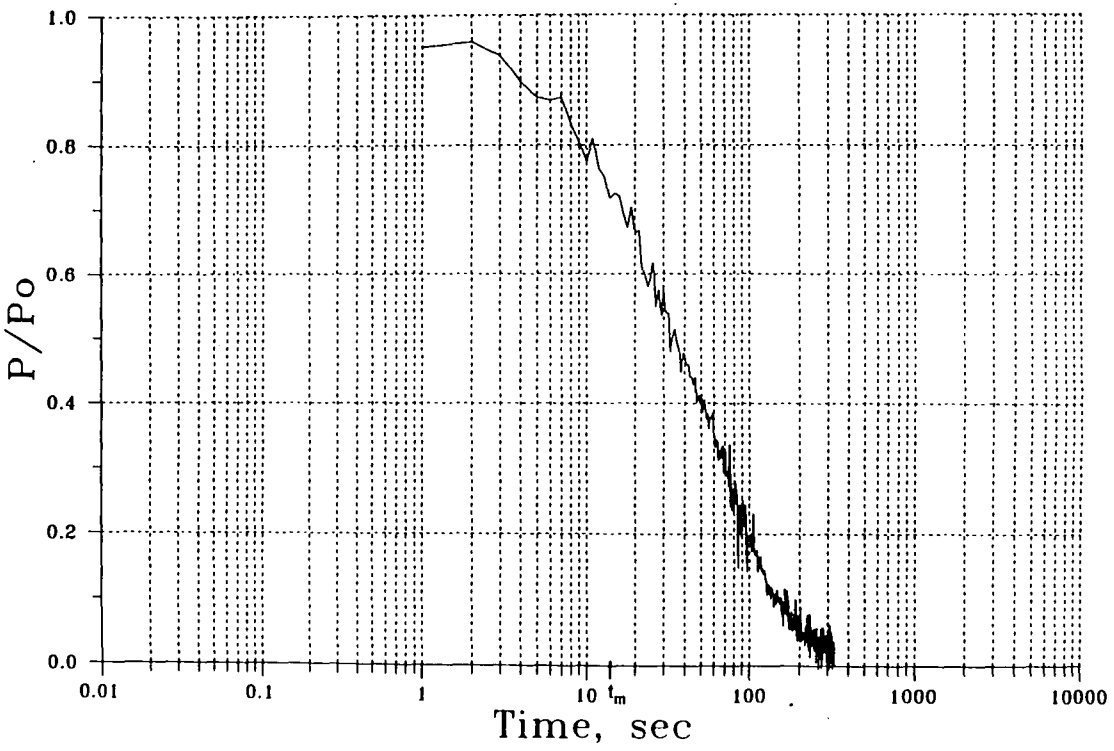

Figure 3.5 Normalized Observed Field Pressure Decay Curve, Station 4.

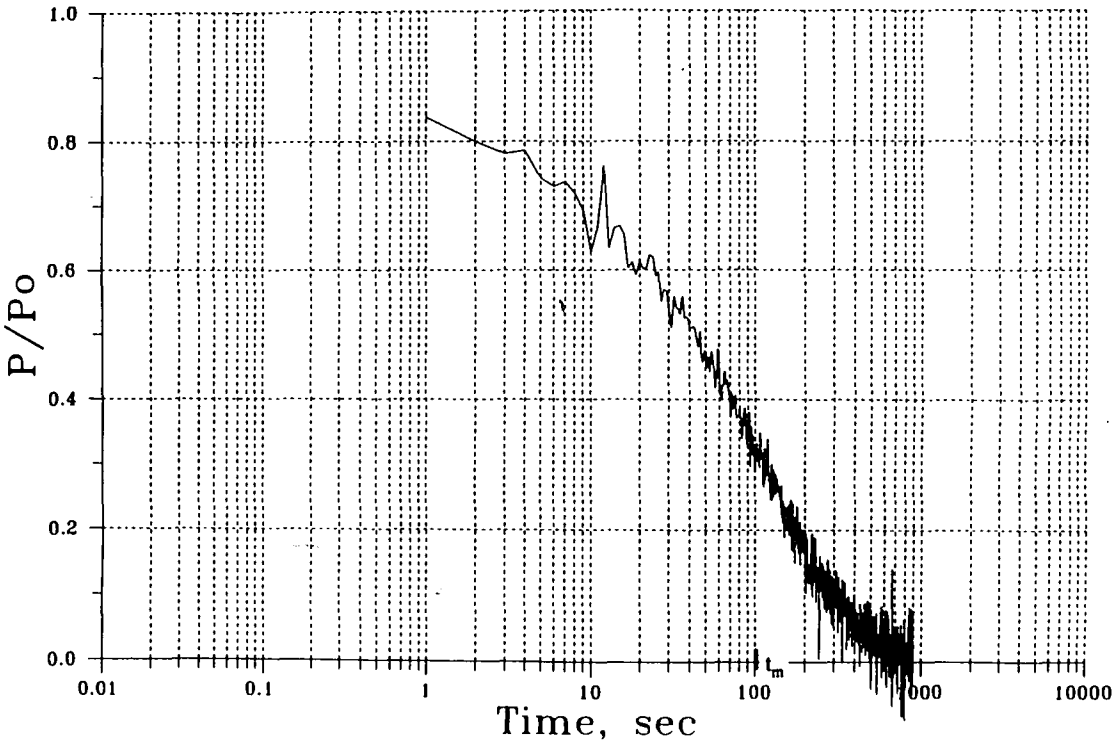

Figure 3.6 Normalized Observed Field Pressure Decay Curve, Station 5.

STATION 6

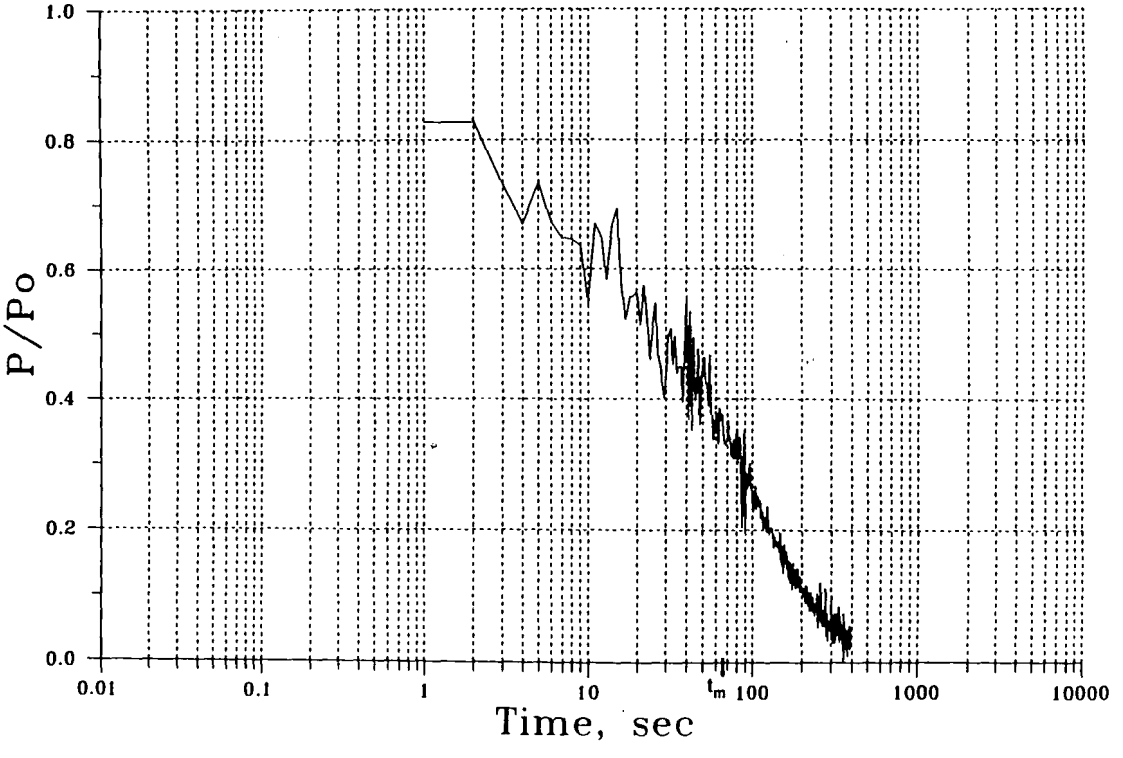

Figure 3.7 Normalized Observed Field Pressure Decay Curve, Station 6.

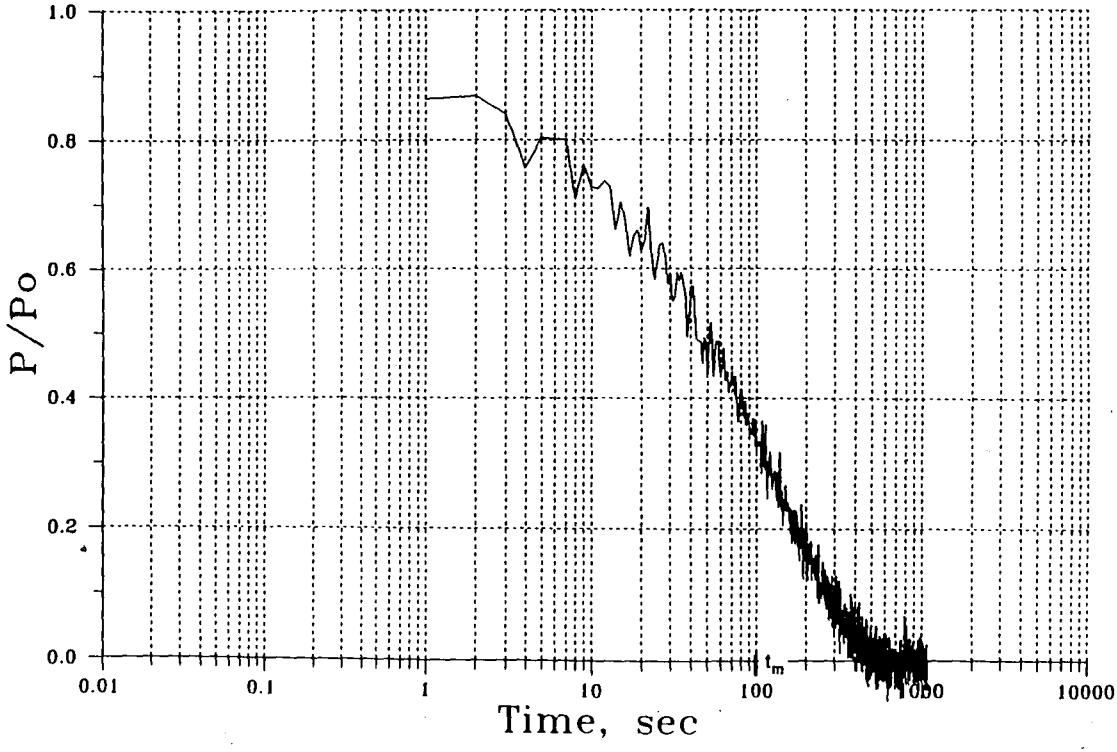

Figure 3.8 Normalized Observed Field Pressure Decay Curve, Station 7.

STATION 8

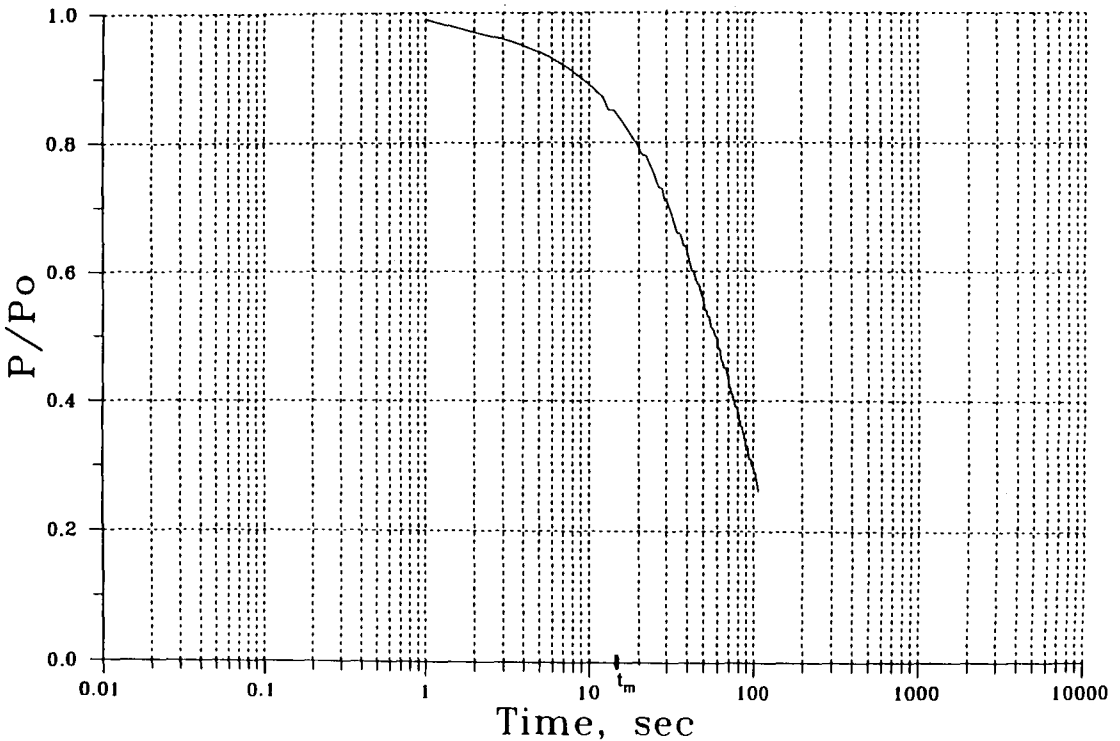

Figure 3.9 Normalized Observed Field Pressure Decay Curve, Station 8.

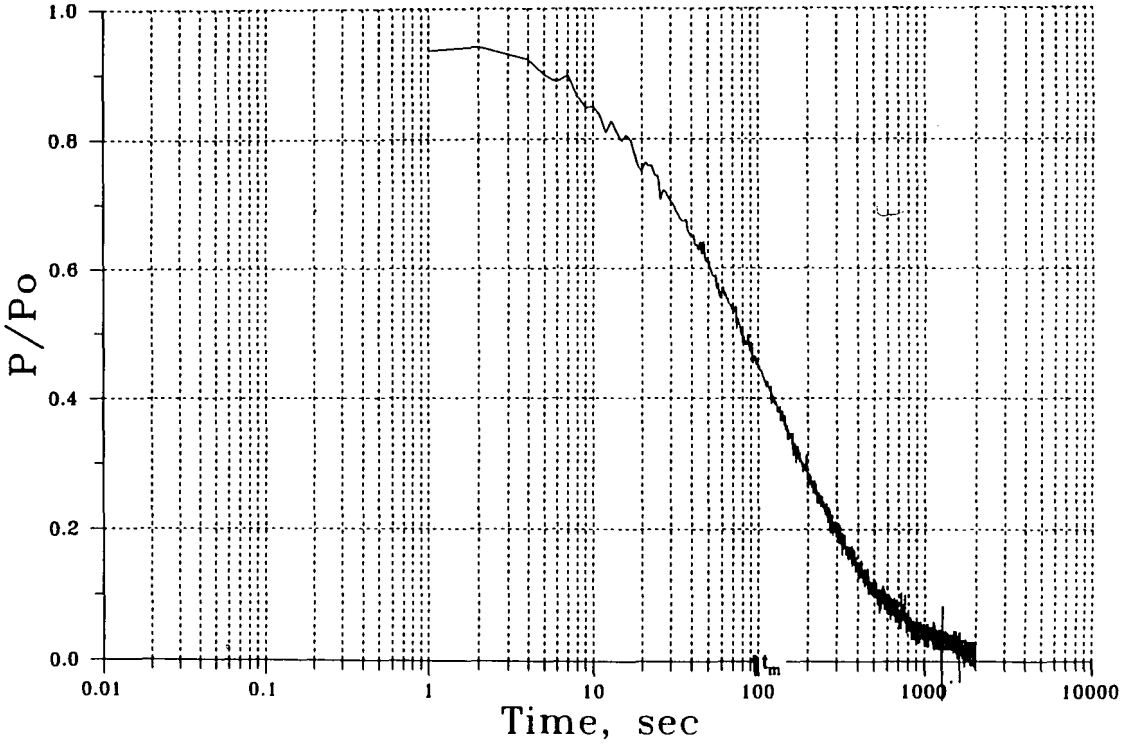

Figure 3.10 Normalized Observed Field Pressure Decay Curve, Station 9.

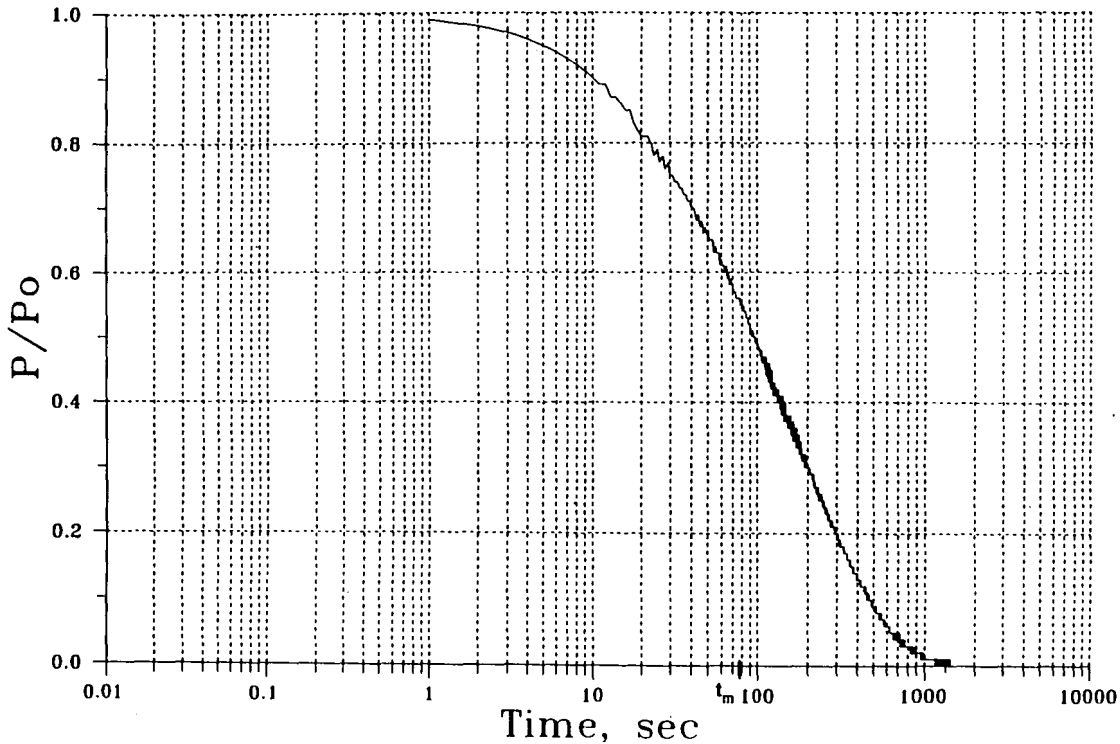

Figure 3.11 Normalized Observed Field Pressure Decay Curve, Station 10.

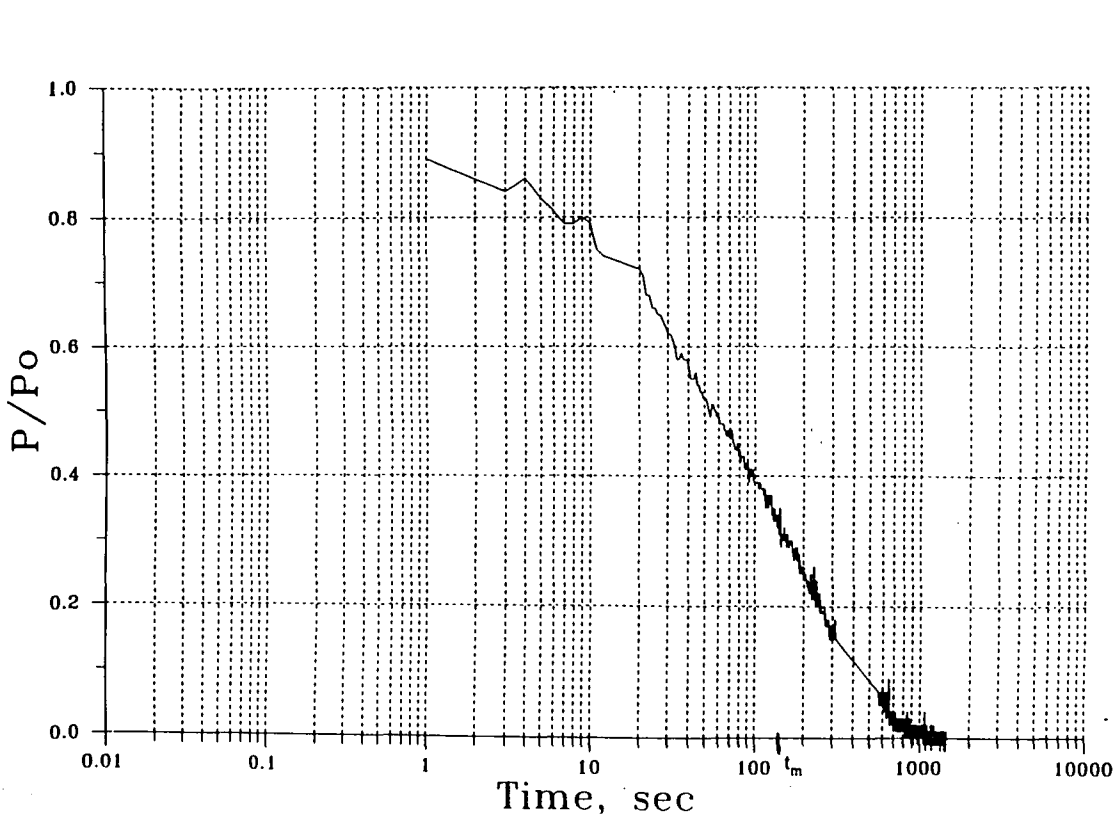

Figure 3.12 Normalized Observed Field Pressure Decay Curve, Station 11.

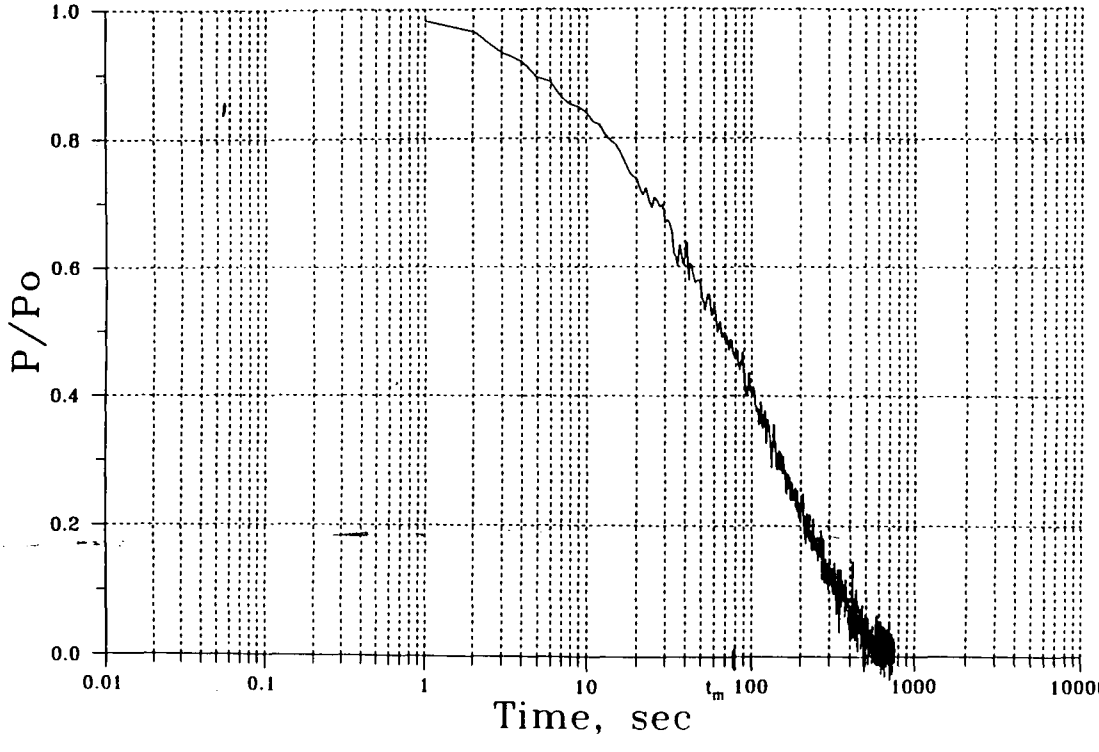

Figure 3.13 Normalized Observed Field Pressure Decay Curve, Station 12.

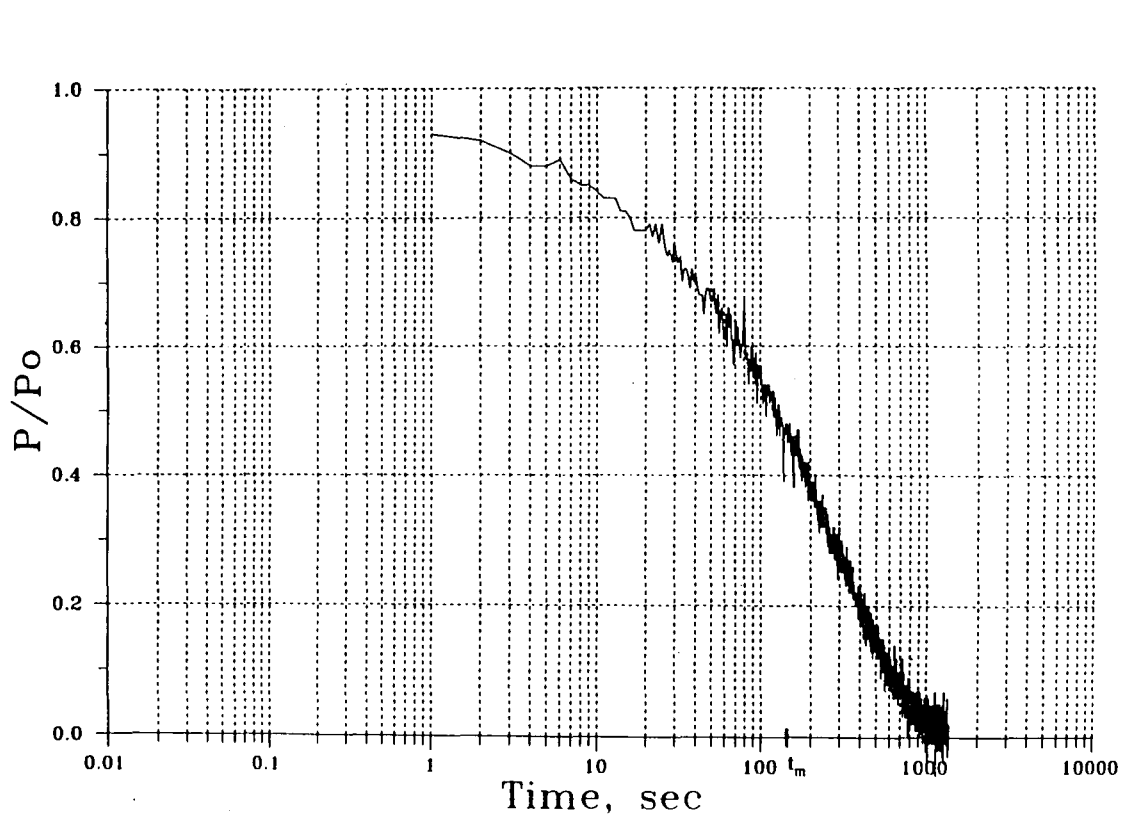

Figure 3.14 Normalized Observed Field Pressure Decay Curve, Station 13.

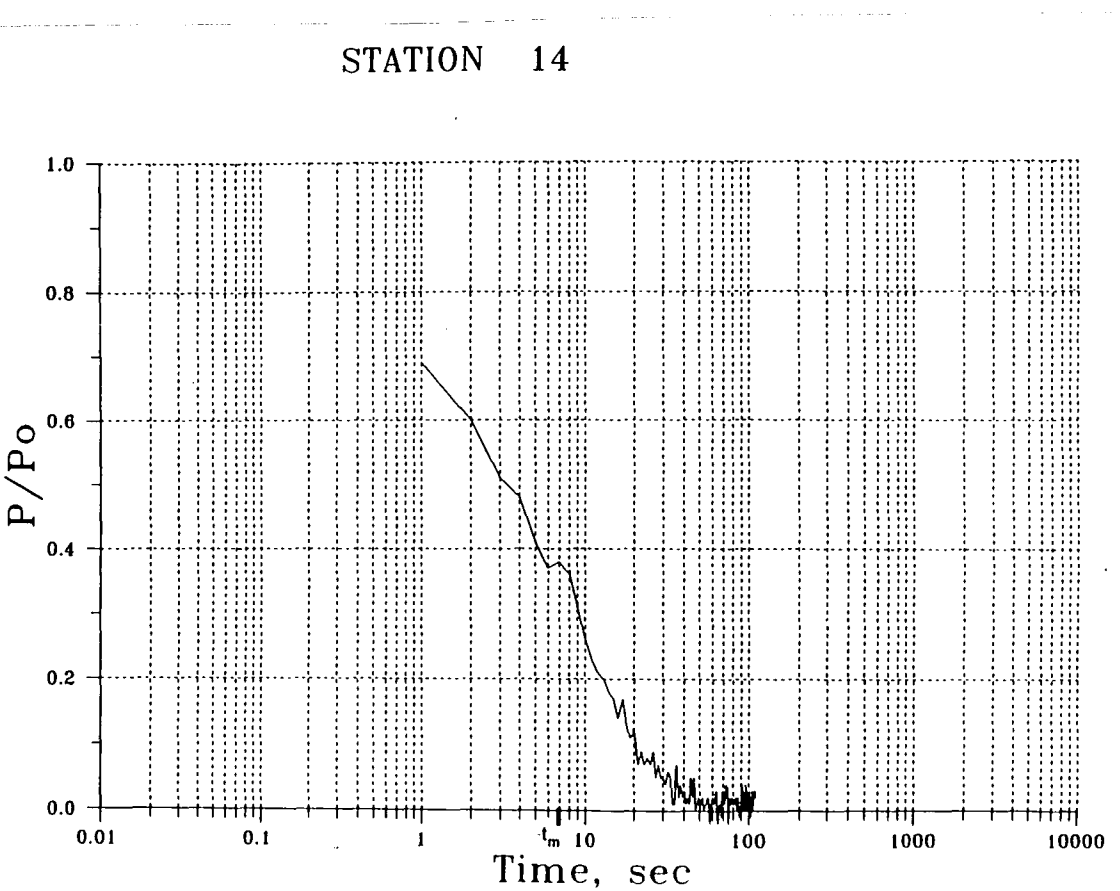

Figure 3.15 Normalized Observed Field Pressure Decay Curve, Station 14.

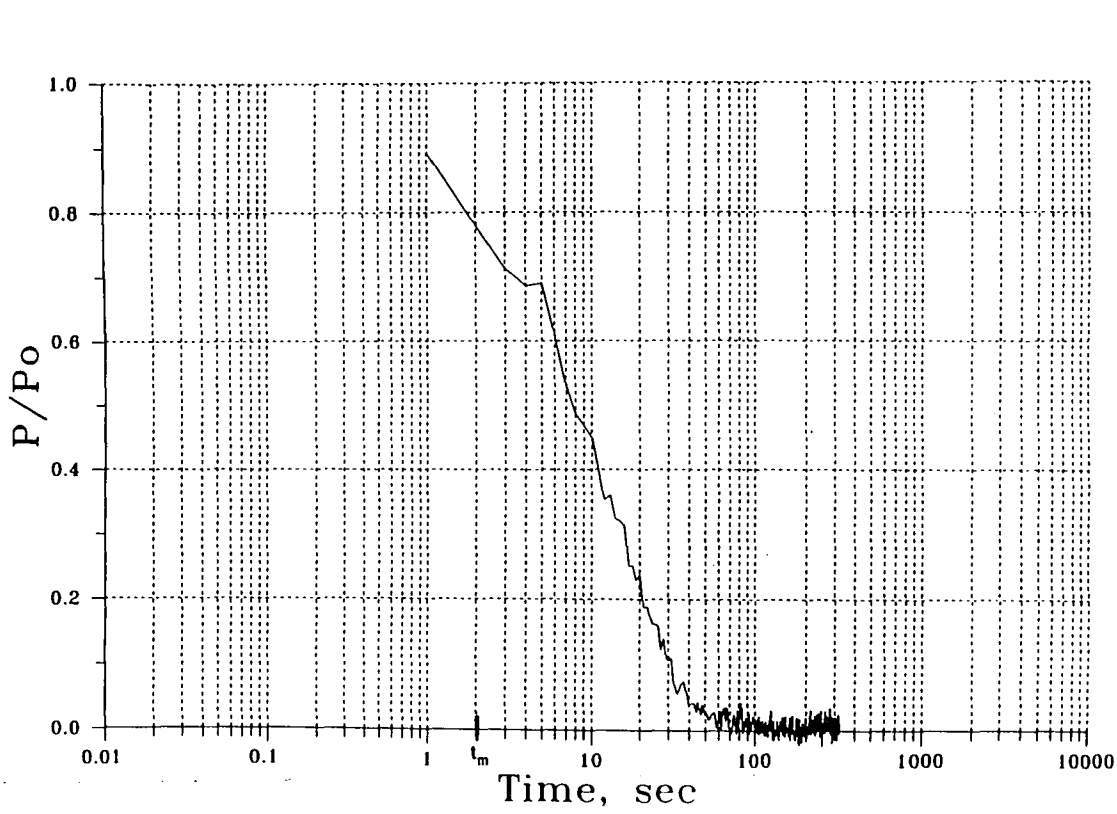

Figure 3.16 Normalized Observed Field Pressure Decay Curve, Station 15.

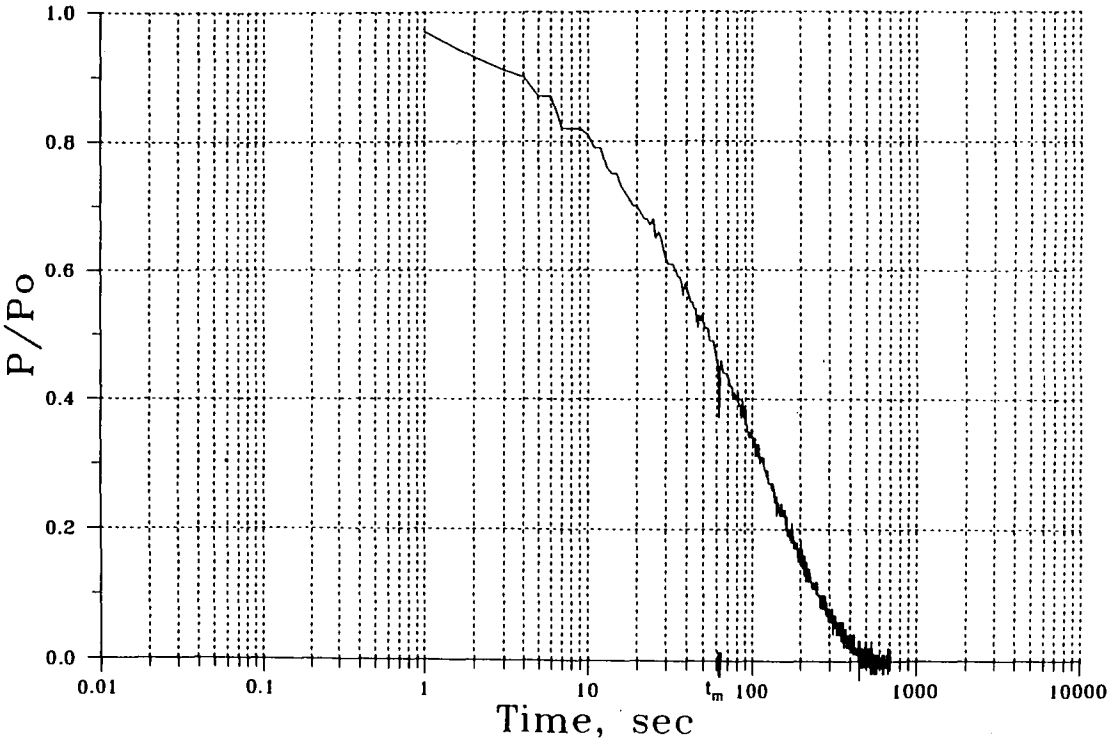

Figure 3.17 Normalized Observed Field Pressure Decay Curve, Station 16.

STATION 17

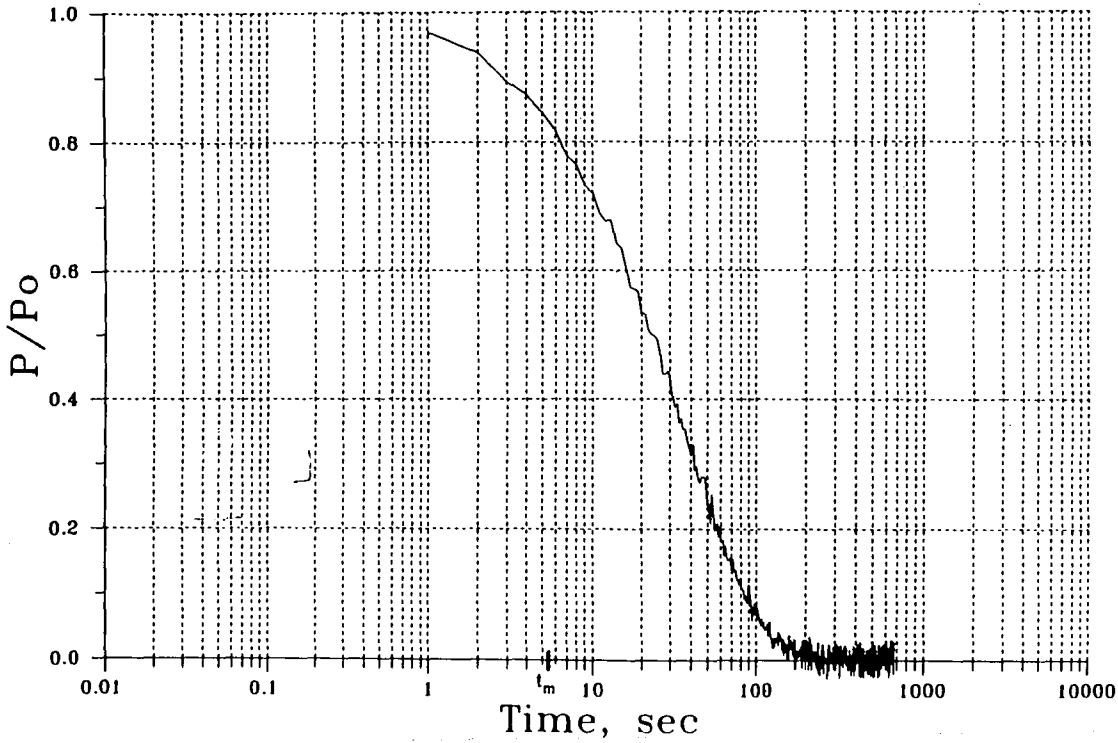

Figure 3.18 Normalized Observed Field Pressure Decay Curve, Station 17.

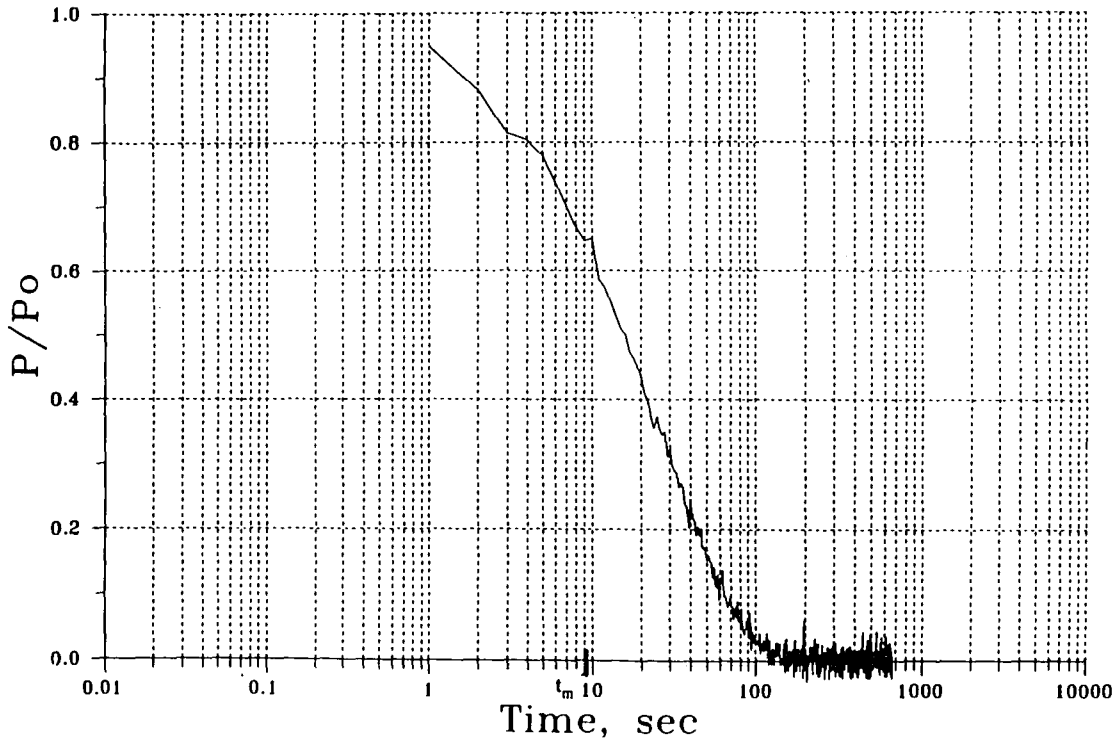

Figure 3.19 Normalized Observed Field Pressure Decay Curve, Station 18.

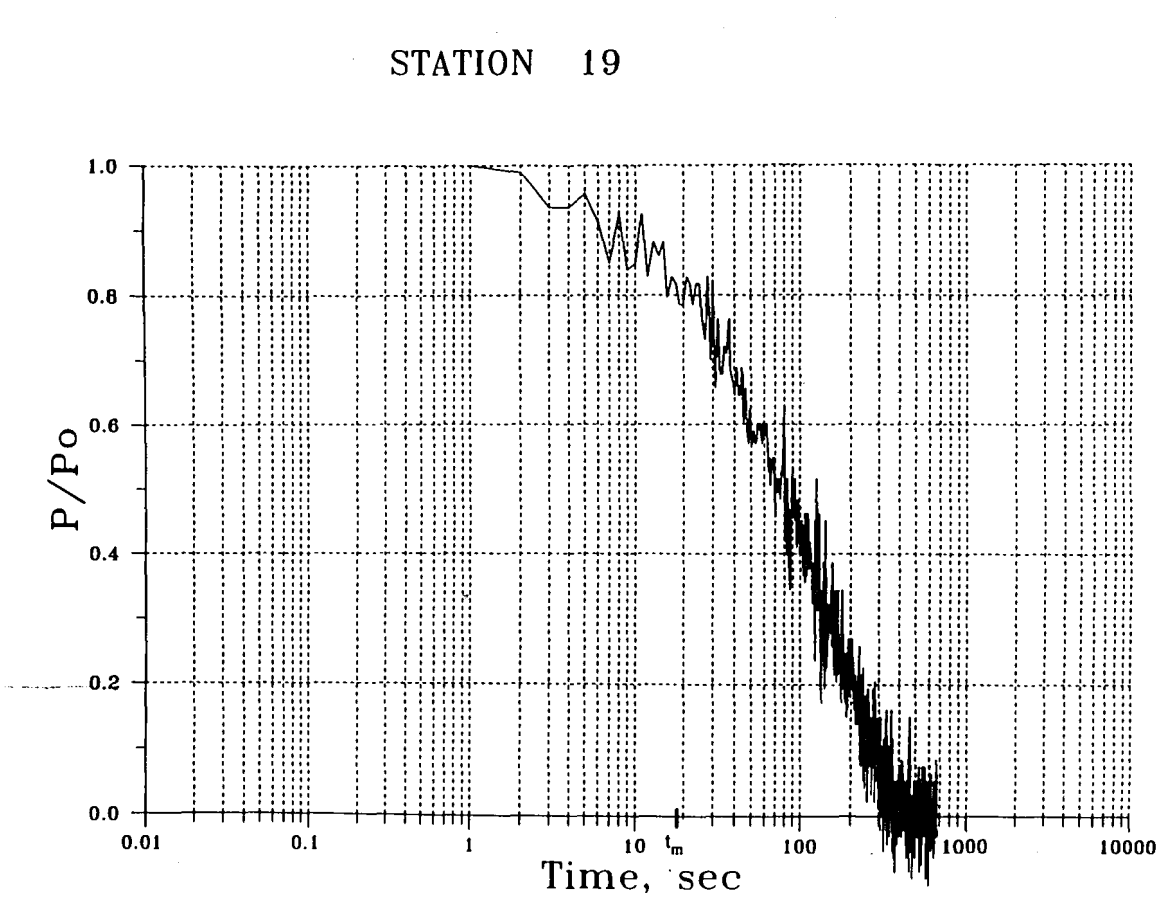

Figure 3.20 Normalized Observed Field Pressure Decay Curve, Station 19.

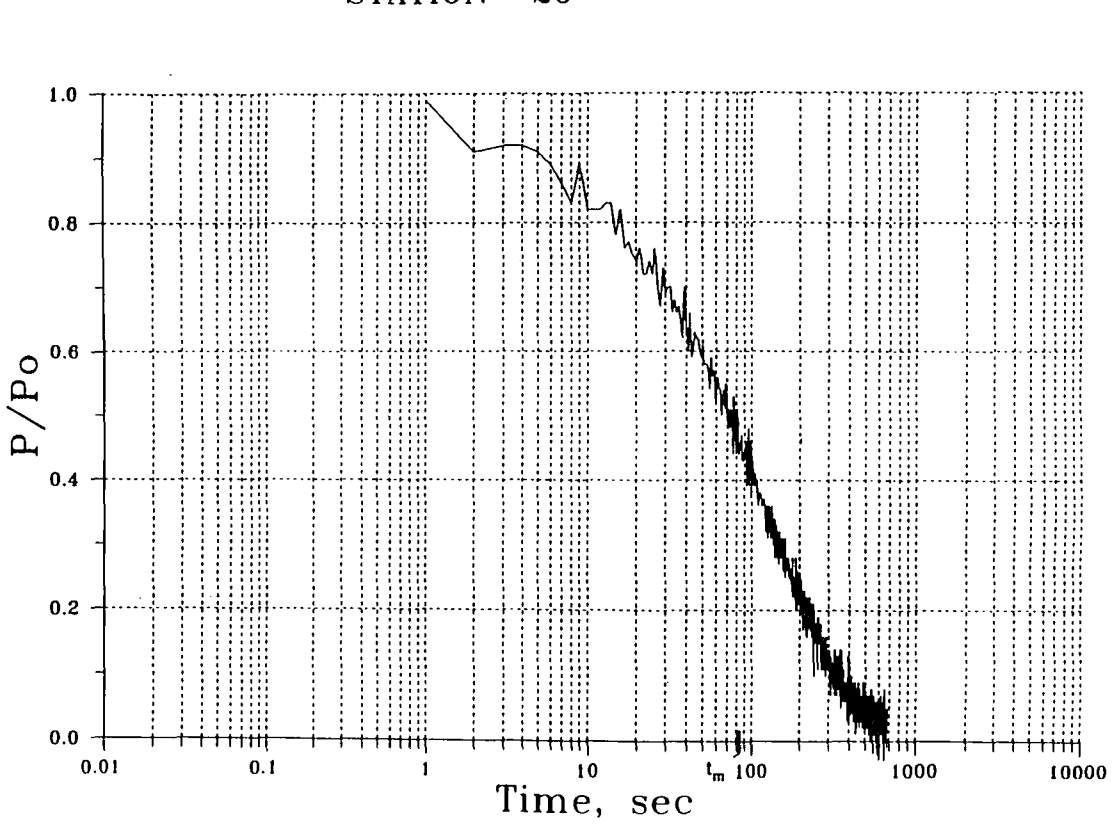

Figure 3.21 Normalized Observed Field Pressure Decay Curve, Station 20.

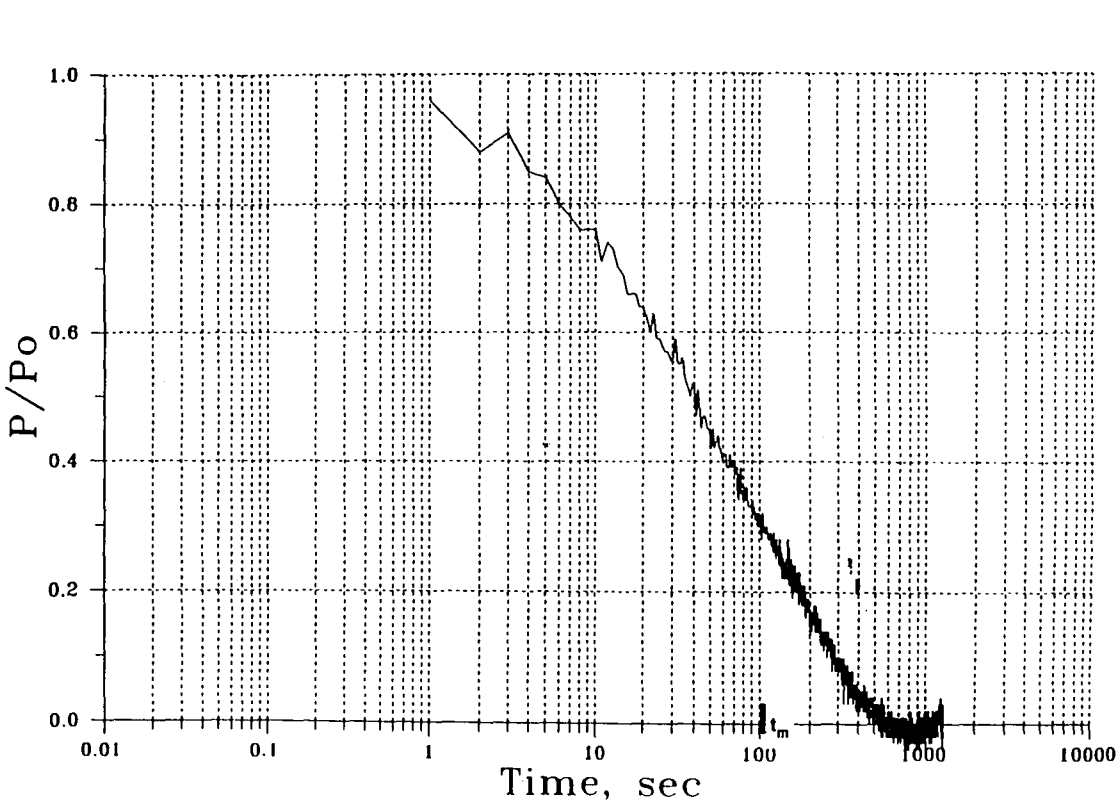

Figure 3.22 Normalized Observed Field Pressure Decay Curve, Station 21.

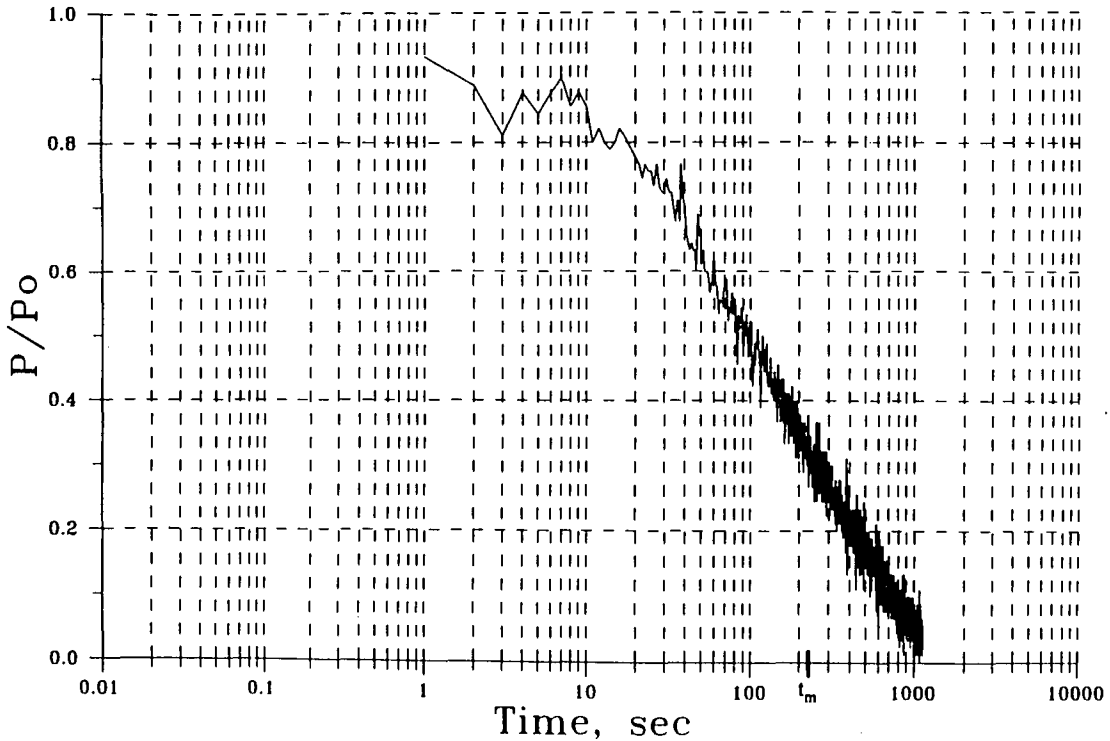

Figure 3.23 Normalized Observed Field Pressure Decay Curve, Station 22.

STATION 23

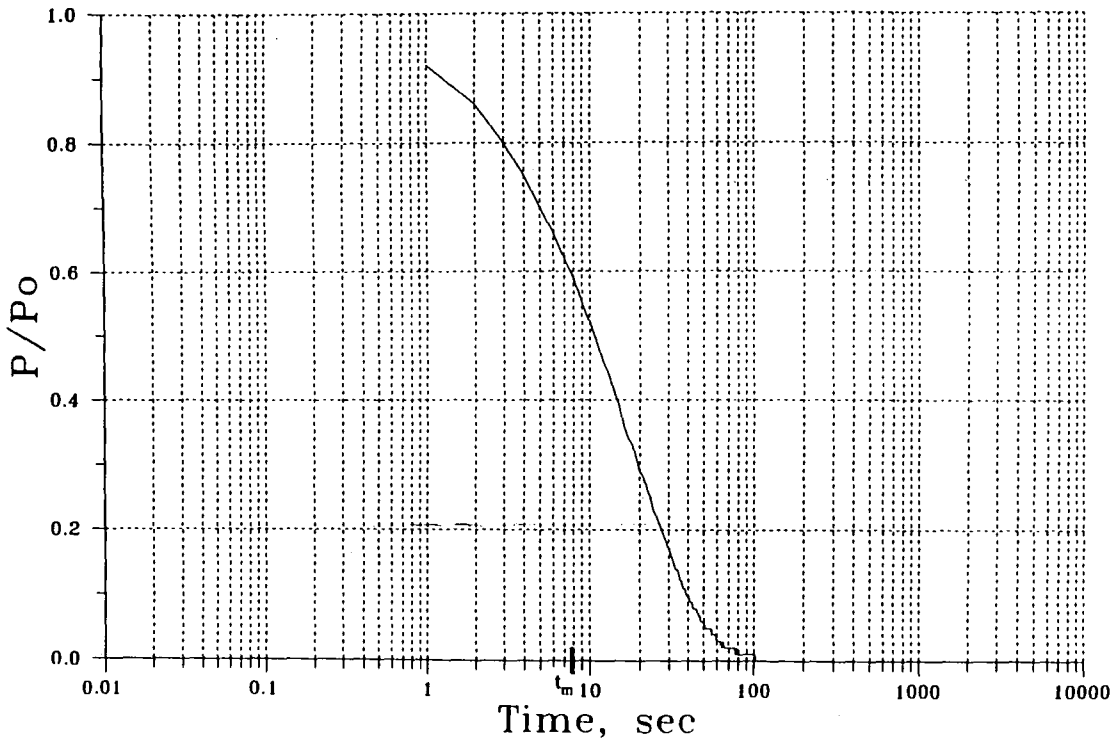

Figure 3.24 Normalized Observed Field Pressure Decay Curve, Station 23.

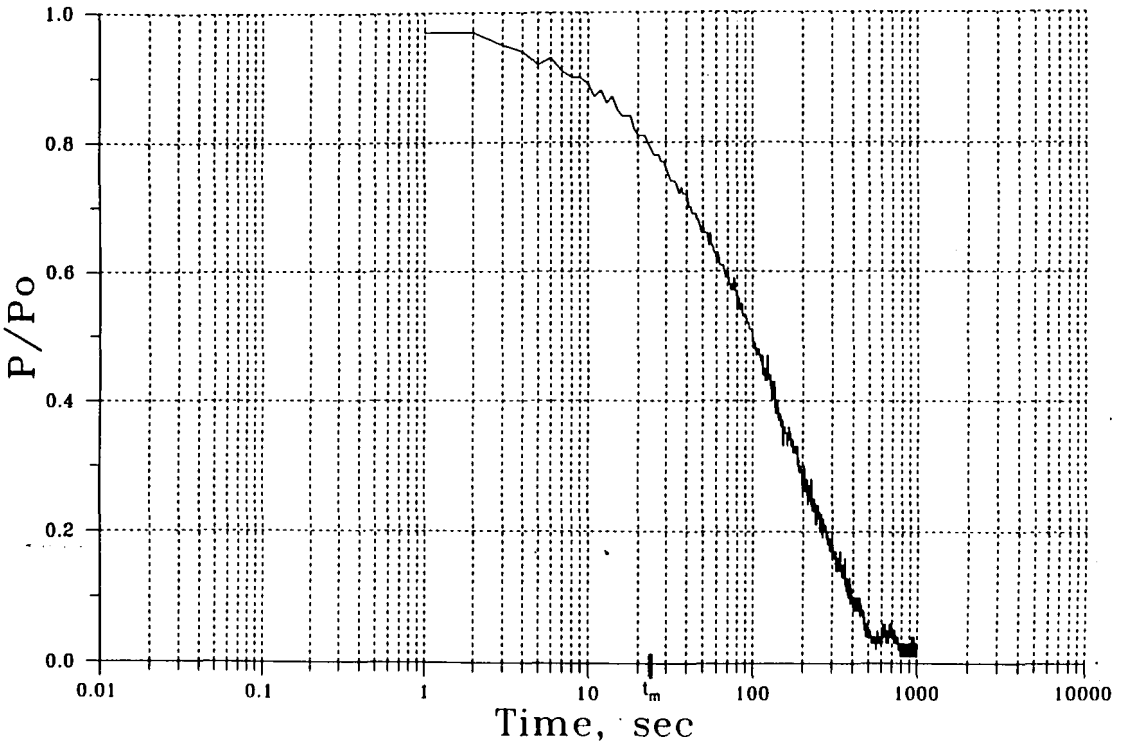

Figure 3.25 Normalized Observed Field Pressure Decay Curve, Station 24.

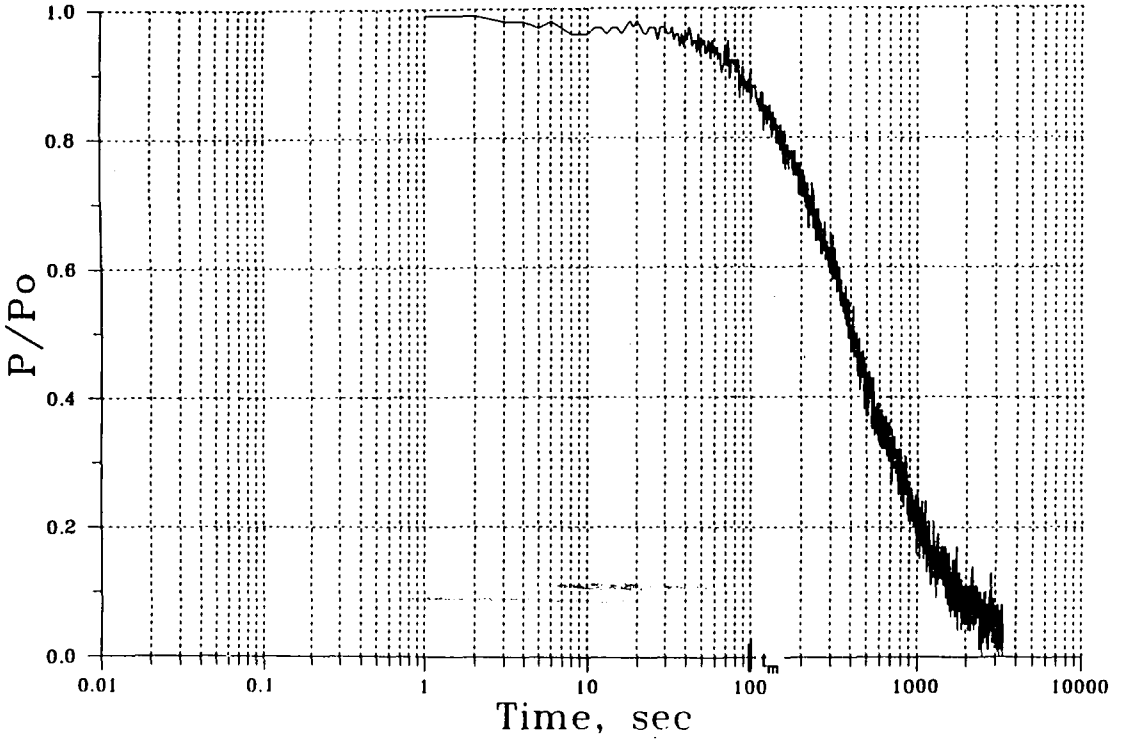

Figure 3.26 Normalized Observed Field Pressure Decay Curve, Station 25.

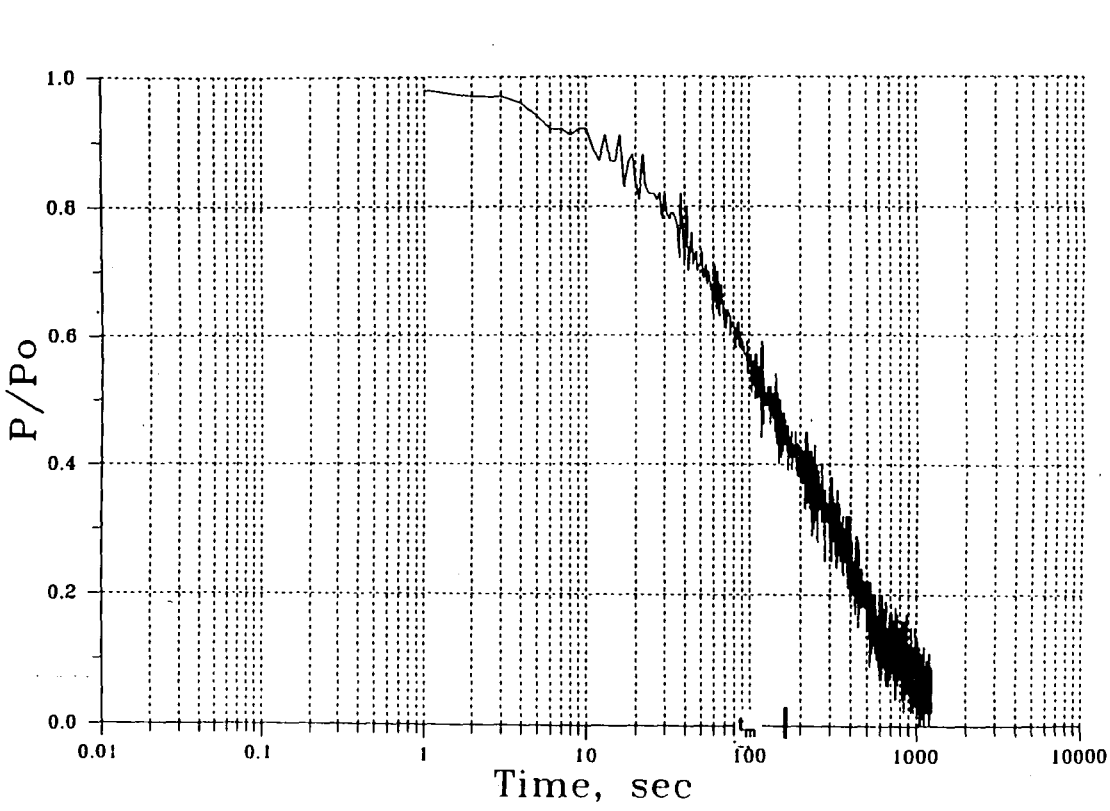

Figure 3.27 Normalized Observed Field Pressure Decay Curve, Station 26.

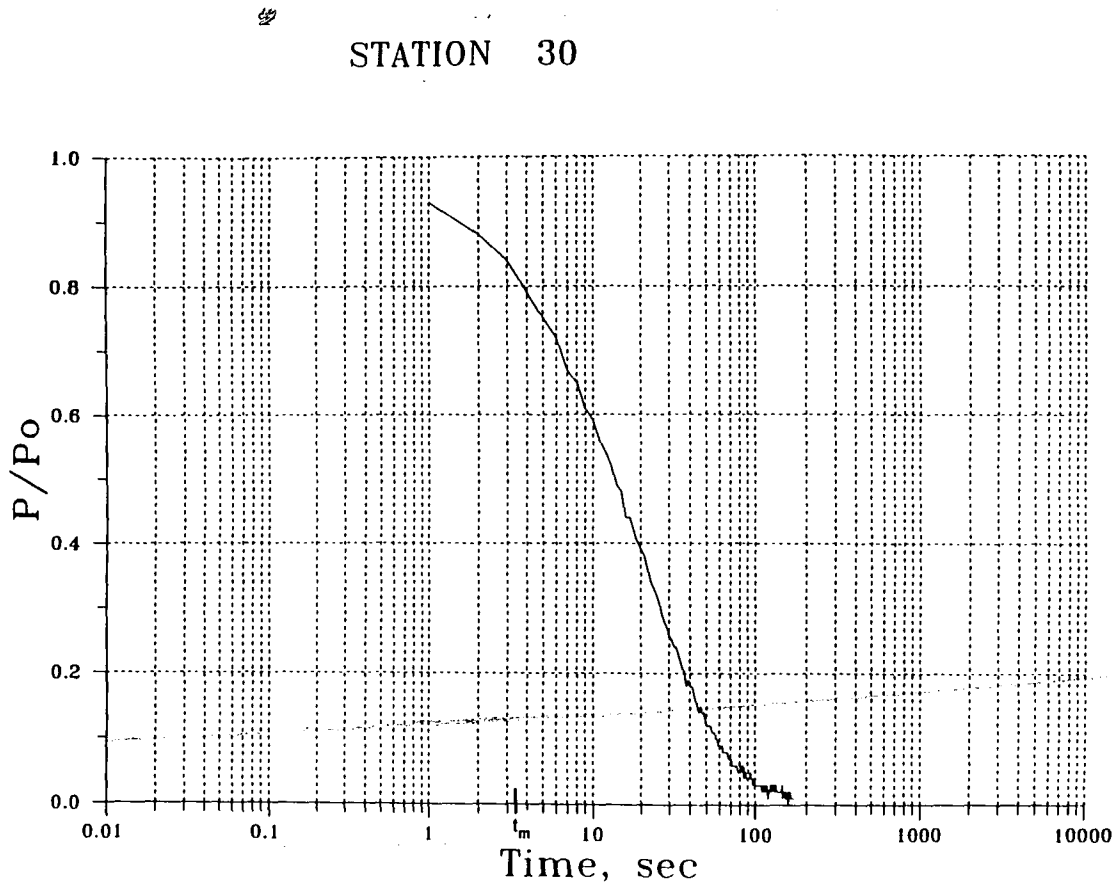

Figure 3.28 Normalized Observed Field Pressure Decay Curve, Station 30.

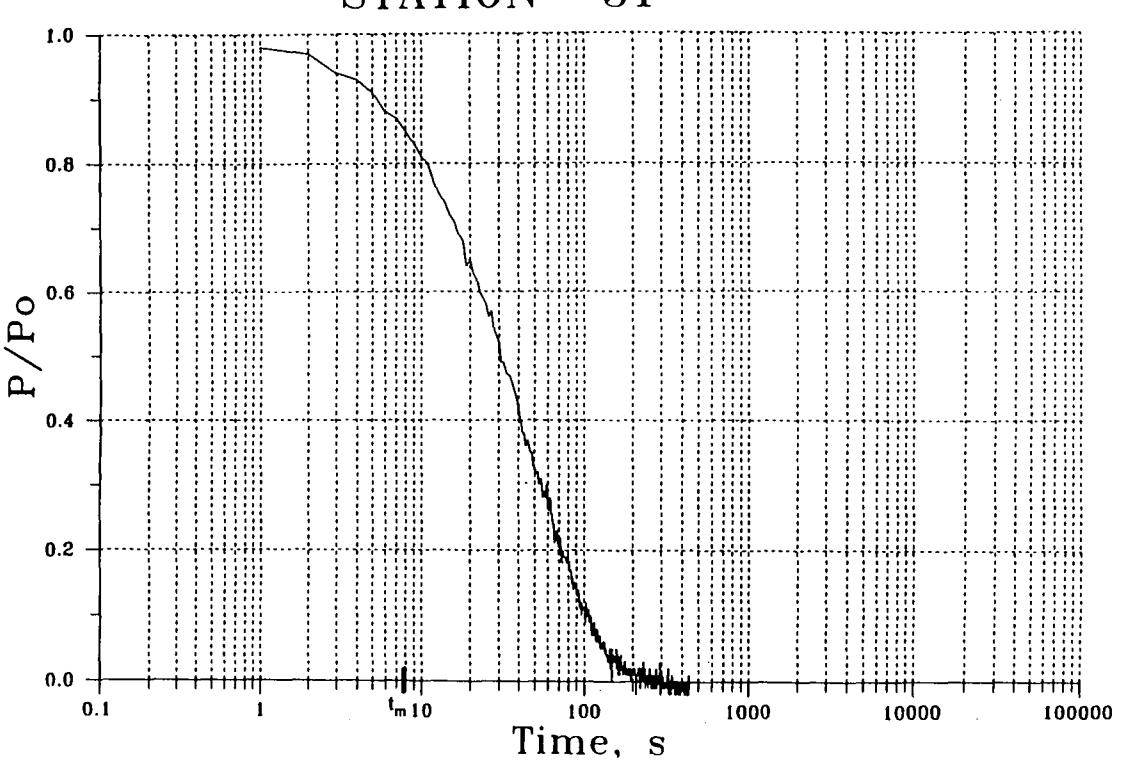

Figure 3.29 Normalized Observed Field Pressure Decay Curve, Station 31.

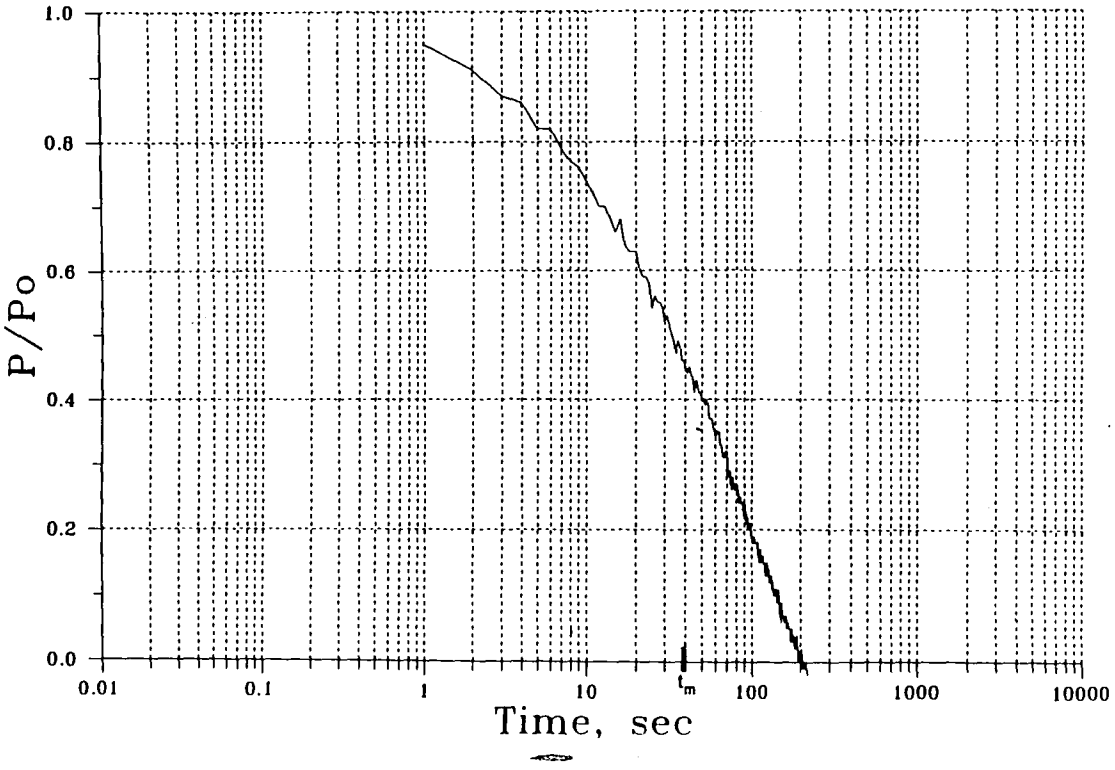

Figure 3.30 Normalized Observed Field Pressure Decay Curve, Station 32.

STATION A

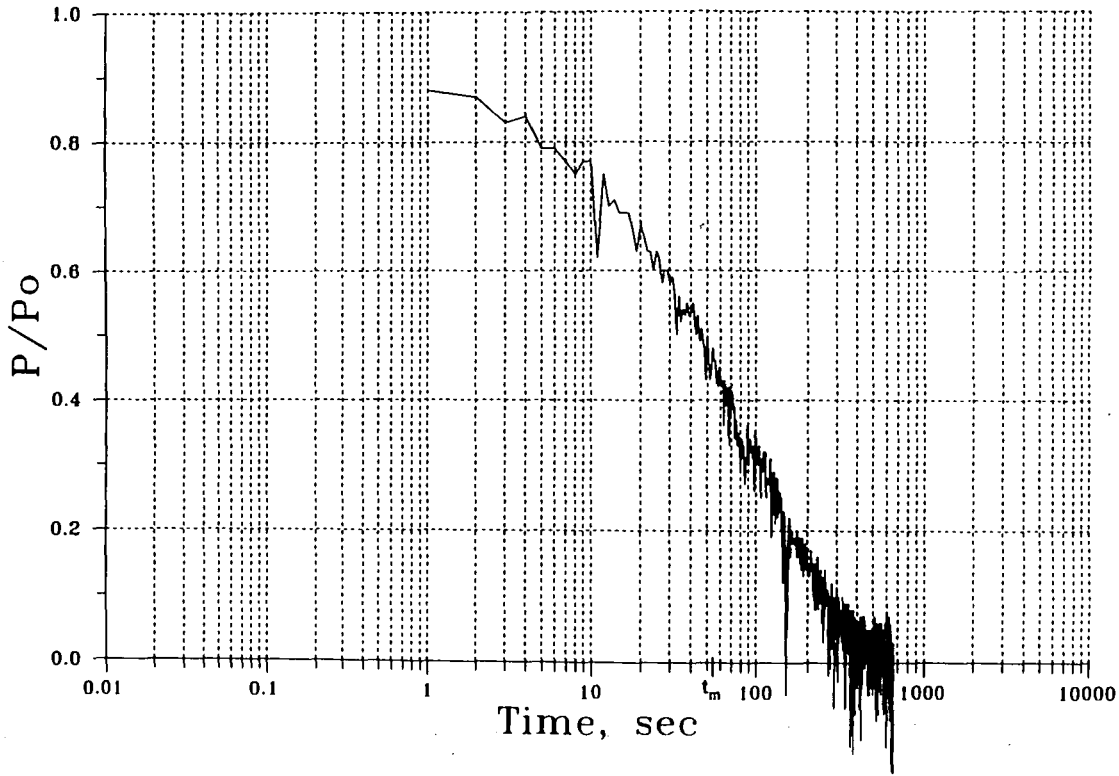

Figure 3.31 Normalized Observed Field Pressure Decay Curve, Station A.

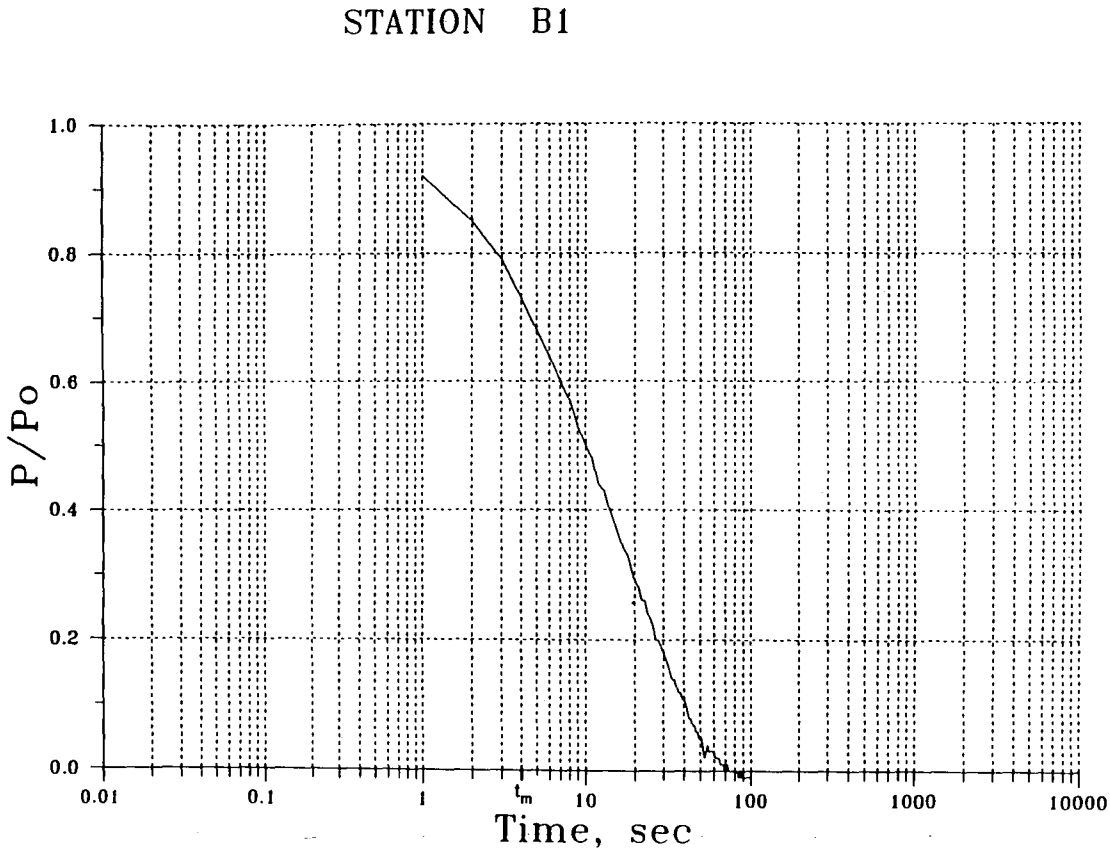

Figure 3.32 Normalized Observed Field Pressure Decay Curve, Station B1.

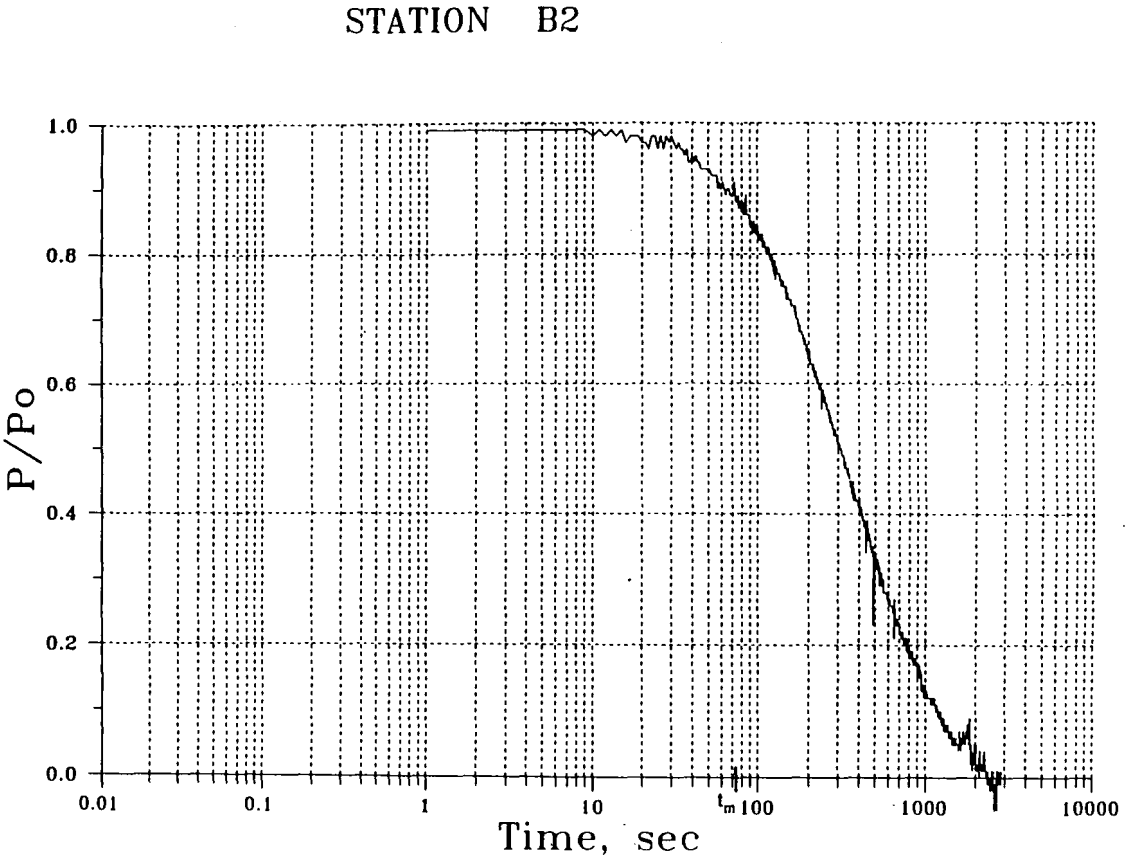

Figure 3.33 Normalized Observed Field Pressure Decay Curve, Station B2.

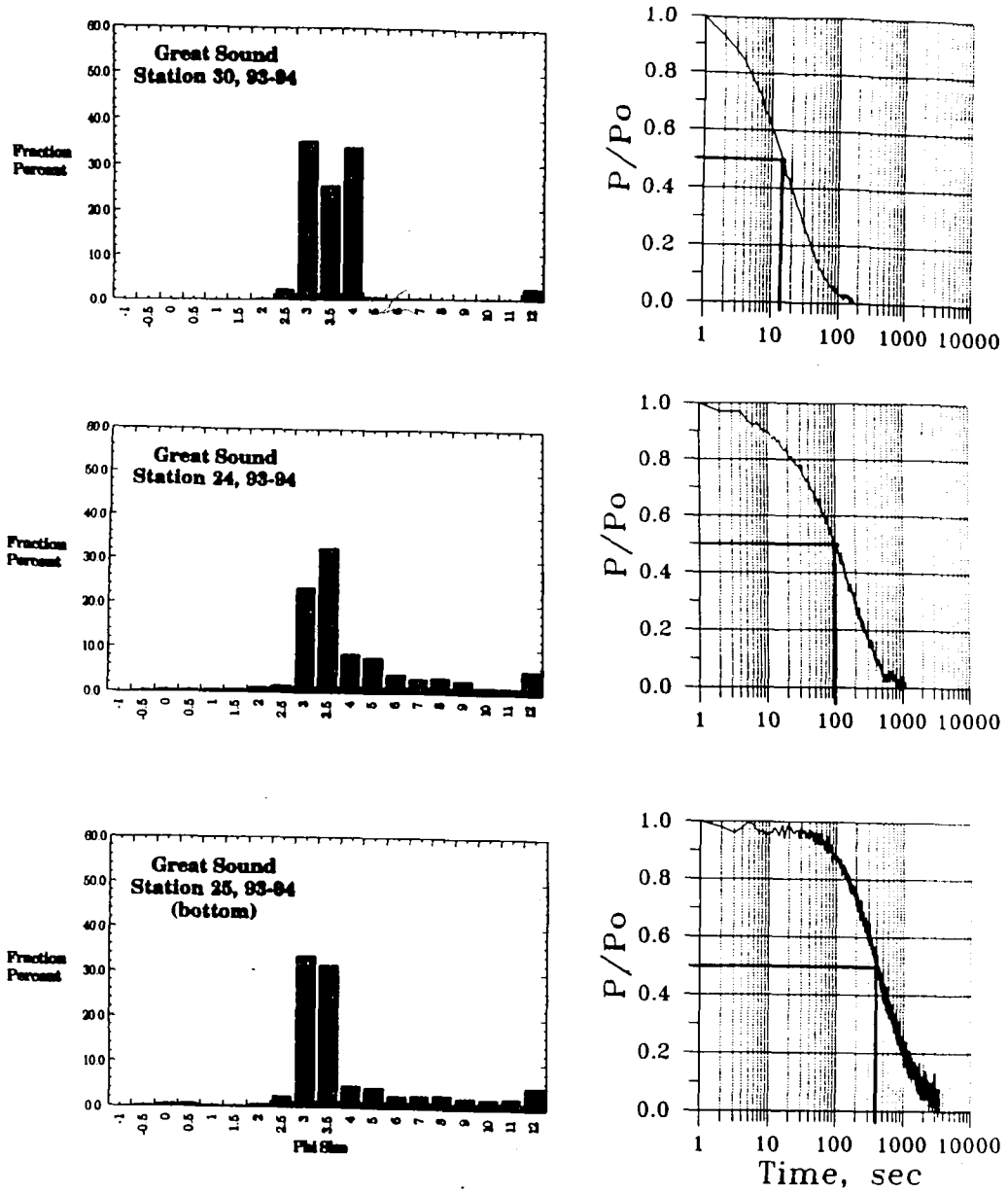

Figure 3.34 Grain Size Distribution and PISPPI-2 Normalized Observed Field Pressure Decay Curves for Selected Stations in Great Sound Proceeding from (a) Coarser (low ϕ units) to (c) Finer (high ϕ units) Sediment.

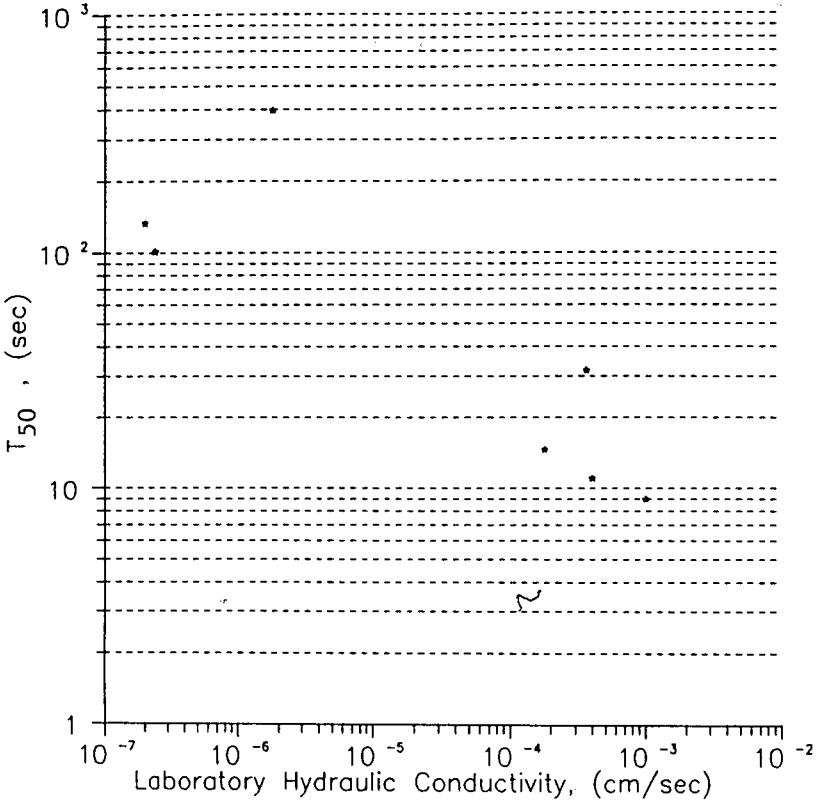

Figure 3.35 T_{50} (Time to 50% Pressure Decay) vs. Laboratory Permeameter Hydraulic Conductivity.

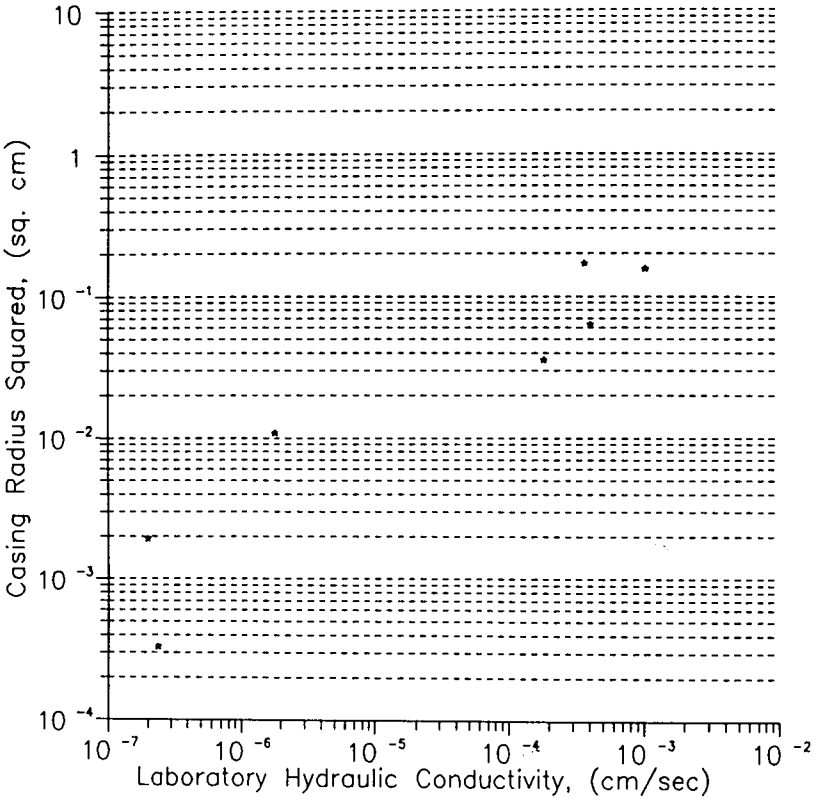

Figure 3.36 Equivalent Casing Radius Squared (r_c^2) vs. Laboratory Permeameter Hydraulic Conductivity (K).

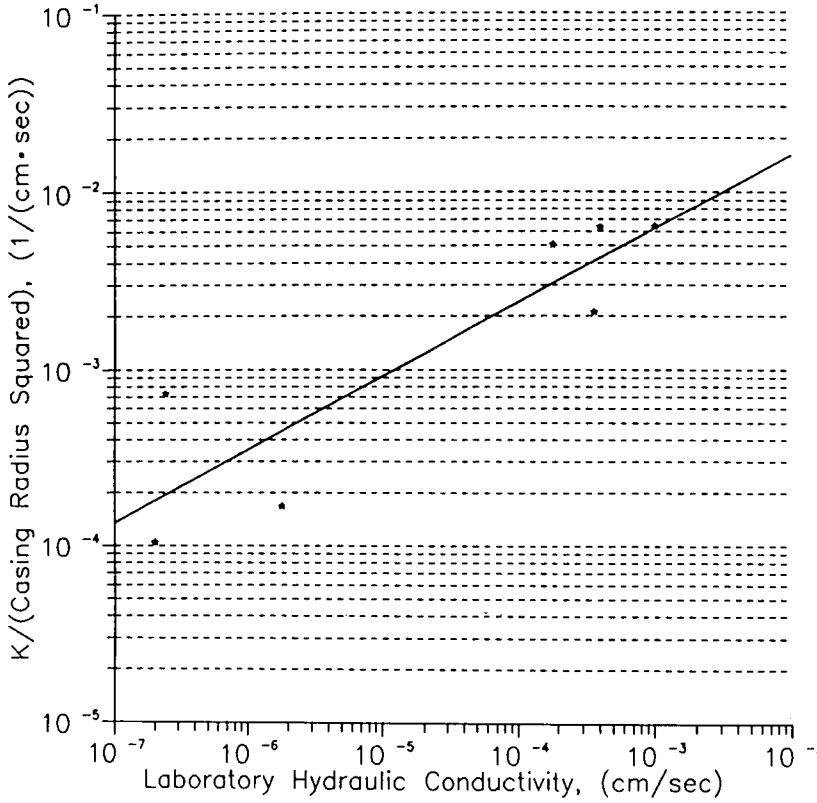

Figure 3.37 Ratio of K to Equivalent Casing Radius Squared (r_c^2) vs. Laboratory Permeameter Hydraulic Conductivity.

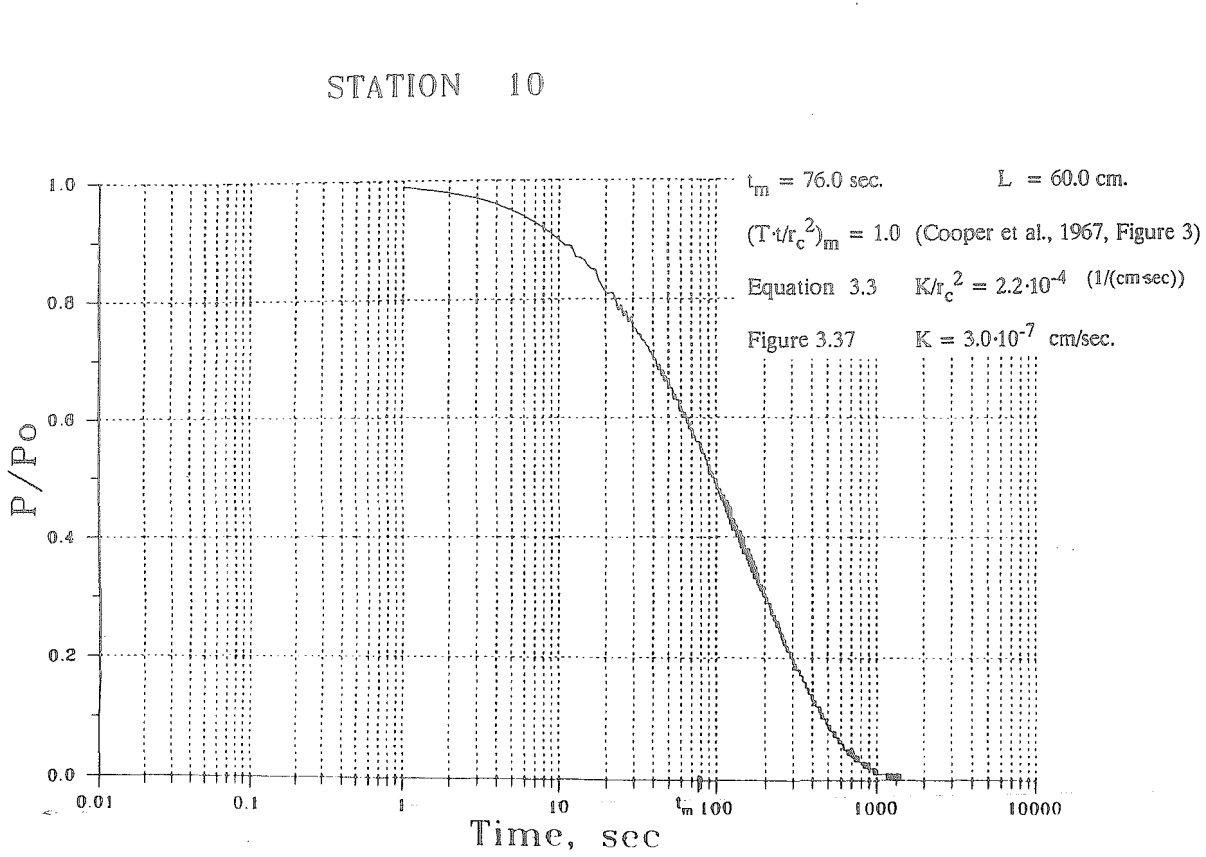

Figure 3.38 Estimate of Hydraulic Conductivity from PISPPI-2 Normalized Observed Field Pressure Decay Using the Equivalent Casing Radius Matching Technique.

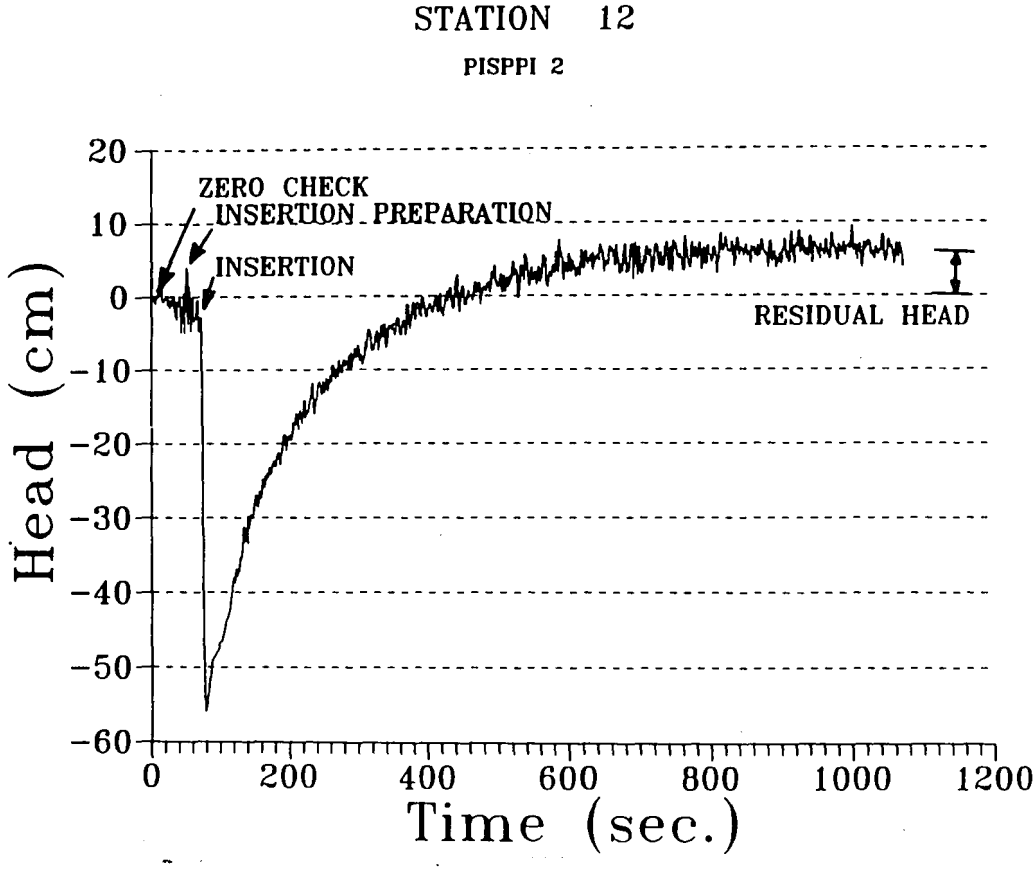

Figure 4.1 Observed Raw Field Pressure Decay Curve with Apparent Residual Pressure.

BIBLIOGRAPHY

ASTM, 1991 Annual Book of ASTM Standards, Philadelphia, pp. 1070-1077.

Bennett, A., Lennon, G.P., Carson, B. and Logue, J.P., 1993. "Hydraulic Conductivity Determination Methods--Laboratory and Computer Simulation Experiments, Imbt Hydraulic Laboratory Report No. IHL-138-93, Lehigh University, Bethlehem, PA.

Bennett, A., "Development of Methods for In Situ Determination of Hydraulic Conductivity in Aqueous Sediment," M.S. Thesis, Department of Civil Engineering, Lehigh University, 1993.

Bennett, R. H.,Burns, J. T., Nastav, F. L., Lipkin, J., and Percival, C. M., 1985. "Deep-Ocean Piezometer Probe Technology For Geotechnical Investigations," IEEE J. Oceanic Engineering, OE-10(1), 17-22.

Bennett, R. H., Burns, J. T., Li, H. Percival, C. M., and Lipkin, J, 1987. "Pore-Water Pressure Events During the In Situ Heat Transfer Experiment Simulation: Piezometer Probe Technology," Sandia National Labs, Albuquerque, NM, Report SAND86-7172, 78 pages.

Bouwer, H., and R. C. Rice. 1963. Seepage meters in seepage and recharge studies. ASCE Proceedings, J. of Irrigation and Drainage Division. 89: 17-42.

Bowles, J. E., Engineering Properties of Soils and Their Measurement, McGraw-Hill Book Company, 1978, pp. 105-109.

Bredehoeft, J. D., and S.S. Papadopulos. 1980. A method for determining the hydraulic properties of tight formations. Water Resources Research. 6(1): 233-238.

Carson, B., G. M. Ashley, G. P. Lennon, R. N. Weisman, J. E. Nadeau, M. J. Hall, R. Faas, M. L. Zeff, R. E. Grizzle, F. E. Schuepfer, C. L. Young, A. J. Meglis, K. F. Carney, and R. Gabriel, 1988, Hydrodynamics and Sedimentation in a Back-barrier Lagoon-salt marsh system, Great Sound, New Jersey - A summary, Marine Geology, 82, 123-132.

Carson, B., E. Suess, and J. Strasser. 1990. Fluid flow and mass flux determinations at vent sites on the Cascadia margin accretionary prism. J. of Geophysical Research. 95(B6): 8891-8897.

Carson, B., Yasko, G., Screaton, E., 1994, PISPPI-II User's Guide and Technical Manual, v. 1.2.

Chang, F. T., 1990, Finite Element Modelling of Coupled Fluid

Expulsion/Deformation Behavior of Dewatering Sediments, PhD Dissertation, Lehigh University, Bethlehem, PA, 150 pp.

Chang, F. T., Lennon, G. P., Pamukcu, S., and Carson, B., Modeling of Fluid Expulsion and Deformation Behavior of Dewatering Sediments, International Journal for Numerical and Analytical Methods in Geomechanics, vol. 17, 531-551, 1993.

Cherkauer, D.A., and McBride, J. M. 1988. A remotely operated seepage meter for use in large lakes and rivers. Ground Water. 26(2): 165-171.

Cherkauer, D.A., and D.C. Nader. 1989. Distribution of Groundwater seepage to large surface-water bodies: The effect of hydraulic heterogeneities. J. of Hydrology. 109: 151-165.

Cooper, H. H., Jr., Bredehoeft, J. D., and Papadopulos, S. S., 1967, Response of a finite diameter well to an instantaneous charge of water, Water Resources Research, 3(1), 263-269.

Davis, E. E., G. C. Horel, R. D. MacDonald, H. Villinger, R. H. Bennett, and H. Li, 1990, Pore Pressures and Permeabilities in Marine Sediments Measured with a Tethered Probe, Journal of Geophysical Research, submitted.

Faas, R. W., and B. Carson, 1988, Short-term deposition and long-term accumulation of lagoonal sediment, Great Sound, New Jersey. In: G. M. Ashley (editor), The Hydrodynamics and Sedimentology of a Back-Barrier Lagoon-Salt Marsh System, Stone Harbor, New Jersey, Marine Geology, 82, 97-112.

Freeze, R. A. and Cherry, J. A., (1979). Groundwater. Prentice-Hall, NJ.

Hvorslev, M. J., 1951. Time lag and soil permeablility in groundwater observations. U.S. Army Corps Engrs. Waterways Exp. Sta. Bull. 36, Vicksburg, Miss.

Karasaki, K., 1991, Prematurely terminated slug tests--a field application, Proceedings of the International Symposium on Groundwater, ASCE, Ed. Gerard P. Lennon & S. Rouhani, July 29-August 2, pp. 163-168.

Kennish, M. J., and Lutz, R. E. (Eds.), 1984, Ecology of Barnegat Bay, New Jersey, Lecture Notes on Coastal and Estuarine Studies 6, Springer-Verlag, NY, 396 pp.

Krabbenhoft, D. P., Anderson, M. P., Bowser, C. J., and Valley, J., 1990, Estimating groundwater exchange with Sparkling Lake, Wisconsin, 1: Use of the stable isotope mass-balance method, Water Resources Research, in press.

Lee, D. R. 1985. Method for locating sediment anomalies in lakebeds that can be

caused by groundwater flow. J. of Hydrology. 79: 187-193.

Lee, D. R. 1977. A device for measuring seepage flux in lakes and estuaries. Limnology and Oceanography. 22(1): 140-147.

Lee, D. R. and J. A. Cherry, 1978. "A Field Exercise on Groundwater Flow Using Seepage Meters and Mini-Piezometers," J. Geological Education, 27, 6-147.

McBride, M.S., and H. O. Pfannkuch. 1975. The distribution of seepage within lakebeds. J. Res. U.S. Geol. Surv. 3: 505-512.

McDonald, M., and Harbaugh, A., 1984, A modular three-dimensional finite-difference groundwater flow model, Scientific Publications Company.

Nicholson, R., "Simulation of Groundwater Flow in the Unconfined Aquifer System of the Toms River, Metedeconk River, and Kettle Creek Basins, New Jersey, Water Resources Investigation Report (in preparation), 1994.

Papadopulos, S. S., Bredehoeft, J. D., and Cooper, H. H., Jr., 1973, On the analysis of 'slug test' data, Water Resources Research 9(4), 1087-1089.

Rad, J. T., and Tumay, M. T., 1985, Pore-pressure response of the piezocone penetrometer, Geotechnical Testing Journal, 8(3), 125-131.

Reay, W. G., Gallagher, D. L., and Simmons, G. M., Jr, 1992, Groundwater discharge and its impact on surface water quality in a Chesapeake bay inlet, Water Resources Bulletin, AWRA, Vol. 28, No. 6.

Schuepfer, F. E., G. P. Lennon, R. N. Weisman, and R. J. Gabriel, 1988, Hydrodynamic model of Great Sound, New Jersey. In: G. M. Ashley (editor), the Hydrodynamics and Sedimentology of a Back-Barrier Lagoon-Salt Marsh System, Stone Harbor, New Jersey, Marine Geology, 82, 1-15.

Schultheiss, P. J., and McPhail, S. D., 1986. "Direct Indication of Porewater Advection from Pore Pressure Measurements in Madiera Abyssal Plain Sediments", Nature, 320(6060), 348-350.

Screaton, E. J., Carson, B., and Lennon, G. P., "In Situ Permeability Tests at Site 892", in Scientific Results, Ocean Drilling Program, Vol. 146, submitted August, 1994.

Shepard, F. P., 1954, Nomenclature based on sand-silt-clay ratios, Journal of Sedimentary Petrology, 24, 151-158.

Todd, K. D. (1976). Groundwater Hydrology, 2nd Edition. John Wiley and Sons,

NY.

Tumay, M. T., Acar, Y. B., and Cekirge, M. H., 1985, Flow field around cones in steady penetration, ASCE Journal of Geotechnical Engineering, 111(2), 193-204.

U.S. Dept. of Commerce, NOAA, Nautical Chart No. 12316, *New Jersey Intracoastal Waterway, Little Egg Harbor to Cape May.*

Winter, T. C., 1983. The interaction of lakes with variably saturated porous media. Water Resources Research. 19: 1203-1218.

Wetzel, M., Lennon, G., and Carson, B., "In situ determination of hydraulic conductivity and hydraulic head in coastal sediments," Imbt Hydraulic Laboratory Report, Lehigh University, 1994 (in preparation).

Woessner, W. W. and Sullivan, K. E., 1984, Results of seepage meter and mini-piezometer study, Lake Mead, Nevada, Ground Water. 22(5). 561-568.

Vita

Michael D. Wetzel was born in Ashland, Pennsylvania on January 9, 1970, to Robert and Diane Wetzel. He received his Bachelor of Science degree in Civil Engineering from Lehigh University in May of 1993. He returned to Lehigh University in the Summer of 1993 to pursue a Master of Science degree in Civil Engineering. He served as a research assistant and as a teaching assistant during his graduate program and expects to graduate in January of 1995.

END OF TITLE